AEDC-TR-72-161

NOV 28 1972

DEC 17 1973

MAR 1 1974

OCT 2 4 1986

RESEARCH AND DEVELOPMENT TESTING OF YTTRIA/RARE EARTH STABILIZED ZIRCONIA MATRIX BRICKS IN THE PILOT TEST UNIT (PTU) AT AEDC

C. R. Tinsley

ARO, Inc.

PROPERTY OF U.S. AIR FORCE
AEDC TECHNICAL LIBRARY

November 1972

TECHNICAL REPORTS
FILE COPY

Approved for public release; distribution unlimited.

B 450

AEDC TECHNICAL LIBRARY
5 0720 00062 7382

ENGINE TEST FACILITY
ARNOLD ENGINEERING DEVELOPMENT CENTER
AIR FORCE SYSTEMS COMMAND
ARNOLD AIR FORCE STATION, TENNESSEE

NOTICES

When U. S. Government drawings specifications, or other data are used for any purpose other than a definitely related Government procurement operation, the Government thereby incurs no responsibility nor any obligation whatsoever, and the fact that the Government may have formulated, furnished, or in any way supplied the said drawings, specifications, or other data, is not to be regarded by implication or otherwise, or in any manner licensing the holder or any other person or corporation, or conveying any rights or permission to manufacture, use, or sell any patented invention that may in any way be related thereto.

Qualified users may obtain copies of this report from the Defense Documentation Center.

References to named commercial products in this report are not to be considered in any sense as an endorsement of the product by the United States Air Force or the Government.

RESEARCH AND DEVELOPMENT TESTING OF YTTRIA/RARE EARTH STABILIZED ZIRCONIA MATRIX BRICKS IN THE PILOT TEST UNIT (PTU) AT AEDC

C. R. Tinsley
ARO, Inc.

Approved for public release; distribution unlimited.

FOREWORD

The work reported herein was sponsored by the Arnold Engineering Development Center (AEDC), Air Force Systems Command (AFSC), Arnold Air Force Station, Tennessee, under Program Element 65802F, Task T-2.

The results of the research presented herein were obtained by ARO, Inc. (a subsidiary of Sverdrup & Parcel and Associates, Inc.), contract operator of AEDC, AFSC, under Contract F40600-73-C-0004. The research testing was conducted in the Engine Test Facility (ETF) from February 1969 to April 1971 under ARO Project Numbers PL3922, KC3002, RR3102, and RR5202. The manuscript for this report was submitted for publication on June 6, 1972.

The author wishes to express appreciation to P. B. Carter and W. W. Muse for the contributions they made to this report, in particular information pertaining to galvanic corrosion, nitric acid erosion, and the matrix restabilization heat soak. Special recognition is given to M. H. Nesbitt who provided much information concerning the 27 heater shakedown runs, and Major L. L. Fehrenbacher and D. F. Frank of ARL, Wright-Patterson Air Force Base, Ohio, for providing the posttest analytical study of various PTU refractories.

This technical report has been reviewed and is approved.

G. M. ARNOLD	R. R. GARREN
Facility Development Division	Lt Colonel, USAF
Directorate of Civil Engineering	Director of Civil Engineering

ABSTRACT

Presented herein are the comprehensive results of research testing accomplished with the Pilot Test Unit (PTU) at AEDC from February 1969 to April 1971. The major objective of this continuing test program is to develop operational techniques and suitable ceramic materials in direct support of a full-scale, intermittent airflow, high enthalpy, high pressure test facility capable of testing aircraft and missile models, components, and engines in the Mach 2 to 8 flight regime. Eighty-four blowdown runs accomplished in the PTU are reported herein. Heater maximum operating conditions of 1850 psi and 4450°R were accomplished during testing. The PTU heater vessel is approximately 3 ft in inside diameter, 21.5 ft long, and contains a 14-in.-diam cored brick matrix which is approximately 15 ft long. The upper 7.4 ft of the matrix are composed of high density yttria-stabilized zirconia, and the lower 7.6 ft are composed of high density alumina. High density (approximately 90 and 95 percent theoretical density) zirconia matrix bricks have been tested with yttria/rare earth content ranging from 9.25 to 16.5 weight percent, and a few low density (approximately 70 percent theoretical density) zirconia matrix brick samples have been tested with yttria/rare earth contents of 12.5 and 14.5 weight percent. Initially, the heater matrix consisted of high-density zirconia and high-density alumina bricks, both manufactured by Coors Porcelain Company. However, during the test program a variety of sample zirconia bricks manufactured by both Coors Porcelain Company and Zirconium Corporation of America were tested in the heater matrix. During the first 27 heater blowdown runs, the zirconia matrix became destabilized. The matrix was subsequently subjected to a 4550°R (maximum matrix temperature) matrix restabilization heat soak which successfully lowered the monoclinic phase content of the matrix bricks and decreased the monoclinic content at the matrix top to below the detectable limit (0.5 percent). After run 85 the monoclinic content of various bricks from throughout the zirconia matrix was below the detectable limit except for a small isolated area at the zirconia/alumina interface, which contained 5.83 percent monoclinic phase.

APPENDIXES

I. ILLUSTRATIONS

Figure		Page
1.	Pilot Heater Schematic	23
2.	Pilot Heater Refractory Configuration	24
3.	Pilot Heater Thermocouple Locations	26
4.	Maximum Matrix Temperature Determination	27
5.	Matrix Centerline Temperature Cycling, Runs 1 through 85	28
6.	Representative Heater Operating Pressure Histories	40
7.	Matrix Configuration, Heat Soak	42
8.	Schematic of Heater Dome and Combustion Chamber Area	43
9.	Matrix Configuration, Runs 28 through 32	44
10.	Post-Run 32 Inspection	45
11.	Matrix Configuration, Runs 33 through 37	48
12.	Matrix Sample Bricks, Post-Run 37	49
13.	Combustion Chamber Bricks, Post-Run 37	50
14.	Matrix Configuration, Runs 38 through 44	51
15.	Matrix Sample Bricks, Posttest 38	52
16.	Post-Run 39 Matrix Inspection	54
17.	Post-Run 44 Matrix Inspection	56
18.	Matrix Configuration, Runs 45 through 69	60
19.	Post-Run 69 Matrix Inspection	61
20.	Matrix Configuration, Runs 70 through 74	65
21.	Second-Generation Burner	66
22.	Matrix Configuration, Runs 75 through 85	67
23.	High Density Sample Bricks, Post-Run 85	68
24.	Low Density Sample Bricks, Post-Run 85	72
25.	Zirconia Matrix Overall View, Post-Run 85	75
26.	Zirconia Matrix Bricks Located Directly below Sample Bricks, Post-Run 85	77
27.	Alumina Matrix, Post-Run 85	78
28.	Various Heater Refractories, Post-Run 85	81
29.	Matrix Brick Exhibiting Stress Marks, Post-Run 44	85
30.	Misalignment in Non-Keyed Bricks, Post-Run 85	86
31.	Bricks Exhibiting Localized Fusion and/or Material Deposits, Post-Run 85	86

II. TABLES

I.	Typical Matrix Reheat Schedule (Maximum Matrix Temperature = 4450°R)	88
II.	Run Summary for Initial Shakedown Runs and Heat Soak	90
III.	Run Summary for Runs 28 through 85	91

CONTENTS

		Page
	ABSTRACT	iii
	NOMENCLATURE	vii
I.	INTRODUCTION	1
II.	APPARATUS	
	2.1 General	2
	2.2 Hardware and Mechanical Systems	2
	2.2.1 Vessel Shell	2
	2.2.2 Insulation Bricks	3
	2.2.3 Cored Brick Matrix	3
	2.2.4 Burner System	3
	2.2.5 Exit Air Restrictor	4
	2.3 Consumables	4
	2.4 Instrumentation	4
	2.5 Recording Systems	4
III.	PROCEDURES	
	3.1 Heater Reheat	4
	3.2 Heater Blowdown	5
	3.3 Heater Cooldown	6
IV.	RESULTS AND DISCUSSION	
	4.1 General	6
	4.2 Shakedown Runs 1 through 27	7
	4.3 Matrix Restabilization Heat Soak	8
	4.4 Blowdown Runs 28 through 37	8
	4.5 Burner Test 38	9
	4.6 Blowdown Runs 39 through 44	9
	4.7 Blowdown Runs 45 through 69	10
	4.8 Blowdown Runs 70 through 85	11
	4.9 Post-Run 85 Inspection	11
	4.9.1 Removal and Analysis of the Refractories	11
	4.9.2 High Density Zirconia Sample Bricks	12
	4.9.3 Low Density Zirconia Sample Bricks	13
	4.9.4 Original Matrix Bricks and Those Installed Pre-Heat Soak	13
	4.9.5 Alumina Matrix Bricks	14
	4.9.6 Insulation Refractories	14
	4.9.7 Heater Vessel	15
	4.10 General Observations	15
V.	CONCLUSIONS	17
	REFERENCES	19

Page

III. COMPARISON OF PREVIOUS SUBSCALE TESTS WITH PILOT HEATER SHAKEDOWN RUNS 96

IV. MATRIX RESTABILIZATION HEAT SOAK 98

V. OPERATING HISTORY OF THE FIRST GENERATION BURNER 102

VI. REACTANT FLOW ANOMALY 108

VII. ANALYTICAL STUDY OF REFRACTORIES FROM AEDC'S AIR STORAGE HEATER: POST MORTEM IN-SERVICE ANALYSES 109

NOMENCLATURE

Destabilization	The transformation of zirconia in the cubic crystalline phase to zirconia in the monoclinic crystalline phase
Equivalence ratio	$\frac{\text{(weight oxidizer per pound of fuel) STOICHIOMETRIC}}{\text{(weight oxidizer per pound of fuel) ACTUAL}}$
Inversion temperature zone	The temperature range at which the reversible monoclinic-tetragonal phase transformation occurs in zirconia
Oxygen enrichment	The number of moles of pure oxygen added as a reactant per mole of pure oxygen in standard air
Percent theoretical density	Percentage of the maximum (zero porosity) density obtainable with a pure material (for example, 80% theoretical density = 20% porosity)
Second phase monoclinic zirconia	Zirconia in the undesirable monoclinic crystalline phase randomly distributed throughout the as-fabricated 9-1/4 w/o yttria matrix bricks originally in the pilot heater
w/o	Weight percentage

SECTION I
INTRODUCTION

For many years, alumina and magnesia ceramic stored energy heaters have been used by industry to produce temperatures simulating supersonic flight conditions. Alumina is relatively economical and has been the most commonly used matrix ceramic in stored energy heaters; however, it has a maximum temperature capability in stored energy heaters of only 3500°R.

Stored energy heaters were not seriously considered for use in supplying conditions for testing in the hypersonic flight regime until about 1954. At that time, ceramic research revealed that zirconia could be utilized to store energy at temperatures up to about 4600°R which was about 1100 deg above the useful range of alumina or magnesia. Therefore, NASA and the Air Force began investigating concepts of stored energy heaters capable of simultaneously producing temperatures and pressures simulating flight conditions up to about Mach 8.

Although zirconia has not been used as a matrix element as widely as alumina, its higher operating temperature capability has made it attractive for use in stored energy heaters. However, its success as a matrix element has been impaired by its tendency to fail because of destabilization wherein the zirconia is reduced to an unacceptable crystalline phase (monoclinic) which causes degradation of the zirconia microstructure.

Zirconia is a polymorphic material for which the crystalline form is altered with temperature. Zirconia can exist in three phases: monoclinic, tetragonal, and cubic. The tetragonal and cubic phases have nearly the same density; whereas, the density of the monoclinic phase is approximately 7 percent less than that of the tetragonal phase. Since a volume change accompanies this change in density, extremely large stresses occur on the microscale which can result in the complete fragmentation of the material.

Zirconia may be produced as a useful stored energy heater matrix element by the addition of other oxides, known as stabilizers, which transform the zirconia into the cubic phase when taken into solid solution at high temperatures and eliminate the phase transformation. Common stabilizing materials are calcia, magnesia, yttria, and yttria/rare earth mixtures.

Considerable research has been devoted to the study of these various stabilizers for zirconia. Tests revealed that calcia stabilized zirconia could withstand temperatures up to 4000°R; however, it could not withstand the combustion environment for long times above this temperature. Magnesia was unacceptable as a stabilizer since it diffused out of the material at temperatures as low as 3400°R. Tests with yttria stabilized zirconia revealed that the fully stabilized material with sufficiently low monoclinic content could be successfully operated at temperatures up to 4600°R.

Since 1963, a program has been in progress at the Arnold Engineering Development Center in support of the development of zirconia matrix bricks suitable for use as the matrix core for high enthalpy, high pressure, intermittent airflow, stored energy heaters.

A pilot stored energy heater (PTU) was subsequently designed and fabricated which would (1) provide the means for testing state-of-the-art heater ceramics, (2) enable the gaining of operational experience and techniques with ceramic stored energy heaters, and (3) provide a future small-scale ceramic stored energy heater test facility with a capability for user testing.

The experience and knowledge gained thus far in the operation of the PTU and that to be gained in the future will prove invaluable in the operation of a full-scale free-jet test facility (APTU), which employs a large ceramic (alumina pebble) stored energy heater.

The AEDC pilot heater was designed so that its length corresponds to that of a full-scale stored energy heater. This permits duplicating longitudinal temperature profiles and approximating the mechanical and thermal stresses within the ceramic matrix which would be produced in a large heater.

Extensive testing of yttria/rare earth stabilized zirconia matrix bricks has been accomplished in the Pilot Test Unit since early 1969. Since the initiation of this research program at AEDC, considerable knowledge has been gained with regard to the behavior of yttria/rare earch stabilized zirconia as a cored matrix material, and to the proper techniques for operation of a stored energy heater test unit. The following is a comprehensive review of ceramic brick testing in the Pilot Test Unit at AEDC.

SECTION II
APPARATUS

2.1 GENERAL

The Pilot Test Unit (PTU) is a high pressure, high temperature, stored energy heater system capable of providing airflows to 10 lb/sec with stagnation pressures and temperatures to 2000 psi and 4450°R, respectively. This is accomplished by storing thermal energy in the cored medium of the heater during a reheat period and then transferring the energy to a high pressure air stream passing through the cored matrix during a blowdown period.

Figure 1 (Appendix I) illustrates the pilot heater installation. The heater consists of a vessel shell and a refractory assembly of insulation and cored bricks. Airflow through the heater is restricted by a nozzle (exit air restrictor) located in the exit flange. Heat-up of the refractories is accomplished by a burner assembly mounted in the top flange of the heater. Burner exhaust gases are passed through the brick matrix and are routed from the base of the heater to an atmospheric exhaust stack. (A portion of the burner exhaust gases bypasses the matrix and is discharged through the exit air restrictor.)

2.2 HARDWARE AND MECHANICAL SYSTEMS

2.2.1 Vessel Shell

The vessel shell is approximately 3 ft on the inside diameter by 21.5 ft long. Nominal shell thickness is 2.25 in. The vessel shell was designed for a working pressure and

temperature of 2000 psi and 1050°R, respectively. Outlets in the shell are located at the top for access to the refractories and for burner insertion, on the side for the air outlet and for five viewports (Fig. 1), and at the bottom for air inlet and exhaust of burner combustion products. The viewports allow viewing of the center of the refractories at the 9-, 11-, 13-, and 15-ft levels (measurement relative to the matrix support grate illustrated in Fig. 1). The vessel is enclosed within an aluminum shroud for forced-air cooling of the shell outside surface.

2.2.2 Insulation Bricks

Various types of insulating bricks fill the annular space between the brick matrix and the vessel shell. Figure 1 identifies the various types of insulation materials utilized and illustrates their location within the heater. The composition insulation is designed to limit vessel shell temperatures to 1050°R maximum.

2.2.3 Cored Brick Matrix

A matrix of hexagon-shaped alumina and zirconia bricks comprises the heat storage and transfer media of the heater. The diameter of the matrix is 14 in., and its length is 15 ft. Sections of the refractory configuration, showing both the brick matrix and the various insulating layers are presented in Fig. 2. The bricks in the lower 7.6 ft of the matrix are a high density alumina material. In the upper portion, the bricks are a higher density yttria/rare earth stabilized zirconia material (approximately 90 and 95 percent theoretical densities). Maximum working temperatures for the alumina and zirconia materials are approximately 3500 and 4600°R, respectively. The matrix bricks are supported off the base of the vessel by a grate assembly. The hexagon-shaped bricks are 2.78 in. across the flats and have a porosity of 0.4. Brick lengths range from 0.5 to approximately 11 in., and the diameter of the holes is about 0.194 in.

2.2.4 Burner System

The burner is utilized for generating thermal energy for heating the brick matrix and is flange mounted through the top of the heater. The burner is a pre-mix type in which fuel and oxidant are pre-mixed in a common cavity and then ignited in the combustion chamber. The fuel is gaseous propane; the oxidant is air, enriched with gaseous oxygen as required to obtain the desired adiabatic flame temperature and to maintain nonreducing combustion products. (Nonreducing combustion products are required to prevent deterioration of the heater refractories.) The burner was designed to remain in-place during heater blowdown.

2.2.5 Exit Air Restrictor

Airflow through the heater is restricted by a restrictor nozzle in the heater air exit flange. A sketch of the restrictor is presented in Fig. 1. The nozzle insert material is Inconel X. The restrictor maximum operating temperature is 1950°R. Restrictor cooling is accomplished by injecting film air into the convergent section of the restrictor liner at a rate typically of 40 to 50 percent of the hot gas flow during heater blowdown.

The back side of the nozzle insert divergent section is cooled during heater reheat and blowdown by passing water through a single-pass, cylindrically wound cooling coil.

2.3 CONSUMABLES

High pressure air (supplied at 2000 psi), low pressure air (supplied at 7 psig), and gaseous oxygen, propane, and nitrogen are provided for burner operation, cooling purges, film cooling, valve control, and emergency cooling. Demineralized and raw water systems are utilized for cooling of the exit air restrictor, exhaust duct, and burner components.

2.4 INSTRUMENTATION

Heater instrumentation consists of thermocouples, optical pyrometers, and pressure sensors. The temperature sensors used to monitor and control the temperature gradients through the heater are the primary heater instrumentation. Figure 3 depicts the location of the thermocouples initially within the heater. (A portion of the thermocouples was destroyed during the matrix restabilization heat soak.) Optical pyrometer measurements are made through the vessel viewports. Heater vessel pressure taps are located on the high pressure air inlet and outlet to record air inlet pressure and differential pressure across the heater.

2.5 RECORDING SYSTEMS

Three types of systems are utilized for recording temperatures, pressures, and flow rates during pilot heater operation. Various matrix, insulation, grate, restrictor, and vessel shell temperatures are recorded on multipoint, null balance, potentiometer-type strip charts during heater reheat, blowdown, and cooldown. All additional temperature and pressure parameters displayed on meters are recorded on film during heater blowdowns. A selected group of these parameters is periodically recorded manually during reheat and cooldown. Thirty-four selected parameters are additionally recorded during heater blowdowns on a digital data system at a rate of ten samples per second.

SECTION III
PROCEDURES

Operation of the pilot heater throughout a series of blowdown runs is grouped into three categories: (1) heater reheat, (2) heater blowdown, and (3) heater cooldown.

3.1 HEATER REHEAT

Reheat involves conditioning the cored matrix from room temperature (or any matrix temperature profile cooler than desired for heater blowdown) to a predetermined longitudinal temperature profile. Reheat is accomplished in two phases.

The first phase is normal reheat and involves heating the matrix until an approximately uniform temperature gradient exists from the bottom to top of the matrix with the top of bed temperature approximately equal to the desired value at blowdown. Normal reheat conforms to a schedule of reactant mixtures and mass flow rates which will increase the

matrix temperature profile in a manner that avoids excessive thermal gradients and thermal shock in the brick matrix. Approximately 70 hr are required for normal reheat from room temperature to maximum temperature.

The second phase of reheat is referred to as fast reheat. This mode of operation is accomplished at an increased burner reactant flow rate for the purpose of producing a near-constant temperature in the upper portion of the matrix. This portion of the temperature profile is known as the "plateau" and encompasses approximately the upper 25 percent of the matrix. During fast reheat, additional energy is stored in the matrix with little or no increase in the top of bed temperature. Fast reheat typically requires approximately three hours of heater operation. When the desired temperature profile is established, the burner is extinguished, and preparations are made for heater blowdown.

During reheat of the pilot heater, adjustments are made to the reactant flow rates in accordance with a predetermined reheat schedule. A typical reheat schedule is presented in Table I (Appendix II) which depicts burner reactant flow rate adjustments required for matrix reheat from room temperature to a top of bed temperature of 4450°R. Of all the 20 step changes shown in the table, only the last two (Steps No. 19 and 20) are held sufficiently long for the top of bed temperature to stabilize. These two settings represent (1) the last setting before initiating fast reheat and (2) the fast reheat setting.

Since many reheats have been conducted with the pilot heater, a relationship has been defined between the burner adiabatic flame temperature, steady-state top of bed temperature, and fuel/oxidizer ratio for a variety of mass flow rates passing through the matrix. This relationship is presented graphically in Fig. 4 for mass flows ranging from 80 to 142 lb/hr and for flows ranging from 450 to 500 lb/hr. The lower range of mass flows corresponds to the last reactant flow setting before fast reheat, and the higher range of flows corresponds to fast reheat. These curves have proved valuable when performing adjustments during reheat to the steady-state top of bed temperature.

3.2 HEATER BLOWDOWN

Immediately after the burner is extinguished, the main valve in the atmospheric exhaust pipe leading from the bottom of the heater is closed. Next the high pressure air system is pressurized, and the film cooling and restrictor flows are switched from the low pressure system to the high pressure system. Film cooling flow is then introduced into the restrictor. Blowdown airflow is initiated from the control room by manually opening a pneumatically controlled high pressure valve. The rate of pressure buildup in the heater and the maintenance of the desired steady-state test pressure are manually controlled from the control room by adjustments to the low pressure pneumatic pilot valve which in turn controls the position of the main high pressure air inlet valve. Heater blowdowns are terminated when the zirconia/alumina interface temperature reaches a predetermined value which, for all runs following run 27, was well above the zirconia monoclinic-tetragonal inversion temperature zone. After blowdown, the heater is isolated from the high pressure air, and either the burner is refired or the heater is allowed to cool.

Maximum mass flow through the pilot heater during blowdown is limited by matrix brick thermal stress. To avoid exceedingly high thermal stresses during blowdown, the maximum allowable heater mass flow is limited, with a safety factor of two, to a value below that at which cracking of the matrix bricks is initiated. This value is determined from Ref. 1 (Eq. 8).

Bed floatation, which is of primary concern with ceramic heaters, is not a problem at the present time in the pilot heater because the exit air restrictor is too small to pass the required mass flow for matrix floatation without exceeding the heater vessel pressure limit.

3.3 HEATER COOLDOWN

After the last heater blowdown in a run series, the heater is permitted to slowly cool to room temperature without addition of air to expedite the cooling process. Cooldown typically requires approximately one week.

SECTION IV
RESULTS AND DISCUSSION

4.1 GENERAL

Operation of the PTU has consisted of 84 heater blowdown runs, one matrix restabilization heat soak, and one burner test without heater blowdown. Chronologically, the test program and major events and anomalies during the program occurred as follows:

A. Heater blowdown runs 1 through 12
B. Minor matrix inspection
C. Blowdown runs 13 through 27
D. Matrix inspection and discovery that zirconia matrix was destabilized
E. Heat soak for restabilization of zirconia matrix
F. Blowdown runs 28 through 32
G. Burner reactant flow anomaly before run 28 resulting in cracking and fracturing of matrix bricks placed in the heater after run 27 and the heat soak
H. Blowdown runs 33 through 37
I. Burner test 38 conducted to determine the cause of burner deterioration
J. Blowdown runs 39 through 44
K. First major matrix inspection and replacement of matrix top foot with new bricks
L. Runs 45 through 69
M. Second major matrix inspection following discovery of a burner water leak
N. Blowdown runs 70 through 85
O. Third major matrix inspection

The events as outlined above are briefly discussed throughout the following sections.

All zirconia matrix bricks tested to-date in the pilot heater have been stabilized with an yttria/rare earth mixture. However, throughout the remainder of this report these bricks will be referred to as "yttria stabilized zirconia", "yttria-zirconia" or "zirconia" for brevity.

Presented in Tables II and III are run summaries containing pertinent statistics including run dates, operating conditions, run times, matrix configurations, remarks, and results of the various heater inspections with the exception of the final inspection after run 85. Results of this inspection are discussed in Sections 4.9 and 4.10. Presented in Fig. 5 are schematic representations of the temperatures through which the matrix was cycled during the test program. Typical heater operating pressure histories for various levels of operating pressure are presented in Fig. 6.

4.2 SHAKEDOWN RUNS 1 THROUGH 27

The objectives of the shakedown runs were to (1) test and evaluate the behavior of the refractory materials within the heater, in particular the upper half of the brick matrix composed of 9.25 w/o yttria/zirconia (95 percent theoretical density) initially containing from 3 to 5 percent monoclinic second phase overall and (2) evaluate the performance of the complete system in support of the design for large, high performance, stored energy heaters.

The zirconia matrix for the shakedown runs was composed of bricks with lengths varying from 4.5 to 11 in. Atop each of the matrix columns were three buffer bricks approximately 1 in. long.

After run 12, the matrix top surface buffer bricks were noted to contain cracks and fractures. However, serious matrix deterioration was not suspected.

After run 27, additional cracking and fracturing of the matrix was noted. Subsequently, several matrix bricks near the top surface were analyzed and found to be destabilized.

Causes of the zirconia matrix destabilization were not immediately apparent since previous subscale tests performed by others had indicated that the pilot heater zirconia matrix would withstand test conditions throughout the range encountered during the shakedown runs. (A discussion of the subscale tests and a comparison of the tests with the pilot heater shakedown runs are presented in Appendix III.) However, the cause of destabilization was accredited to the presence of 3 to 5 weight percent second-phase monoclinic zirconia randomly distributed throughout the as-fabricated bricks. The kinetics for the destabilization apparently resulted from a combination of thermal stress cycling, water vapor from the combustion products, and monoclinic/tetragonal stresses realized in the zirconia bricks as a result of force cooling the zirconia matrix (four times) through the inversion zone during the shakedown runs. After run 27, the decision was made to avoid force cooling the zirconia matrix below 1950°R on future runs.

4.3 MATRIX RESTABILIZATION HEAT SOAK

After discovery of the zirconia matrix destabilization, it was determined by others[1] that the matrix brick microcracks could be resintered and the matrix restabilized by subjecting the matrix to a high temperature heat soak. (Details related to the heat soak are presented in Appendix IV.)

Prior to the heat soak, additional yttria stabilized zirconia bricks were placed in the matrix (as shown schematically in Fig. 7) to replace those which had been removed for inspection and analysis. These bricks were manufactured by Coors to approximately 95-percent theoretical density. A portion of the bricks contained 9.25 w/o yttria/rare earth stabilizer and the remainder contained 10.4 w/o stabilizer.

The heat soak consisted of generating a matrix centerline temperature profile consisting of approximately 4550°R at the matrix top and 3450°R at the zirconia/alumina interface. These conditions were held constant for 94 hr, followed by heater cooldown without passing air through the matrix.

After the heat soak, selected bricks were analyzed from the matrix top along with various small matrix brick samples which had been placed in the matrix before the test by way of the view port holes. Analysis of the various bricks and small samples revealed that the heat soak successfully lowered the monoclinic content of the zirconia matrix bricks and changed those bricks inspected from weak, friable, and chalky white to strong, hard, and grayish in color.

Inspection of the burner revealed severe erosion of the combustion chamber. Details of this inspection and other burner inspections during the test program are provided in Appendix V.

Visual inspection of the heater combustion chamber bricks and arch bricks adjacent to the dome skew bricks (see Fig. 8) revealed fracturing, spalling, and crumbling in these areas. However, replacement of the refractories was not deemed necessary.

4.4 BLOWDOWN RUNS 28 THROUGH 37

The objectives of these runs were to (1) determine the permanence of stability and evaluate the structural integrity of the restabilized, resintered zirconia cored bricks and (2) evaluate the integrity of sample[2] cored bricks manufactured by Coors with yttria contents of 10.9, 12.6, and 13.8 w/o when subjected to thermal cycling conditions.

---

[1]Major participants in this effort were Dr. Robert Ruh, Air Force Materials Laboratory and Dr. J. D. Plunkett, Materials Consultants, Inc.

[2]These matrix bricks were the first of the "sample bricks" referred to throughout this report. All new matrix bricks added to the matrix beginning prior to run 28 are referred to as sample bricks. These bricks were manufactured by both Coors Porcelain Company and Zirconium Corporation of America (Zircoa) and varied in overall dimensions, yttria content, and density.

In support of the second objective, six new zirconia bricks (manufactured by Coors) were added to the matrix. These bricks possessed about 90-percent theoretical density. The locations of the bricks in the matrix are presented schematically in Fig. 9. These sample matrix bricks were to contain 12, 14, and 16 w/o yttria; however, analysis of the bricks by others after kiln firing revealed that the yttria contents were 10.9, 12.6, and 13.8 w/o, respectively.

During fast reheat for run 28, an irregularity occurred in the reactant flow to the burner resulting in a drop in the top of bed temperature from 3220 to 2400°R. A detailed discussion of the anomaly is presented in Appendix VI.

Inspection of the matrix revealed that excessive fracturing and cracking had occurred as a result of the reactant flow anomaly. Of particular note was the tendency of relatively long bricks to fracture into shorter segments. All matrix bricks inspected including the original cored bricks were hard indicating no destabilization. Pertinent photographs taken during the inspection are presented in Fig. 10.

Prior to run 33, additional sample bricks with 10.9, 12.6, and 13.8 w/o yttria were added to the matrix to replace the broken ones and to level the bed at a nominal height of approximately 15 ft (measured relative to the grate). The orientation of these bricks in the matrix is presented in Fig. 11.

Inspections after run 37 revealed (1) that the sample matrix bricks installed before run 33 were in good condition with some hairline cracking and (2) that heater combustion chamber insulation refractories exhibited further degradation. Pertinent photographs taken during the inspection are presented in Figs. 12 and 13.

New combustion chamber refractories were installed prior to test 38. Also, two new bricks were added to the matrix as depicted in Fig. 14.

4.5 BURNER TEST 38

Burner test 38 was conducted, without heater blowdown, to positively identify either galvanic corrosion or nitric acid erosion (resulting from the formation of nitric acid from burner products of combustion) as the main cause of burner damage as incurred during the heat soak and during runs 33 through 37.

Posttest 38 inspections revealed (1) that nitric acid erosion was the prime factor causing burner deterioration and (2) that selected matrix bricks inspected were in good condition with only a few additional hairline cracks. Pertinent photographs taken during the inspections are presented in Fig. 15. The bricks depicted in Figs. 15a and b were also photographed after run. 37 (see Fig. 12) so that the effects of testing could be documented in typical matrix bricks.

4.6 BLOWDOWN RUNS 39 THROUGH 44

The primary objective of these runs was the continued evaluation of the cored matrix integrity when subjected to thermal cycling conditions.

Run 39 was unsuccessful because of a leaking high pressure air control valve. The remaining runs which had been scheduled for the test period were subsequently cancelled.

Inspection of selected matrix bricks revealed them to be in good condition and practically unchanged since inspected after test 38. Pertinent photographs taken during the inspection are presented in Fig. 16. The matrix bricks presented in Fig. 16 were also photographed after test 38 (Fig. 15).

After runs 40 through 44, the top foot of the cored matrix was removed for the first major inspection. Laboratory analysis of selected bricks did not indicate destabilization. Pertinent photographs taken during the inspection are presented in Fig. 17. By referring to Fig. 14, all bricks shown in Fig. 17 can be identified as to location and number of runs that they remained in the matrix.

Prior to run 45, new Coors and Zircoa sample bricks were installed in the matrix to replace those which had been removed. The replacement matrix bricks are shown schematically in Fig. 18. Details concerning the new bricks are listed in Table III.

4.7 BLOWDOWN RUNS 45 THROUGH 69

The primary objectives of these runs were to (1) comparatively evaluate the integrity of the high density, high yttria content Coors and Zircoa sample bricks, (2) evaluate the feasibility of using low density matrix bricks in regions of large temperature gradients, and (3) continue evaluation of the restabilized, resintered original cored matrix and the 9.25 and 10.4 w/o yttria bricks installed before the heat soak with regard to permanence of stability and structural integrity.

The second major inspection of the matrix refractories was conducted after run 69. Inspections revealed that a water leak had developed at the burner tube tip exterior; therefore, a complete examination was made of all sample matrix bricks placed into the heater before run 45. All high density sample bricks were found to contain hairline cracks. Coors high-density sample bricks in one column beneath the burner were all fractured into small pieces as a result of the water leak. All sample bricks remained stabilized throughout the test series. However, in general, the high density bricks appeared to be more susceptible to vertical fracture with increasing yttria content.

Presented in Fig. 19 are photographs typical of the various high density bricks removed from the heater for inspection. It may be noted that practically all cracks are in the vertical (longitudinal) direction.

The exact location of the sample bricks presented in Fig. 19 may be determined by their respective brick number. For example in Fig. 19a, brick "16-7" was located in column 16, seventh from the top.

With a few exceptions, the matrix bricks removed for inspection were returned to the matrix prior to run 70. Replacement details are presented in Table III and the location in the matrix of the various replacement bricks is shown schematically in Fig. 20.

The new stainless steel burner (depicted in Fig. 21) was installed in the heater prior to run 70. Also installed were new combustion chamber bricks to accompany the new burner.

4.8 BLOWDOWN RUNS 70 THROUGH 85

The primary objectives of these runs were to (1) continue evaluation of the Coors and Zircoa high density sample bricks and the Zircoa low density sample bricks, (2) evaluate the performance and integrity of the second generation burner, and (3) continue evaluation of the restabilized, resintered original cored matrix and the 9.25 and 10.4 w/o yttria bricks installed before the heat soak with regard to permanence of stability and structural integrity.

Inspections after run 74 revealed the sample bricks to be in very good condition with some hairline cracks and the new burner to be in excellent condition. Matrix bricks replaced before run 75 are shown schematically in Fig. 22.

After run 85, the third major heater inspection was accomplished. Approximately one-half of the ceramics was removed from the heater. A detailed description of the inspection is presented in the following paragraphs.

4.9 POST-RUN 85 INSPECTION

4.9.1 Removal and Analysis of the Refractories

Access to the heater refractories was provided by removal of the top heater flange. All combustion chamber and heater dome refractories were then removed down to the steel shelf which supports all refractories above the 15-1/2-ft heater level (measured relative to the grate). Below the support shelf, the matrix bricks and insulation bricks were removed one layer at a time. Refractories located below the shelf were composed of the cored brick matrix, the matrix liner bricks, and two layers of insulation bricks. The outer layer of insulating bricks was not removed below the support shelf with the exception of the first layer of bricks located directly under the shelf. Refractory removal was continued until all of the zirconia matrix and the top layer of the alumina matrix had been removed. Details concerning condition of the various types of heater refractories are presented in Sections 4.9.2 through 4.9.6.

Samples of various matrix, combustion chamber, bed liner, and 3250°R firebricks were subjected to analytical study by Major L. L. Fehrenbacher, at ARL/WPAFB. Results of the various analyses have been summarized in the report entitled, "Analytical Study of Zirconia Refractories from AEDC's Air Storage Heater: Post Mortem In-Service Analyses," by Major L. L. Fehrenbacher and D. F. Frank. The report has been included as Appendix VII of this report. However, it should be noted that included in the report are results of analyses performed on various additional samples not taken from the AEDC Pilot Test Unit. These samples are denoted by a double asterisk in the report.

Of primary interest is the fact that, with one exception, monoclinic phase was not detected throughout the zirconia matrix. (A small isolated area at the zirconia/alumina interface contained 5.83-percent monoclinic phase.)

4.9.2 High Density Zirconia Sample Bricks

Inspection of all high density sample bricks revealed them to be in good condition overall. A comparison was made between bricks from the two suppliers and between bricks of the several yttria contents by considering only those bricks which had remained in the matrix throughout runs 45 through 85. The only variable eliminated by this comparison is the number of runs experienced by the bricks; therefore, other variables such as brick position in the columns or column position in the matrix are not considered.

Inspection of the sample bricks which had remained in the heater since run 45 did not reveal any significant difference in integrity of bricks with regard to manufacturer. However, bricks of both manufacturers appeared to be more susceptible to vertical fracture with increasing yttria content.

Presented in Fig. 23 are representative photographs obtained after run 85 which depict typical crack and fracture patterns. These photographs are not intended to indicate statistics such as percentage of fractured or cracked bricks. Many of the bricks shown in Fig. 23 were also photographed during the post-run 69 inspection and were previously presented in Fig. 19. Therefore, any degradation of these bricks resulting from runs 70 through 85 may be noted. Listed in the following table are those bricks for which photographs after runs 69 and 85 are presented and the respective figure numbers.

Brick Number	Manufacturer and Yttria Percentage	Post-Run 85 Fig. 23	Post-Run 69 Fig. 19
16-7	Coors, 12.6	a	a
19-2	Coors, 13.8	b	b
19-5	Coors, 13.8	c	c
14-3	Zircoa, 10.8	d	d
17-4	Zircoa, 12.5	e	e
18-5	Zircoa, 16.5	f	f
18-7	Zircoa, 16.5	g	g

Brick 2-2 (Zircoa 12.5 w/o) was placed in the matrix before run 75 and is typical of approximately one dozen of the sample bricks which contained fractured corners. A photograph of brick 2-2 is presented in Fig. 23h.

Shown in Fig. 23i is a photograph of brick 1-8 (Zircoa, 16.5). This photograph is included because only a very few of the sample bricks exhibited this varied pattern of hairline cracks during the post-run 85 inspection. (A discussion of crack and fracture patterns is presented in Section 4.10).

The seven sample bricks in column three (Coors, 12-5) were placed in the matrix before run 75. However, in general, they were in poorer condition than bricks of the same composition in column 5 which had remained in the matrix since run 45.

4.9.3 Low-Density Zirconia Sample Bricks

Zircoa low-density sample bricks were located atop matrix columns 6 and 11 and a portion of columns 7 and 10. Previously tested high density 1/2-in. buffer bricks were utilized as a level base for the oversized bricks. This is illustrated schematically in Fig. 22. All of these bricks remained in the heater throughout runs 45 through 85.

The three 12.5 w/o low-density sample bricks were located atop columns 6 and 7 and consisted of two 4-1/2-in. bricks and one 1-1/2-in. brick. Photographs of bricks 6-2 and 6-3 are presented in Figs. 24a and b. Although the bricks contained no cracks or fractures, the bricks tended to distort (creep) at high temperature. This may be noted in Fig. 24b.

The four 14.5 w/o low-density sample bricks were located atop columns 10 and 11 and consisted of three 2-1/2-in. bricks and one 1-1/2-in. brick. Photographs of bricks 11-2 through 11-4 are presented in Figs. 24c through 24e. One small open crack was present in brick 11-1; however, the other three bricks contained no cracks or fractures. Photographs showing high temperature creep in brick 11-4 are presented in Figs. 24d and 24e. A slight creep was noted in brick 11-3 at the mating surface with brick 11-4; however, the deformation was too slight to be observed in a photograph.

4.9.4 Original Matrix Bricks and Those Installed Before Heat Soak

During removal of the bricks installed before the heat soak and the original zirconia matrix, it was discovered that the bricks which were located directly below the sample bricks at matrix heights ranging from approximately 13 to 14 ft exhibited areas of serious degradation. Although the bricks were in place in these areas prior to removal, a portion was reduced to small pieces when removal was attempted. Below this region, down to approximately the 10-ft bed level, the original matrix bricks were in better overall condition. All of these bricks contained cracks, and most contained fractures which lay in various planes. However, there was a definite trend in the fractures which tended to reduce the bricks to shorter lengths. Also, much fusion was present between bricks in the individual columns. That is, between a given brick and the brick located directly above or below it rather than between bricks located side-by-side.

Below approximately the 10-ft level, the bricks were once again seriously degraded. Most bricks located below the 10-ft level were removed in small pieces and large irregular blocks. However, as was noted previously, the brick pieces remained in place until removal was attempted. This may be verified in that no discernible increase in matrix pressure drop occurred throughout the PTU test program.

The condition of the matrix as described in the preceding paragraphs is evident in Fig. 25 which presents photographs of the overall zirconia matrix. (In Fig. 25b the top

course of alumina bricks is also shown in columns 6 and 10.) The deteriorated condition of the zirconia matrix is attributed to the earlier destabilization which occurred during the 27 heater shakedown runs.

Presented in Fig. 26 are three matrix bricks which were located directly below the sample bricks in their respective columns. The brick shown in Fig. 26a was located in matrix column 3 (the center column) and was placed in the matrix before the heat soak. Except for the sample bricks, the condition of this brick was better than any of the zirconia bricks. This is a Coors brick stabilized with 9.25 w/o yttria.

Shown in Fig. 26b is another Coors brick which was placed in the matrix before the heat soak. This brick is stabilized with 10.4 w/o yttria and was located directly below the sample bricks in matrix column 11.

Presented in Fig. 26c is a photograph of a 9.25 w/o original heater brick which was located in matrix column 6. This brick was situated at approximately the 13-ft bed level.

4.9.5 Alumina Matrix Bricks

The top course of alumina bricks at the zirconia/alumina interface was removed from the matrix. Brick length was approximately 11 in. A photograph of the alumina matrix at the interface is presented in Fig. 27a. Three of the alumina bricks had been removed from the matrix before the photograph was taken. During removal of the top course, seven bricks located centrally in the matrix were fused together and were removed as a unit. A photograph of these bricks is presented in Fig. 27b. It is evident in Figs. 27a and b that, at the interface, the centrally located bricks had become plastic and distorted as a result of high temperature. This distortion was only present at the top surface of the bricks. Presented in Figs. 27c through e are additional photographs of alumina bricks from the top course. These photographs are presented so that crack and fracture patterns in the alumina bricks may be observed.

With the exception of the first course of alumina matrix bricks, the remainder of the matrix appeared to be in excellent alignment and in good condition. However, the amount of cracks or fractures present in the matrix is unknown since the remainder of the alumina matrix was not removed for inspection.

A flood light was inserted into the bottom of the heater which permitted inspection of the matrix air passages when viewed from the top. Approximately one-tenth of the passages contained small pieces of bricks which had become lodged in the passages during removal of the zirconia matrix.

4.9.6 Insulation Refractories

Overall condition of the insulation refractories was very good. Specifically, replacement refractories are required for 23 percent of the hot face insulation above the heater shelf, 26 percent of the remaining (backup) insulation above the shelf, and 3 percent

of all insulation below the shelf with the exception of the outer layer of insulation. (The steel shelf supports the heater insulation refractories above the matrix.) Only the top row of outer insulation bricks, located directly below the heater shelf, requires replacement.

Presented in Fig. 28 are photographs of various heater insulation refractories taken during the removal process. The condition of typical dome hot face refractories is illustrated in Fig. 28a. The steel shelf may be noted in Fig. 28b along with the bed liner bricks and the first layer of insulation. The outer layer of insulation cannot be seen in this photograph because of the heater shelf. Presented in Figs. 28c through h are photographs of various heater insulation and liner bricks. Crack and fracture patterns shown in these bricks are typical for the various types of insulation refractories.

4.9.7 Heater Vessel

The interior surface of the heater vessel was inspected after removal of the heater ceramics and was found to be in excellent condition. The vessel wall was not inspected below the heater shelf with the exception of the area directly below the shelf for a distance of approximately 5 in. The top course of insulation bricks located directly below the shelf was removed and permitted this inspection. Dark discoloration was noted on the under surface of the shelf indicating that hot gases had been present in this region. However, the heater vessel remained in excellent condition in this region. The vessel interior surface paint had remained intact on practically all of the surface inspected.

4.10 GENERAL OBSERVATIONS

A comparison was made between the zirconia high density sample bricks which had remained in the matrix since run 45. These bricks may be identified from Figs. 18, 20, and 22, and they consisted of columns 5, 13, 14, 16, 17, 19, bricks 1-1 through 1-7 and bricks 18-2 through 18-10. The results of this comparison were similar to those obtained during the post-run 69 inspection in that bricks of both manufacturers appeared to be more susceptible to vertical fracture with increasing yttria content.

Throughout the pilot heater test program, fusion of the zirconia bricks has been noted. Occasionally, a small brick particle or chip was found fused inside a brick air passage, or a piece of one brick was sometimes found fused to the side of another brick, as illustrated in Fig. 23g. Also two or more bricks were sometimes found fused together. A sudden shock will usually separate the two. A typical example of this type of fusion is shown in Fig. 24d.

Occasionally stress marks will be discovered on the matrix bricks which are typical of those shown in Fig. 29. These horizontal indentations are caused by bricks becoming slightly misaligned as the matrix shifts with changing temperature. In cases of pronounced indentations such as these, the air passages in the brick adjacent to the surface and at the point of indentation remain slightly distorted, indicating that, because of elevated temperature, the brick was relatively soft at the time the indentation was made.

Most of the sample matrix bricks contain keys machined into the bricks to ensure alignment of the brick air passages. However, in some cases where the sample bricks were received from the manufacturer in longer lengths than desired, they were cut to the desired lengths before placement in the matrix. Therefore, some of these bricks contained no keys, and the possibility existed of these bricks becoming misaligned. An example of this misalignment is shown in Fig. 30. In this case, after the misalignment occurred, the bricks became fused together.

During the post run 69 and post run 85 sample brick inspections, it was noted that, although hairline cracks were present in some of the sample bricks at various odd angles, all fractures in the sample bricks were longitudinal. By far, the majority of the hairline cracks present in the sample bricks during the post run 85 inspection were also longitudinal. One of the very few exceptions is shown in Fig. 23g in which a horizontal hairline crack may be noted to extend around the center of the brick, tending to divide it into two 1-in. wafers.

Following the removal of the zirconia matrix and the top course of alumina matrix bricks, a type of crack-or-fracture-pattern was noted which was unlike those found in the sample bricks. With this type of cracking, an oval-shaped portion of a brick side appears to have partially collapsed toward the inside of the brick. However, some bricks appear just the opposite; that is, the outer brick surface appears to have expanded radially outward leaving the oval midsection. This crack pattern may be noted in both the alumina bricks and the original 9.25 w/o heater bricks as is depicted in Figs. 26c and 27c. This phenomenon is also present in Fig. 17g which shows an original heater brick removed from the matrix after run 44.

Presented in Fig. 31 are matrix bricks, photographed during the post run 85 inspection, upon which material has been deposited and/or removed. The composition of material in these areas was analyzed and found to vary only slightly from the remainder of the bricks. Bricks which possessed this appearance were as follows: brick numbers 10-1, 10-2, 10-3, 12-2, 12-3, 13-5, 13-6, and 16-5. All of these bricks were situated in matrix columns adjacent to the bed liner. Brick 10-1 (Fig. 31a) appears to have experienced localized melting, resulting in the removal of material from the brick. To a lesser extent, this may also be observed of brick 13-6 (Fig. 31b). Presented in Fig. 31c are bricks 10-2 and 10-3 which are fused together. Again a localized area of the brick appears to have melted. In addition, deposits of yttria/zirconia material are fused to the bricks.

Remarks presented in previous sections of this report concerning integrity of the low density Zircoa sample matrix bricks may lead one to the conclusion that this type of brick is vastly superior to the high density matrix brick. This conclusion would be erroneous based solely on the results of the matrix inspections discussed in this report. As noted from the various matrix inspections, the low density matrix bricks possess a greater resistance to cracking and fracturing than the high density bricks. However, the disadvantages of the low density brick have not been investigated in the pilot heater tests nor discussed in this report. Not the least of these disadvantages being the decreased heat storage ability of these bricks or the potential for increased "dusting" associated with the low density bricks. The zirconia dust, formed primarily from rubbing of one

brick against another, would be forced out of the heater at high velocity during heater blowdown and could produce a sand blast effect on a test article downstream of the heater air exit.

The decision of whether to utilize low or high density zirconia matrix bricks should be made only after carefully weighing all advantages and disadvantages of both types of bricks against the purposes for which the stored energy heater is being utilized.

To avoid excessively long starting transients in a stored energy heater facility, it is imperative that a fast-acting valve be incorporated into the system which controls heater exit air and permits pressurization of the heater vessel prior to the initiation of heater blowdown. The need for this type of valve is clearly evident in Fig. 6d wherein heater operating pressure is plotted as a function of run time for run 85. It may be noted that for a maximum matrix temperature of 4450°R approximately 50 sec of heater blowdown operation were required to pressurize the heater vessel to an operating pressure to 1850 psi. An operating pressure of 2000 psi had been planned for this run; however, the run was terminated after 52 sec to avoid force-cooling the zirconia/alumina interface below 1950°R.

SECTION V
CONCLUSIONS

An extensive test program was conducted from February 1969 until April 1971 with the Pilot Test Unit at AEDC to investigate the integrity of yttria/rare earth stabilized zirconia as a stored energy heater matrix element. The results of 84 heater blowdown runs at maximum heater operating conditions of 1850 psi and 4450°R are summarized as follows:

1. Refinements to the yttria/zirconia brick specifications which should permit the production of a satisfactory cored brick matrix have been determined from the PTU test program. These refinements are concerned with brick length, stabilizer content, and the absence of second-phase monoclinic zirconia in the as-fabricated bricks.

2. Destabilization of the zirconia matrix during the 27 shakedown runs is accredited to the presence of 3 to 5 weight percent second-phase monoclinic zirconia randomly distributed throughout the as-fabricated bricks. The kinetics for the destabilization apparently resulted from a combination of monoclinic/tetragonal stresses realized in the zirconia bricks as a result of force cooling the zirconia matrix through the inversion zone during the shakedown runs, thermal stress cycling, and water vapor from the combustion products.

3. The 4550°R heat soak successfully lowered the monoclinic content to an undetectable level and resintered the microcracks in the matrix bricks at the top of the matrix.

4. Inspection of samples throughout the complete zirconia matrix after run 85 revealed no detectable monoclinic content with the exception of one small isolated area at the zirconia/alumina interface. A sample from this area possessed 5.83-percent monoclinic phase.

5. Extreme stresses experienced by the zirconia matrix due to force cooling the matrix through the inversion zone during the shakedown runs led to the decision that, on future blowdown runs, the zirconia matrix would not be force cooled below 1950°R. This criterion proved satisfactory with regard to preventing adverse conditions which could contribute toward the destabilization process.

6. Early in the test program it was determined that—especially near the matrix top—the lengths of the original matrix bricks (with L/D up to four) were unsatisfactory. Shorter sample bricks (with L/D of one or less) proved entirely satisfactory.

7. Severe temperature changes such as those experienced by the zirconia matrix as a result of the reactant flow anomaly and the burner cooling water leak cannot be tolerated in stored energy heaters without imparting serious damage to the matrix refractories.

8. Vertical fractures in the high-density sample matrix bricks appeared more numerous in bricks containing the highest percentages of stabilizer.

9. The importance of proper keying of the matrix bricks to maintain alignment of air passages was demonstrated by noting the misalignment which occurred in nonkeyed bricks.

10. Low-density zirconia sample bricks performed exceptionally well with much less tendency toward cracking than the high-density bricks. However, the low-density bricks proved readily susceptible to high temperature creep.

11. Performance of the alumina matrix bricks was very good throughout the test program with only the top layer of bricks requiring replacement.

12. Overall performance of the insulation refractories was very good with only about 25 percent of those located above the matrix requiring replacement and less than 3 percent of the remainder requiring replacement after completion of the 85-run test program.

13. The original burner which utilized an integral combustion chamber was unsuccessful because it was incompatible with nitric acid, formed as a product of combustion. However, the second generation burner fabricated of stainless steel and utilizing a ceramic combustion chamber proved entirely satisfactory.

REFERENCES

1. DeCoursin, D. G., Hagford, D. E., Arnold, G. M., and Male, D. W. "Recent Development of Storage Heaters to Provide Flight Simulation for Airbreathing Propulsion Systems." AIAA Third Propulsion Joint Specialist Conference, Washington, D. C., 1967.

2. DeCoursin, D. G. and Hagford, D. E. "Yttria-Zirconia Destabilization in the Tripltee Pilot Heater–Preliminary Review." Prepared under Air Force Contracts AF40 (600)-1094 and AF40600-68-(0002) by FluiDyne Engineering Corporation, July 1969.

APPENDIXES

I. ILLUSTRATIONS
II. TABLES
III. COMPARISON OF PREVIOUS SUBSCALE TESTS TO PILOT HEATER SHAKEDOWN
IV. MATRIX RESTABILIZATION HEAT SOAK
V. OPERATING HISTORY OF THE FIRST GENERATION BURNER
VI. REACTANT FLOW ANOMALY
VII. ANALYTICAL STUDY OF REFRACTORIES FROM AEDC'S AIR STROAGE HEATER: POST MORTEM IN-SERVICE ANALYSES

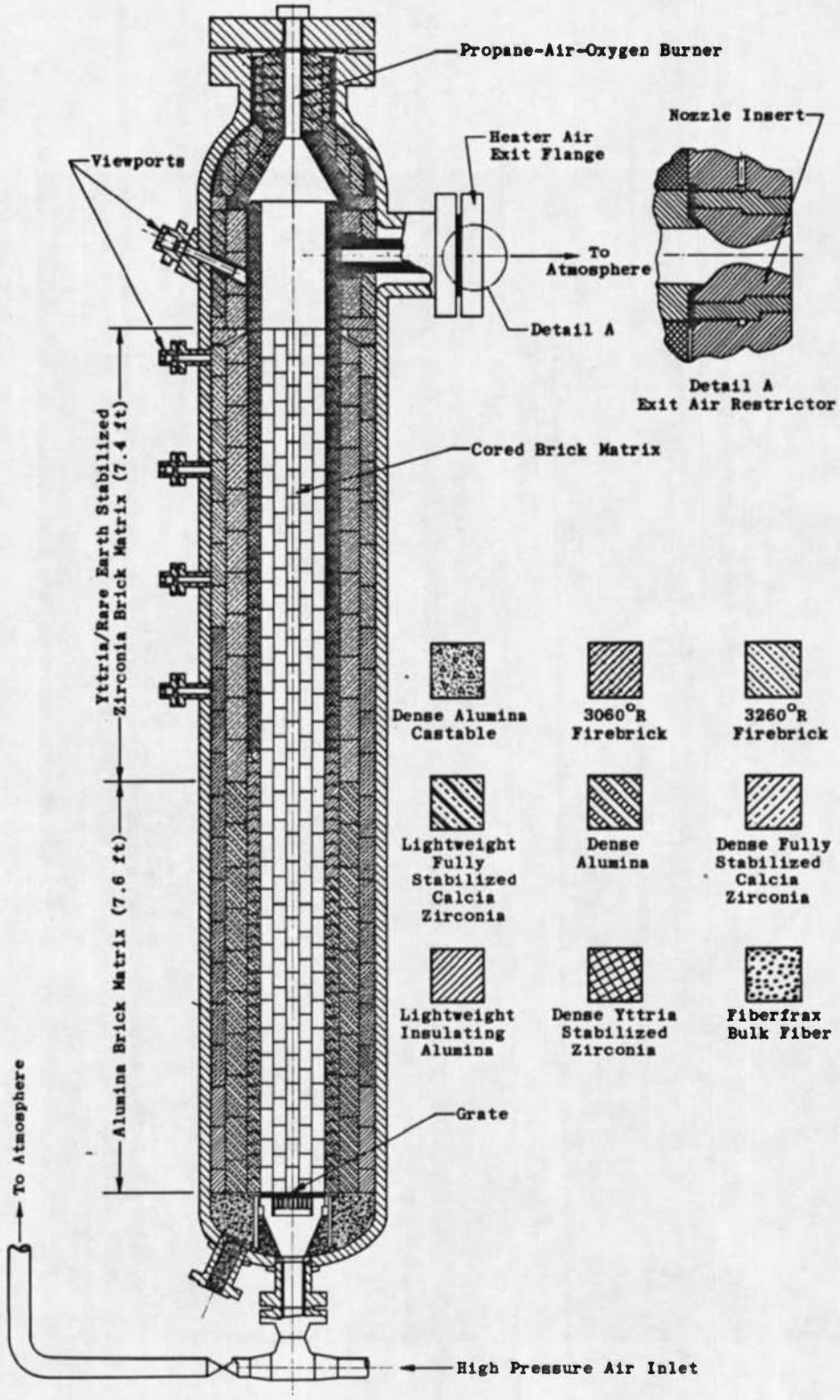

Fig. 1 Pilot Heater Schematic

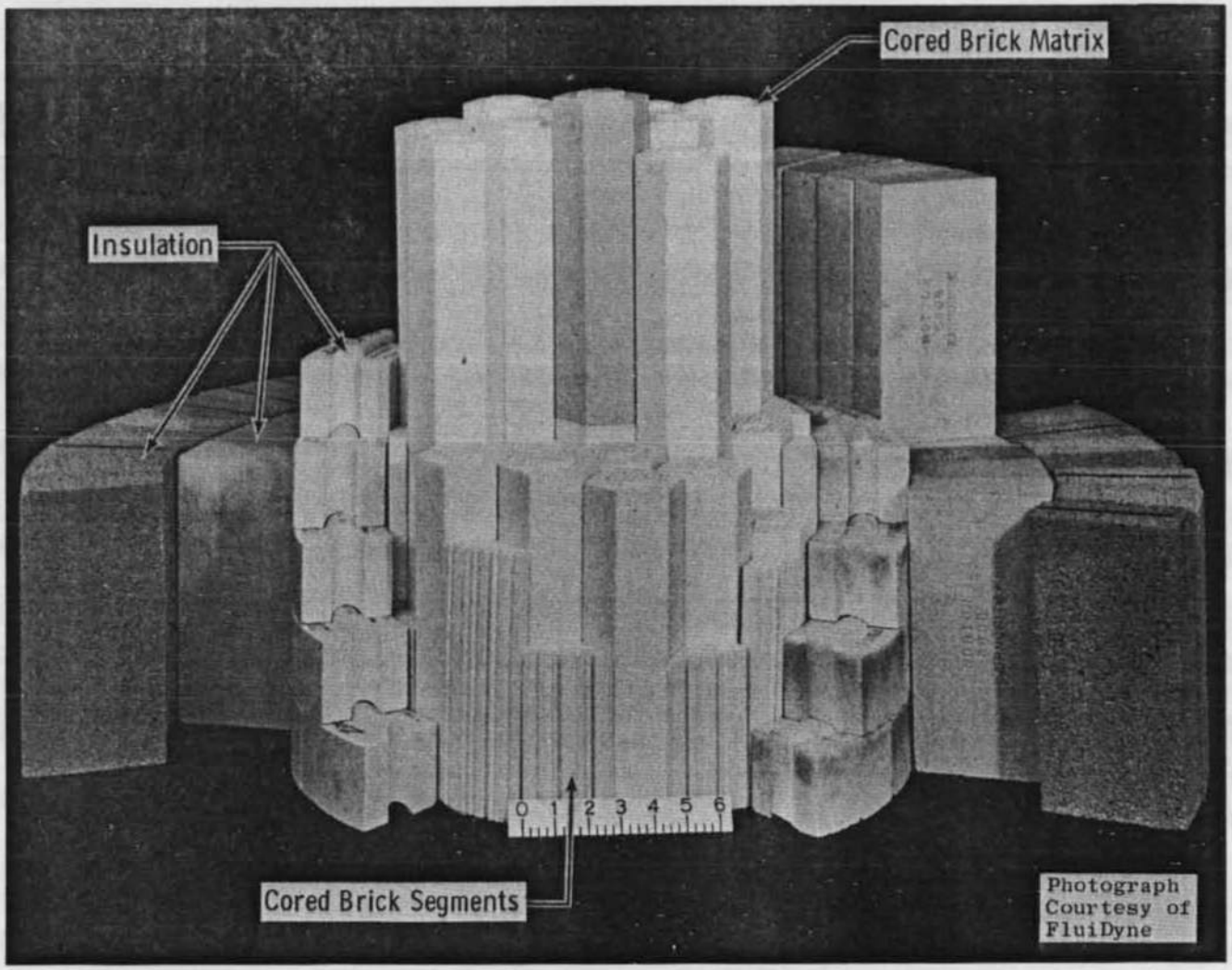

a. Typical Refractory Layout
Fig. 2 Pilot Heater Refractory Configuration

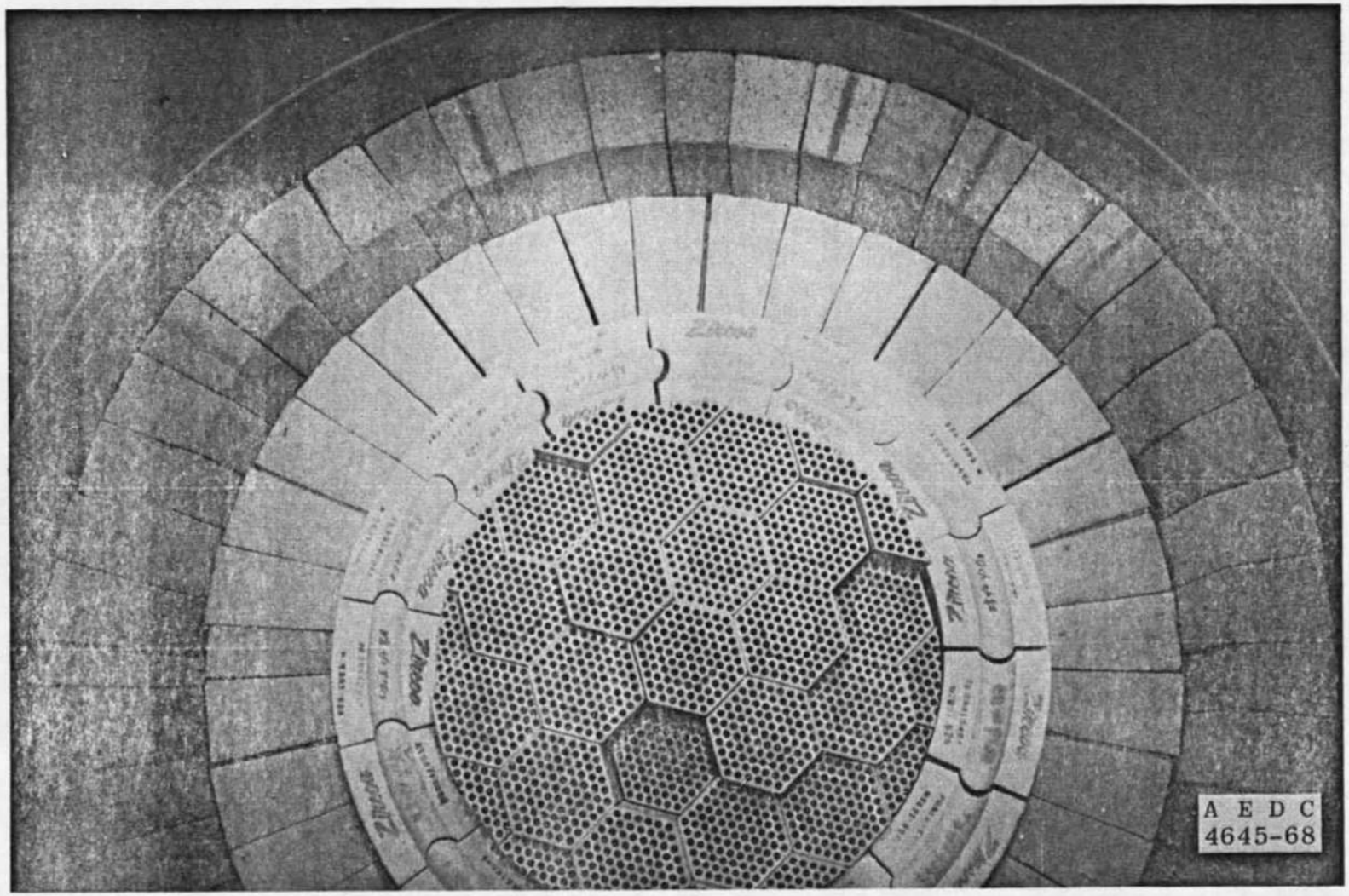

b. 10.5-ft Matrix Level Photographed during Original Installation
Fig. 2 Concluded

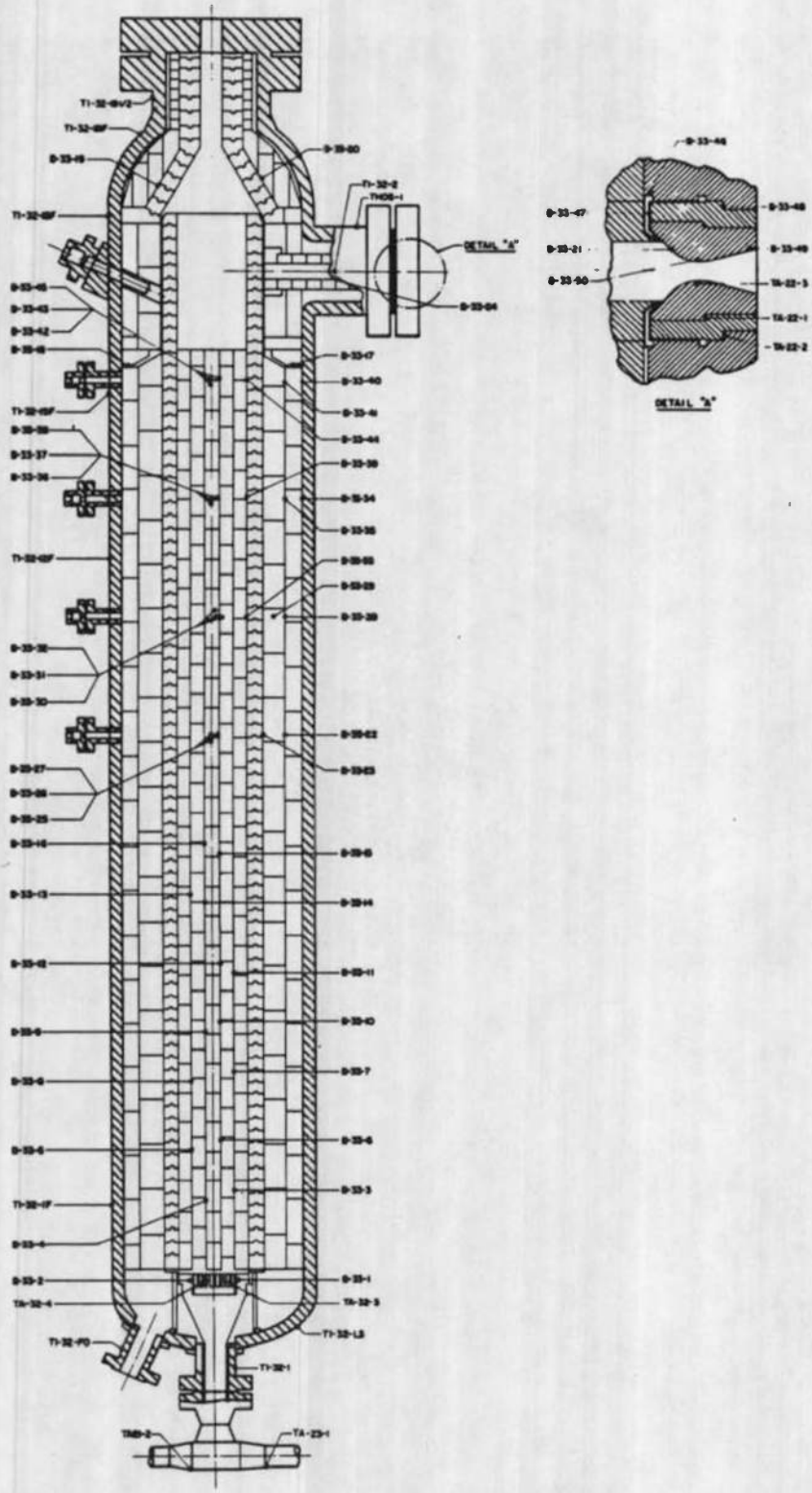

Fig. 3 Pilot Heater Thermocouple Locations

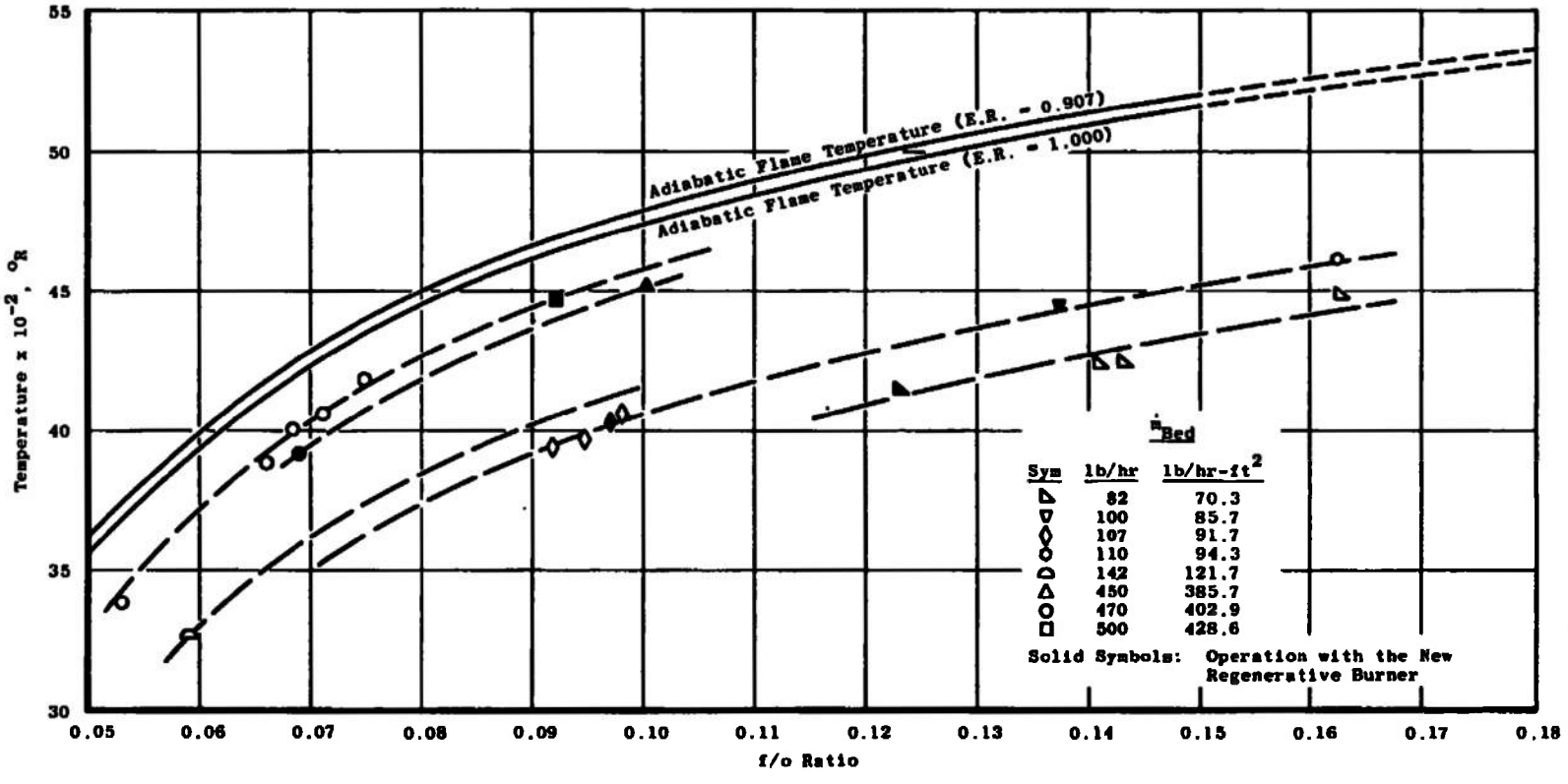

Fig. 4 Maximum Matrix Temperature Determination

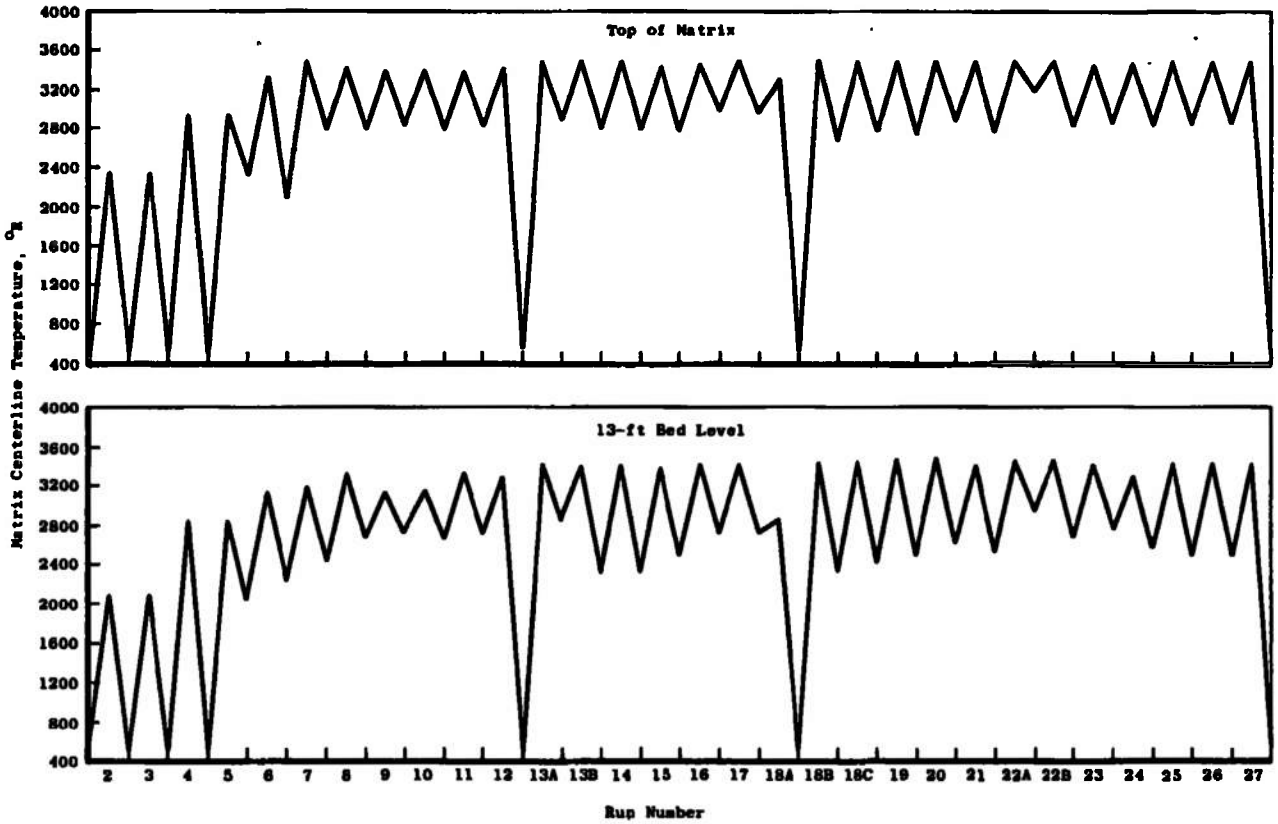

a. Runs 1 through 27

Fig. 5 Matrix Centerline Temperature Cycling, Runs 1 through 85

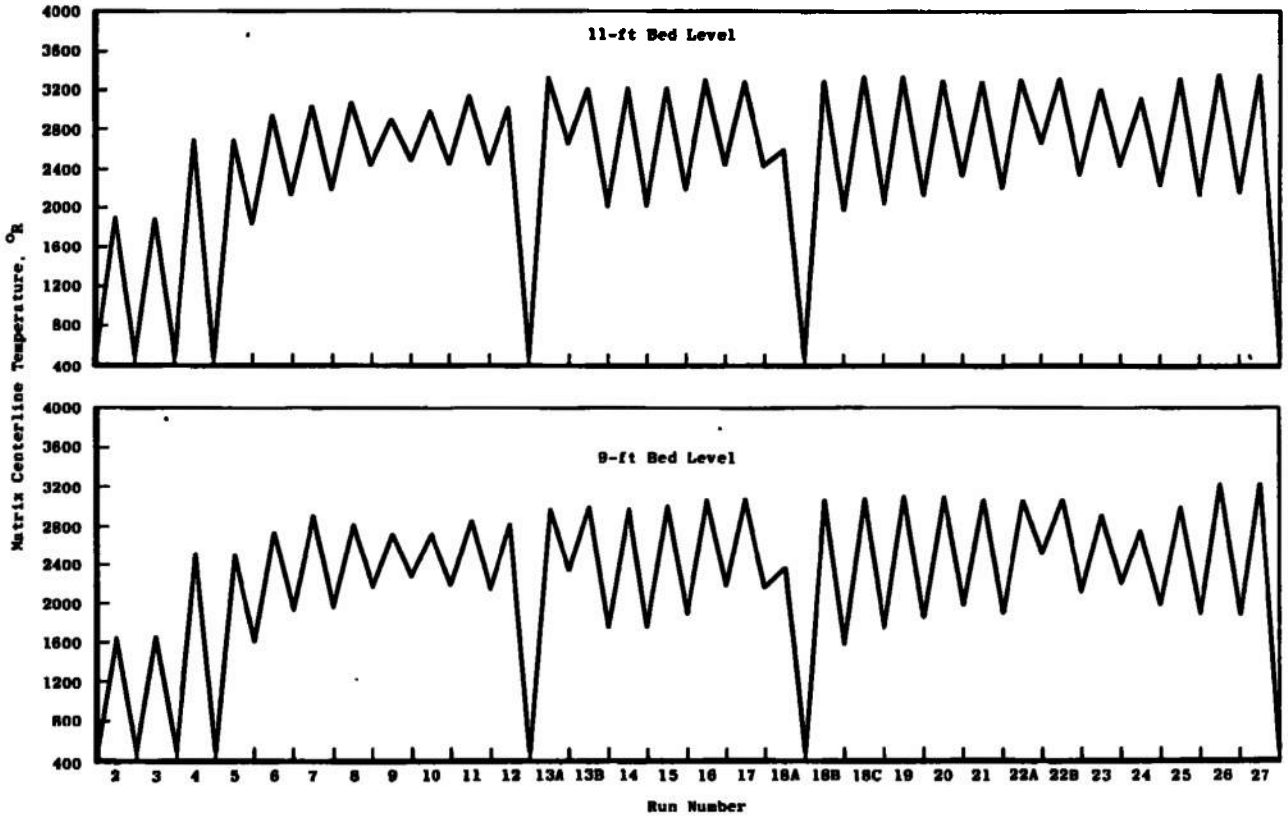

a. Concluded
Fig. 5 Continued

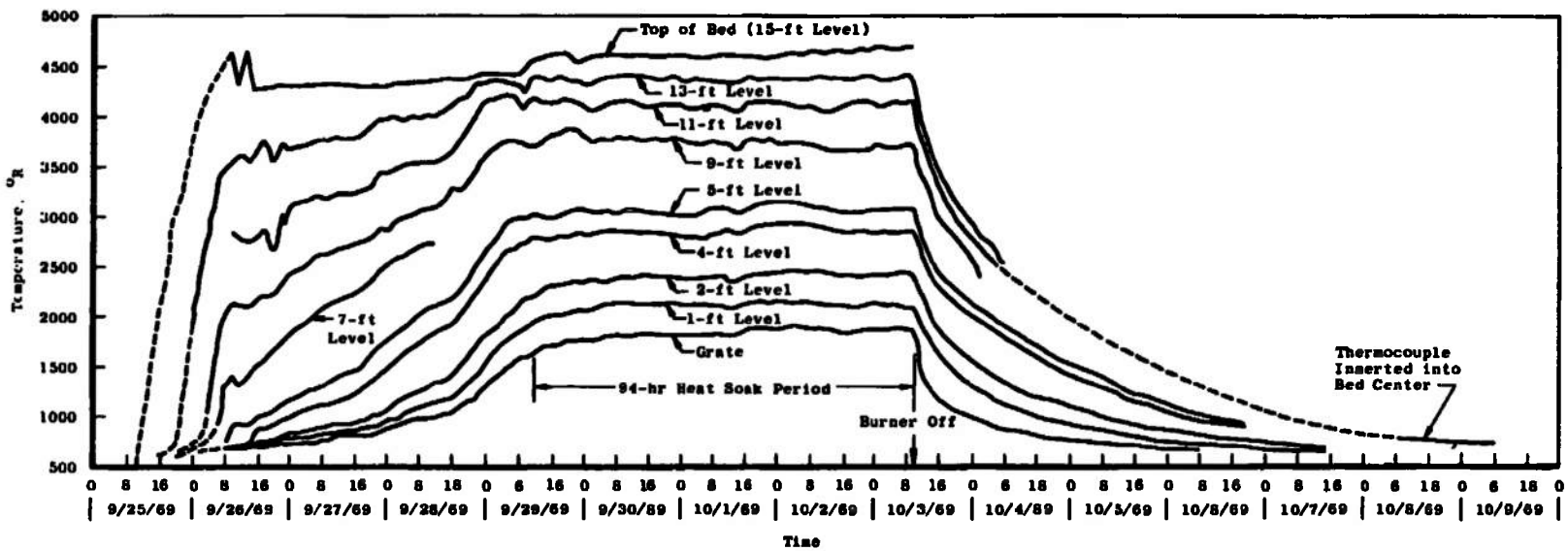

b. Heat Soak
Fig. 5 Continued

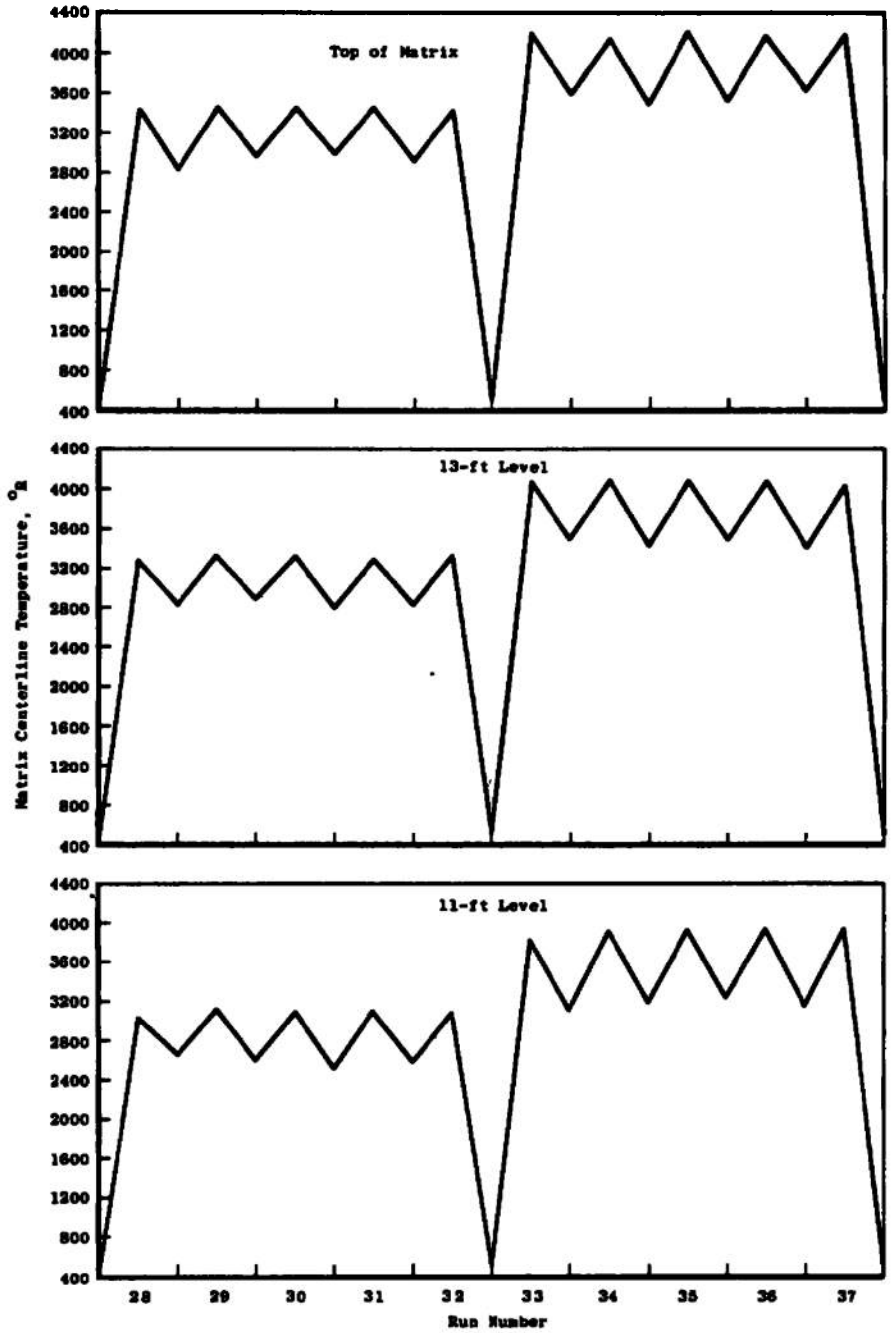

c. Runs 28 through 37
Fig. 5 Continued

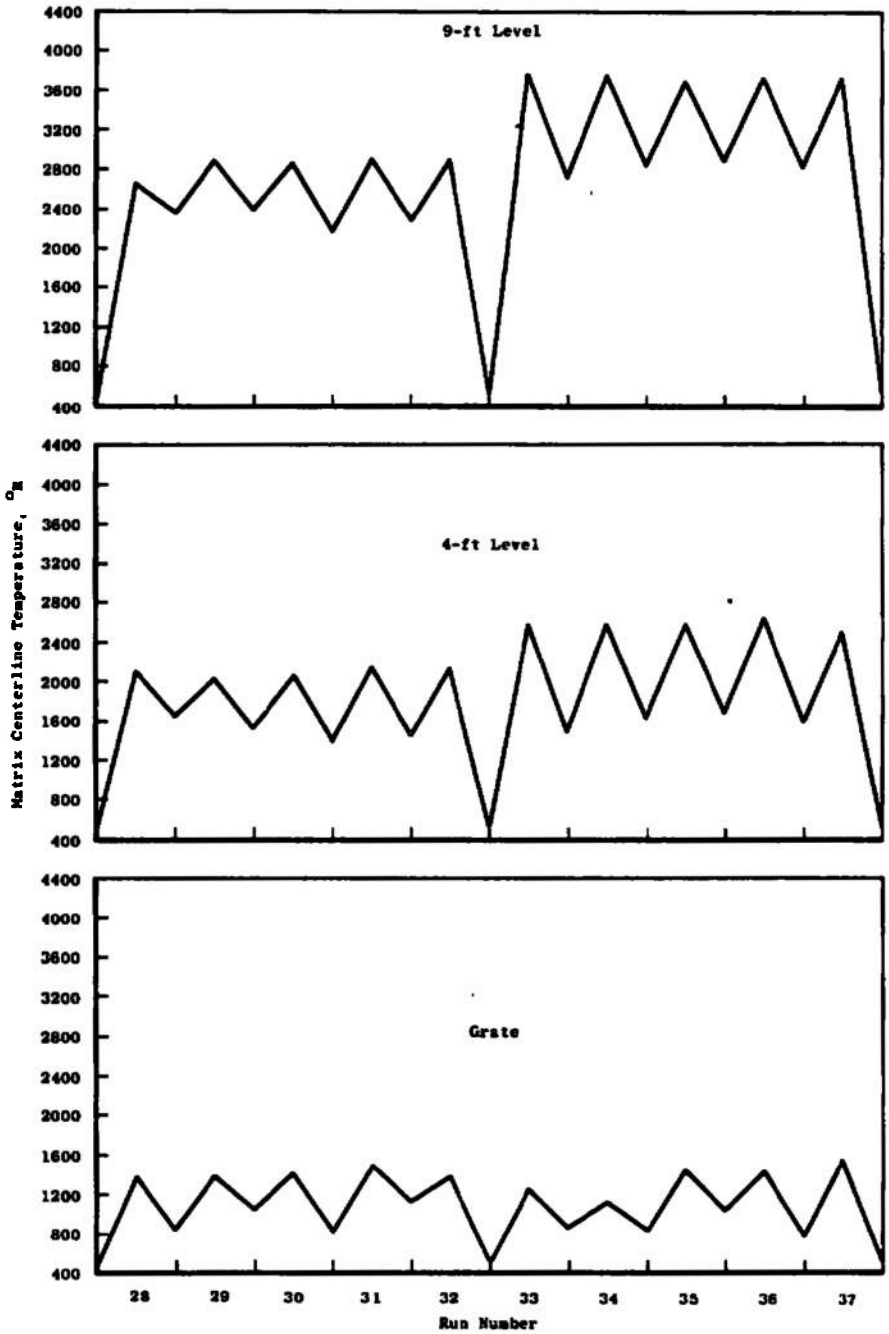

c. Concluded
Fig. 5 Continued

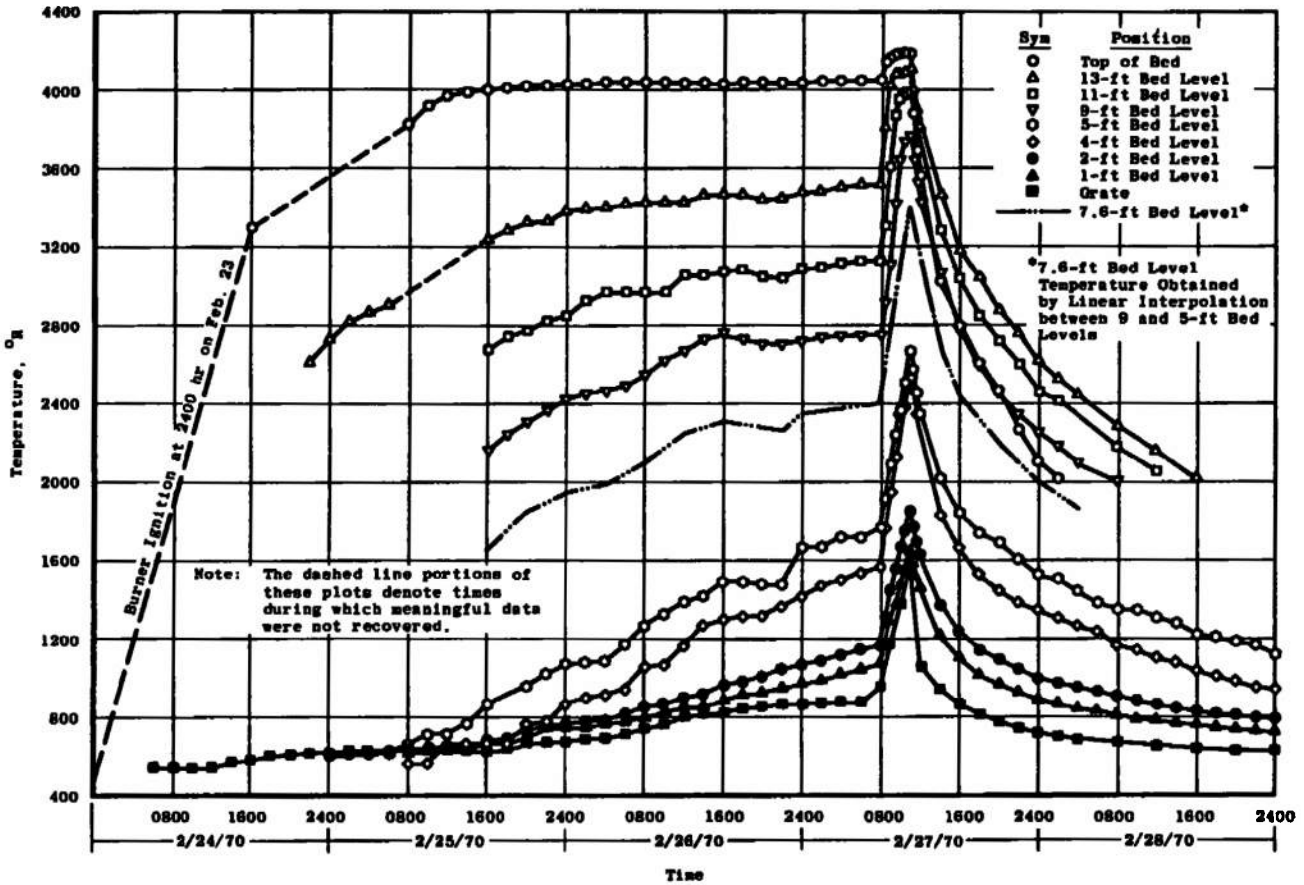

d. Test 38
Fig. 5 Continued

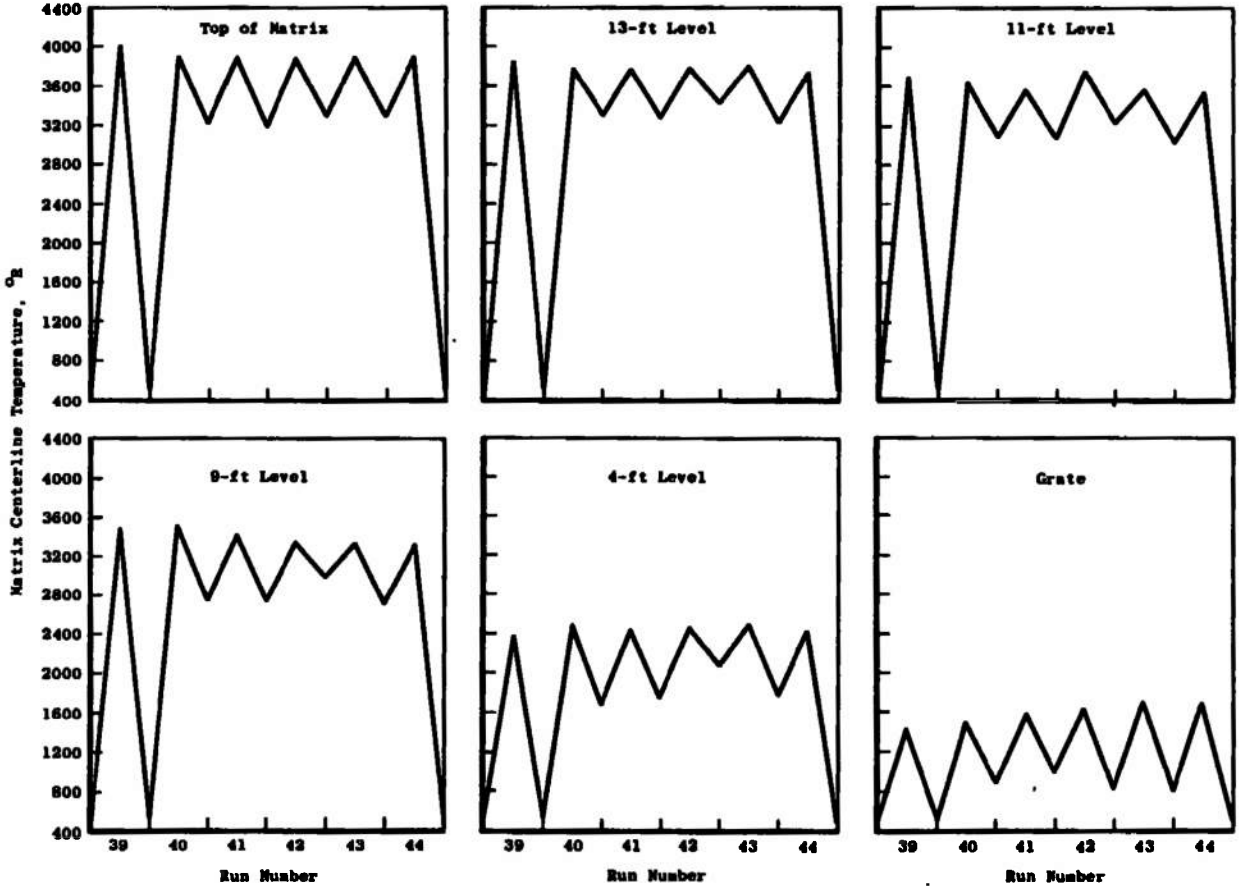

e. Runs 39 through 44
Fig. 5 Continued

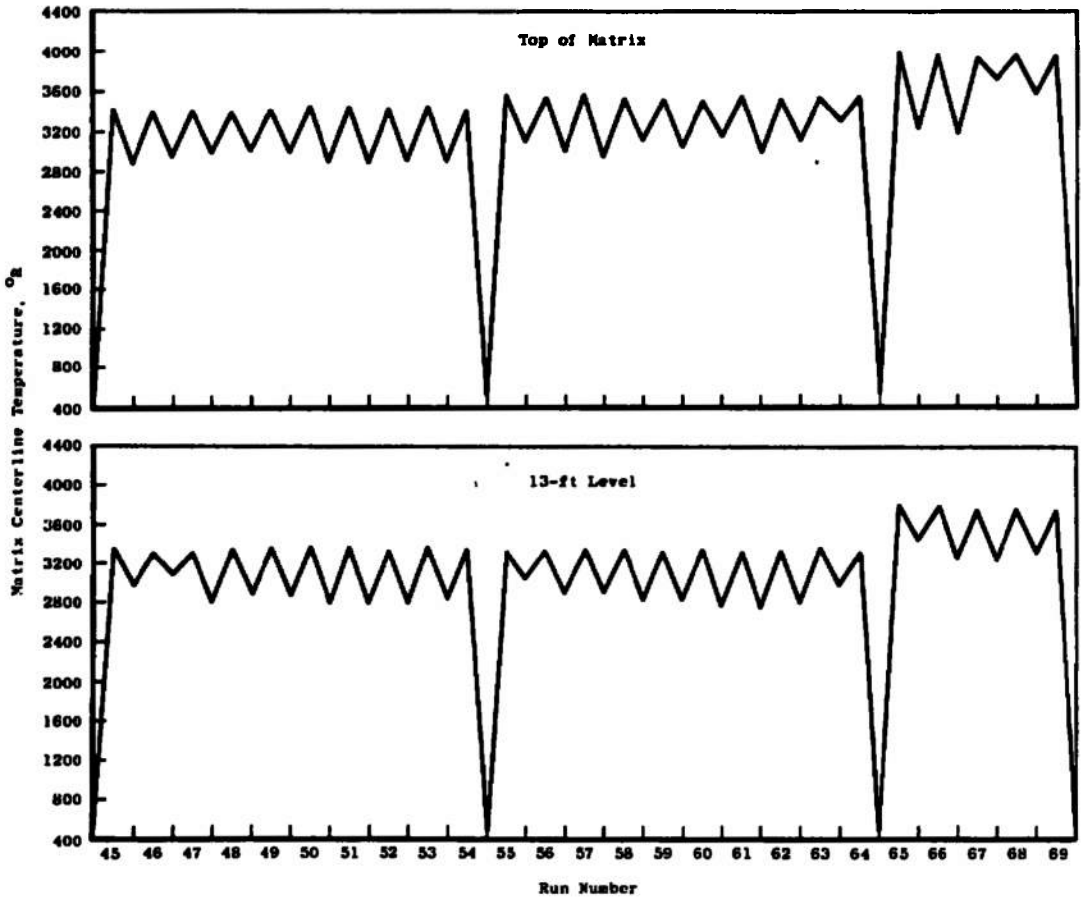

f. Runs 45 through 69
Fig. 5 Continued

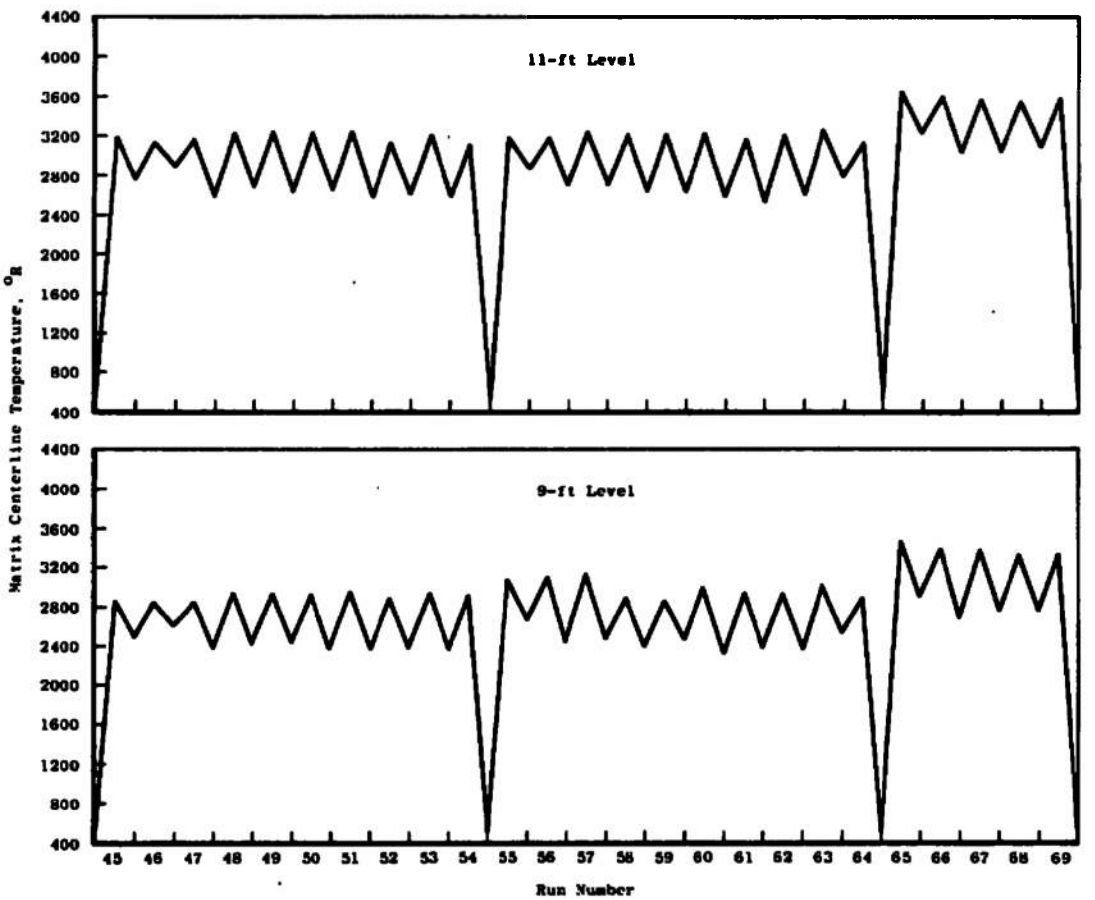

f. Continued
Fig. 5 Continued

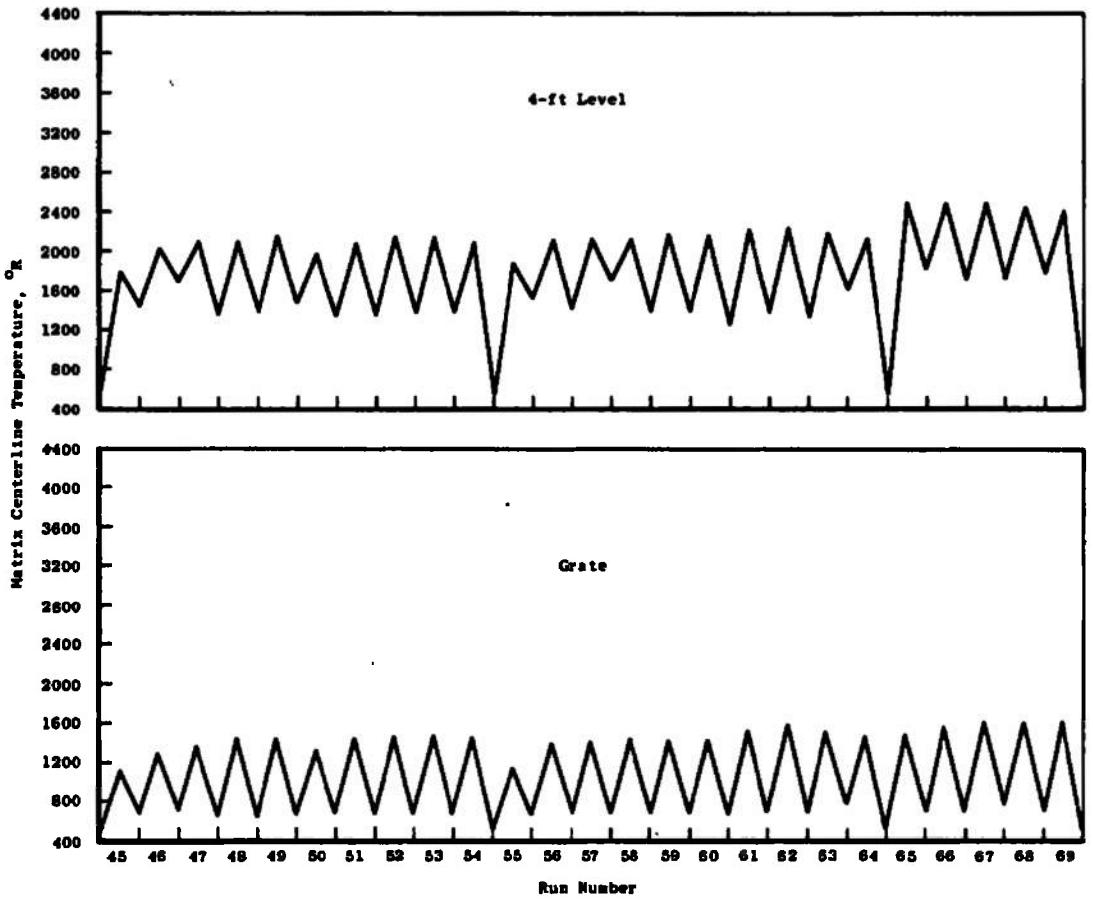

f. Concluded
Fig. 5 Continued

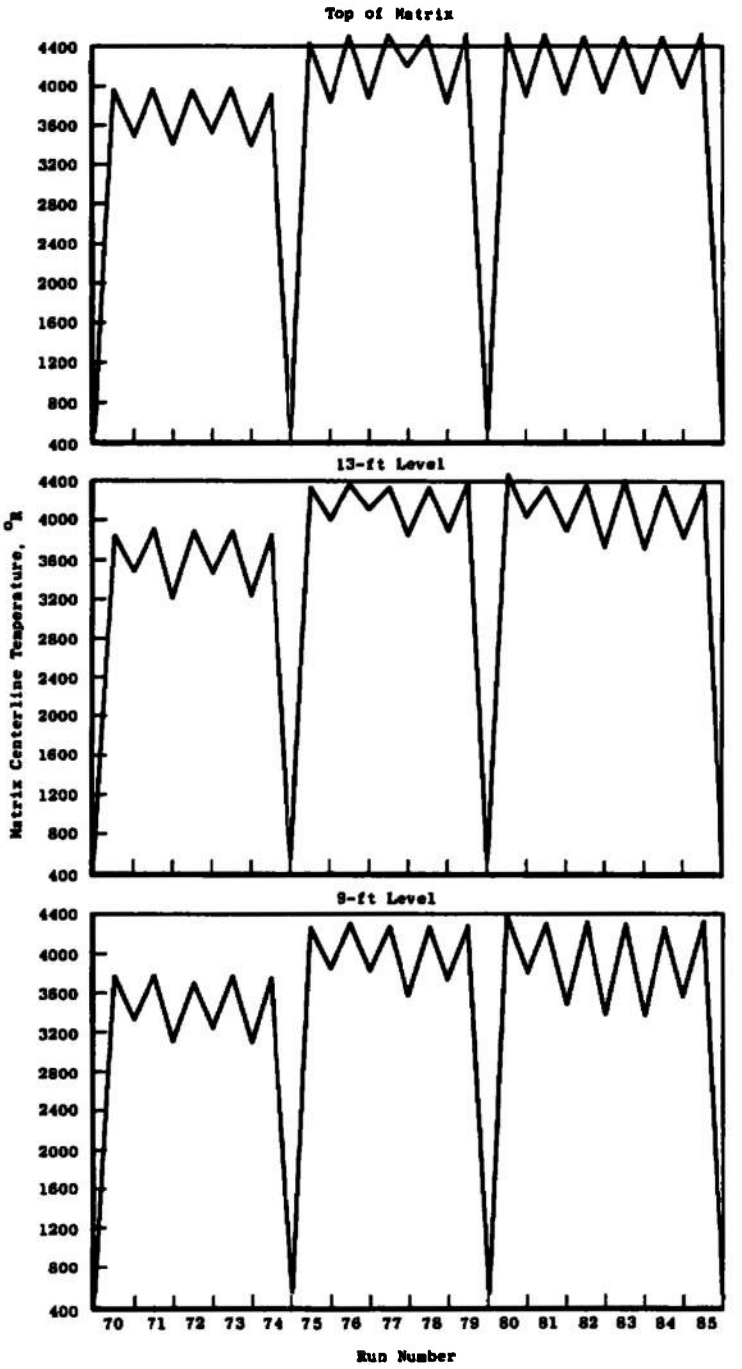

g. Runs 70 through 85
Fig. 5 Continued

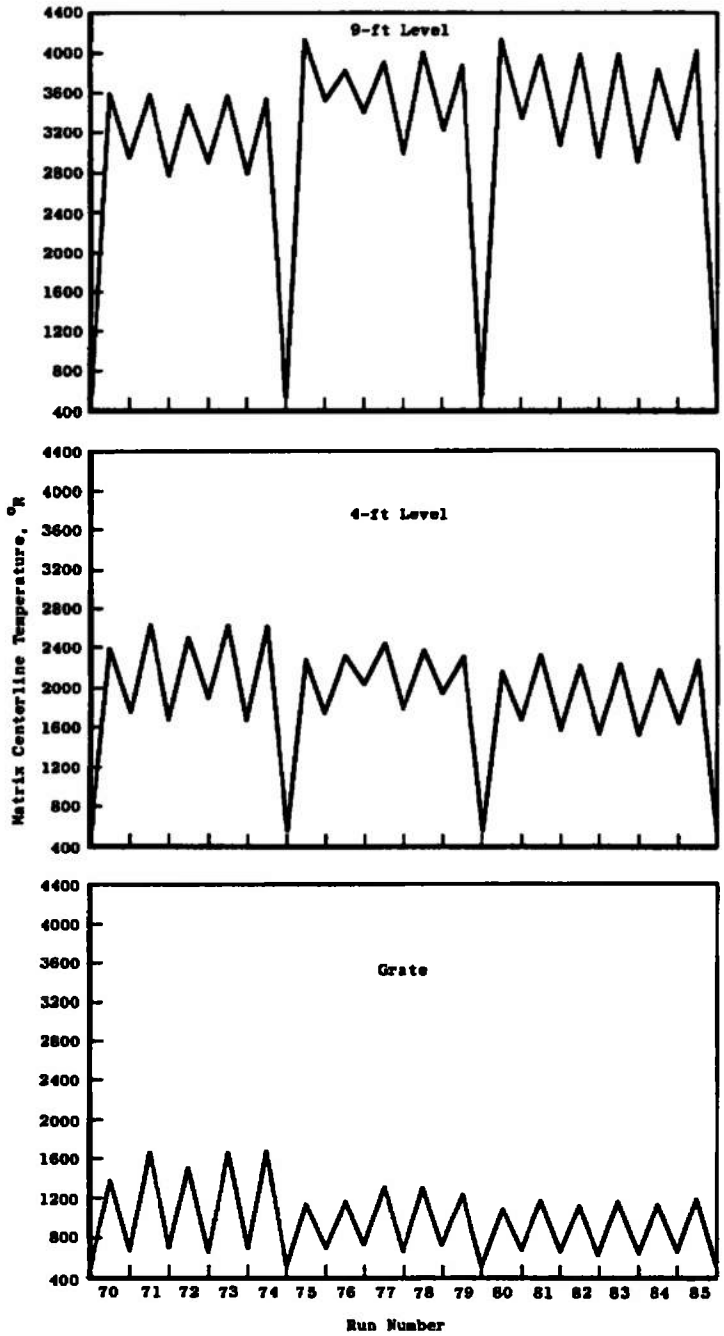

g. Concluded
Fig. 5 Concluded

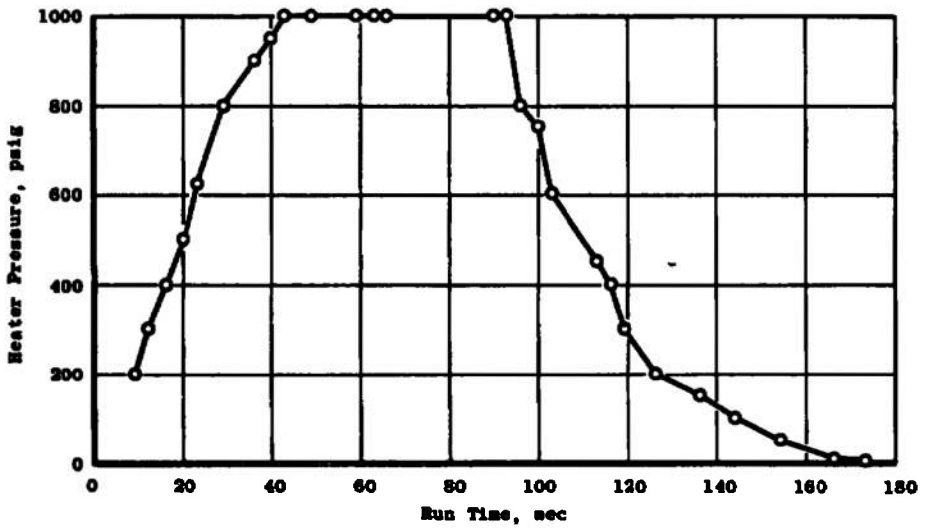

a. Run 30 (3450°R Maximum Matrix Temperature)

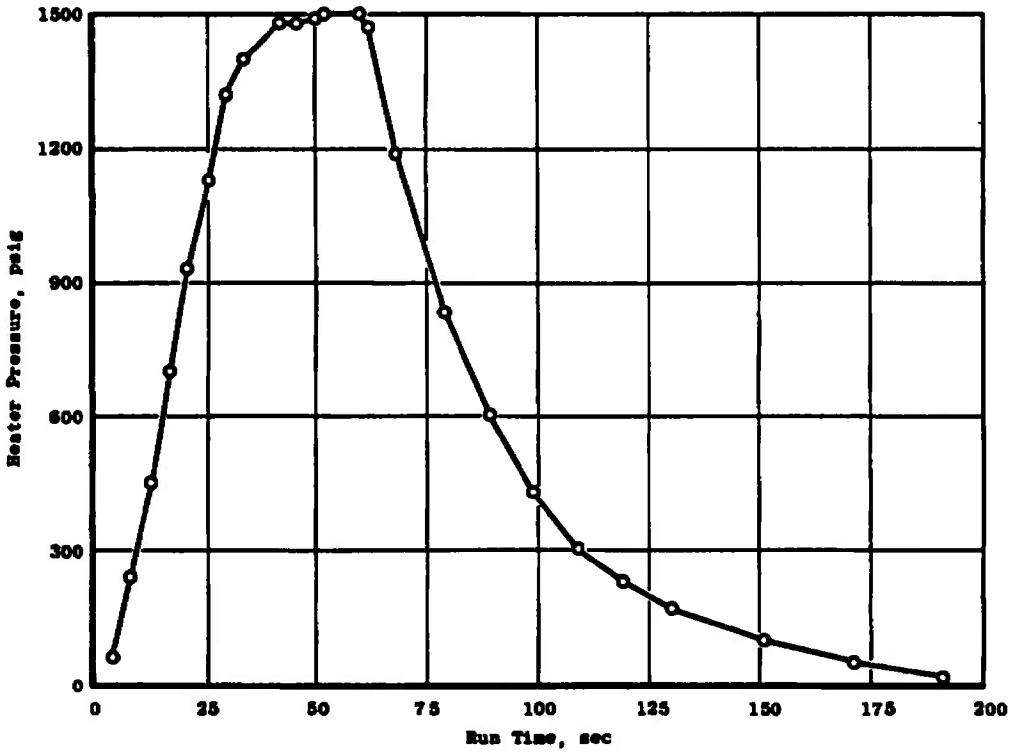

b. Run 59 (3450°R Maximum Matrix Temperature)

Fig. 6 Representative Heater Operating Pressure Histories

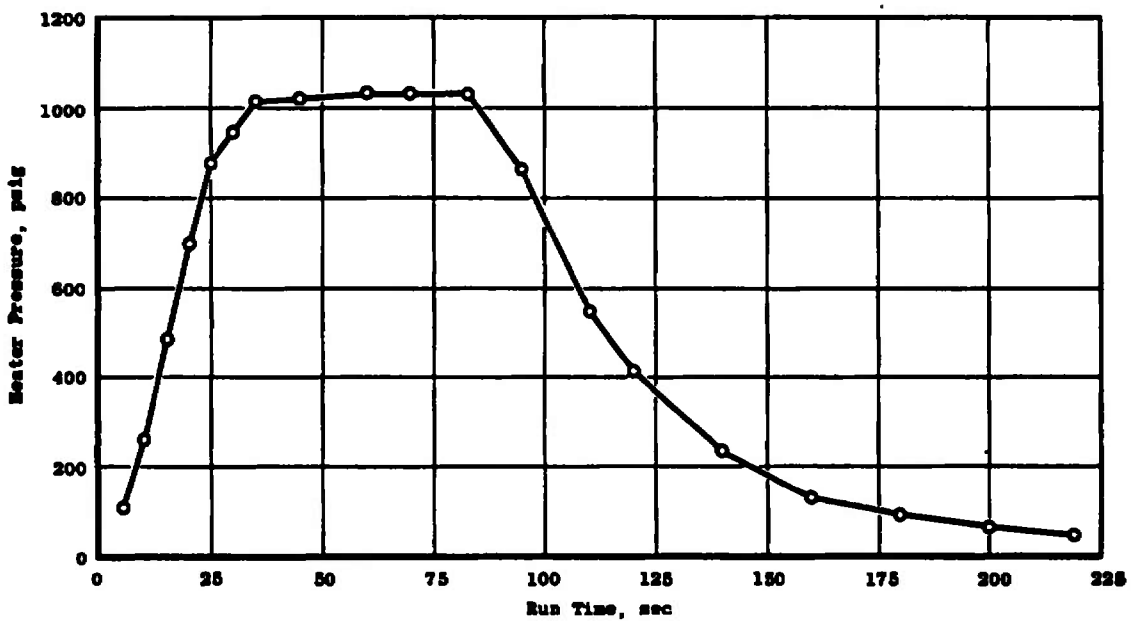

c. Run 72 (3950°R Maximum Matrix Temperature)

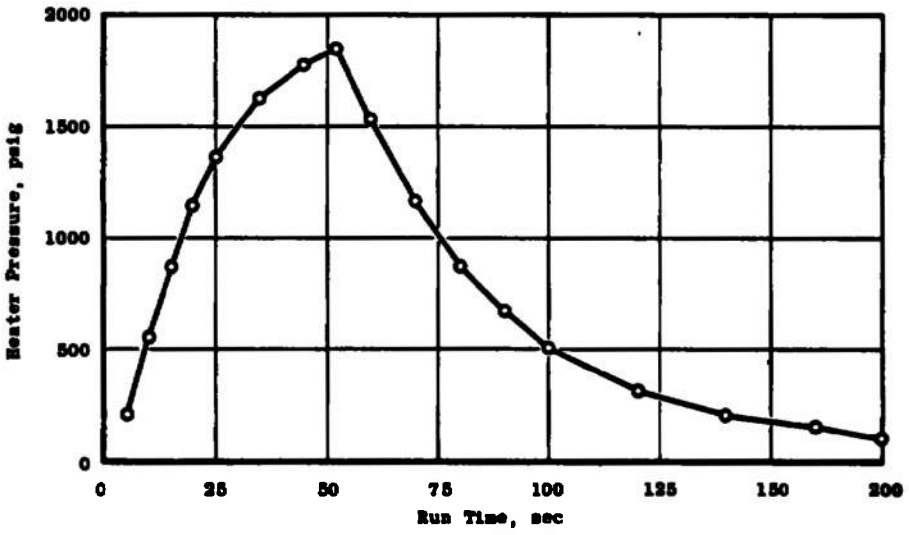

d. Run 85 (4450°R Maximum Matrix Temperature)

Fig. 6 Concluded

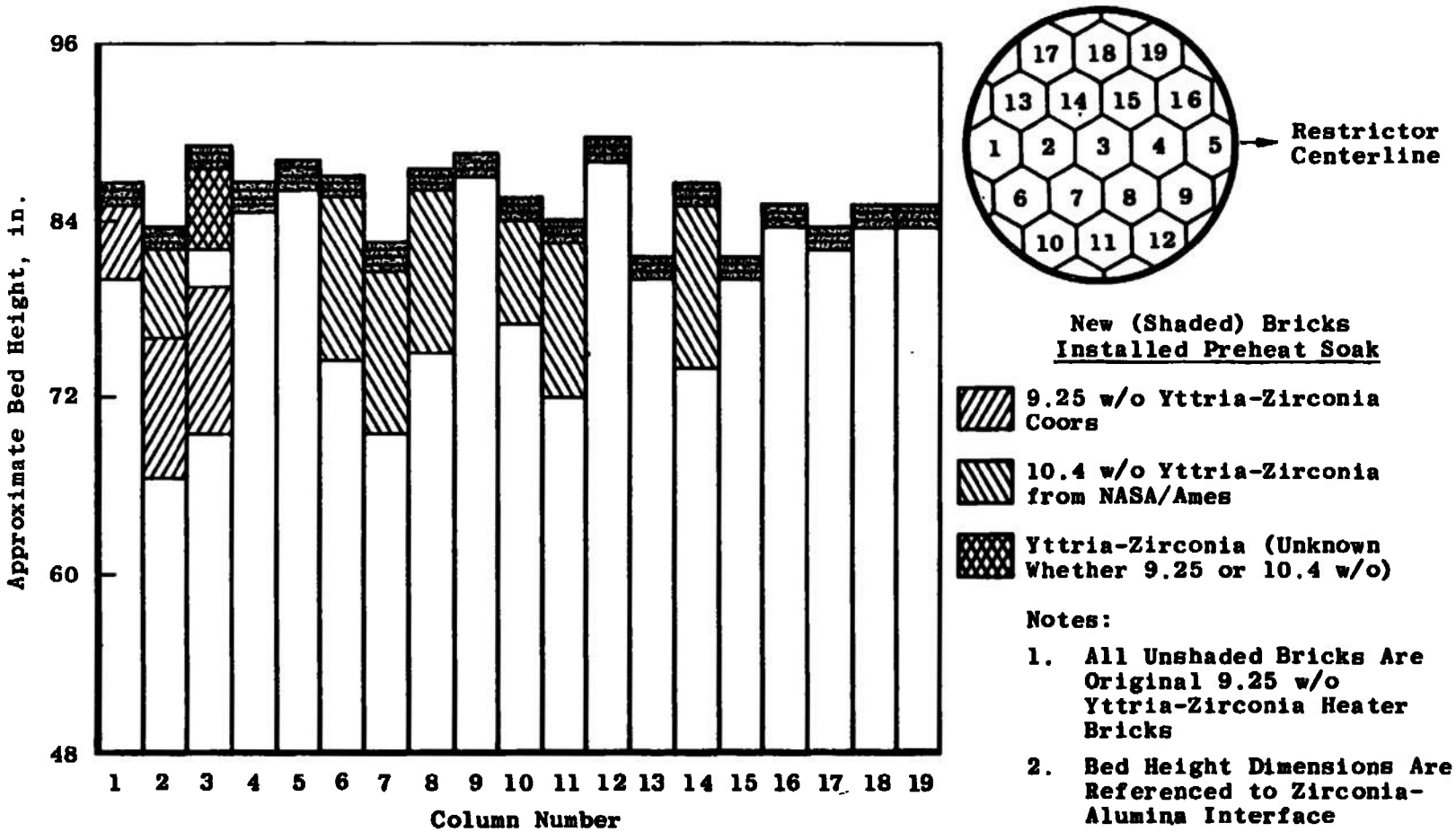

Fig. 7 Matrix Configuration, Heat Soak

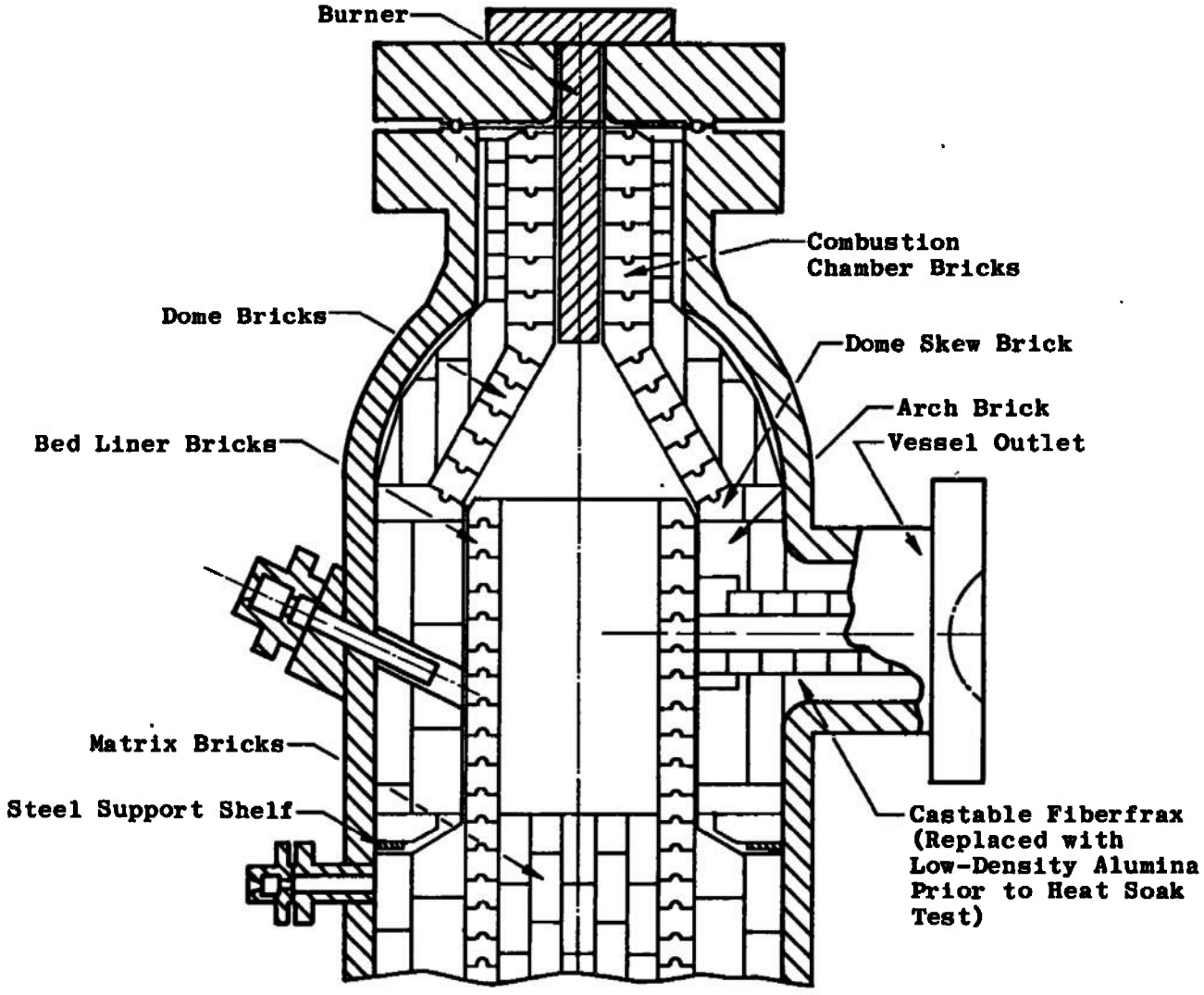

Fig. 8 Schematic of Heater Dome and Combustion Chamber Area

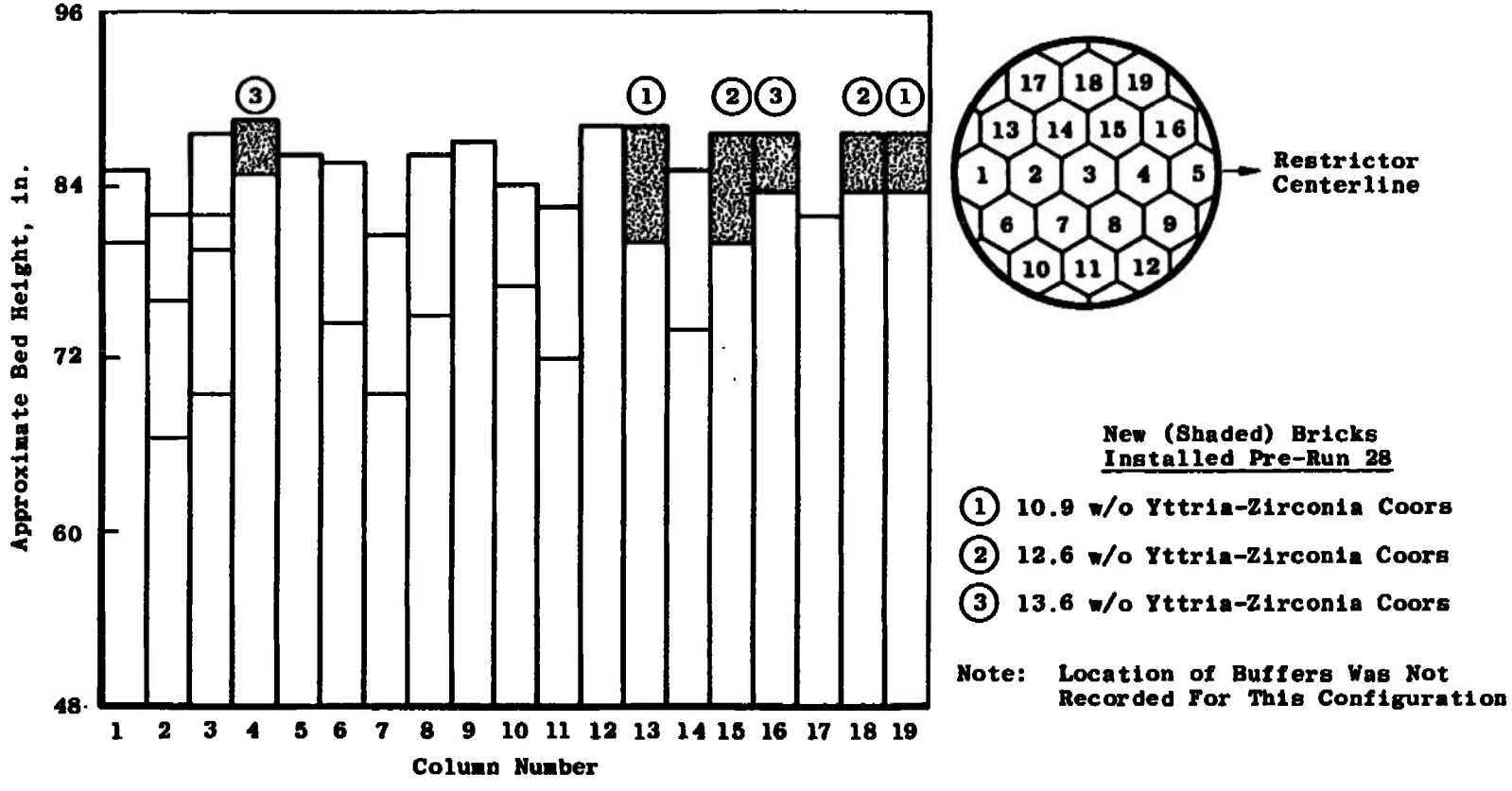

Fig. 9 Matrix Configuration, Runs 28 through 32

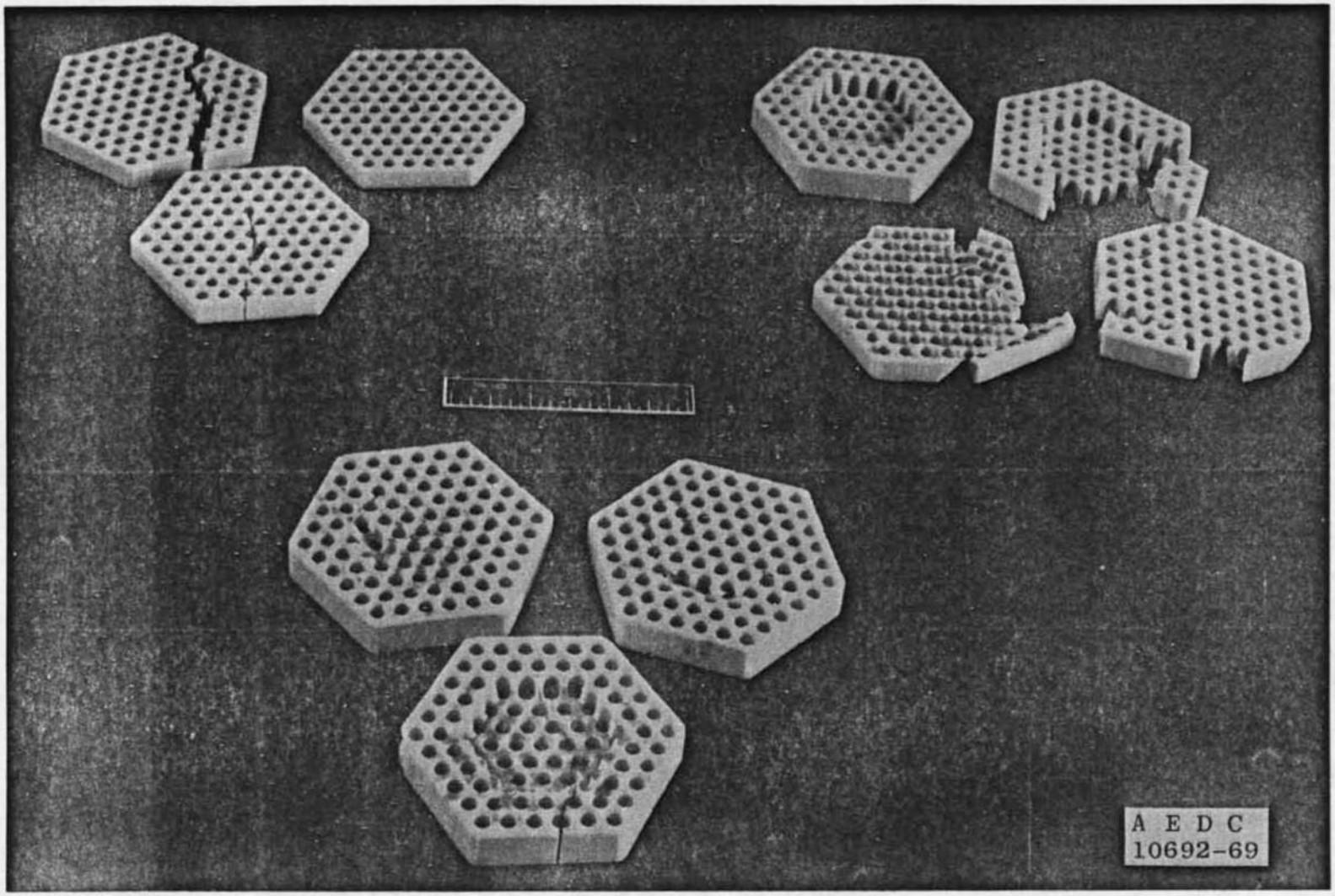

a. Buffer Bricks, Coors

Fig. 10 Post-Run 32 Inspection

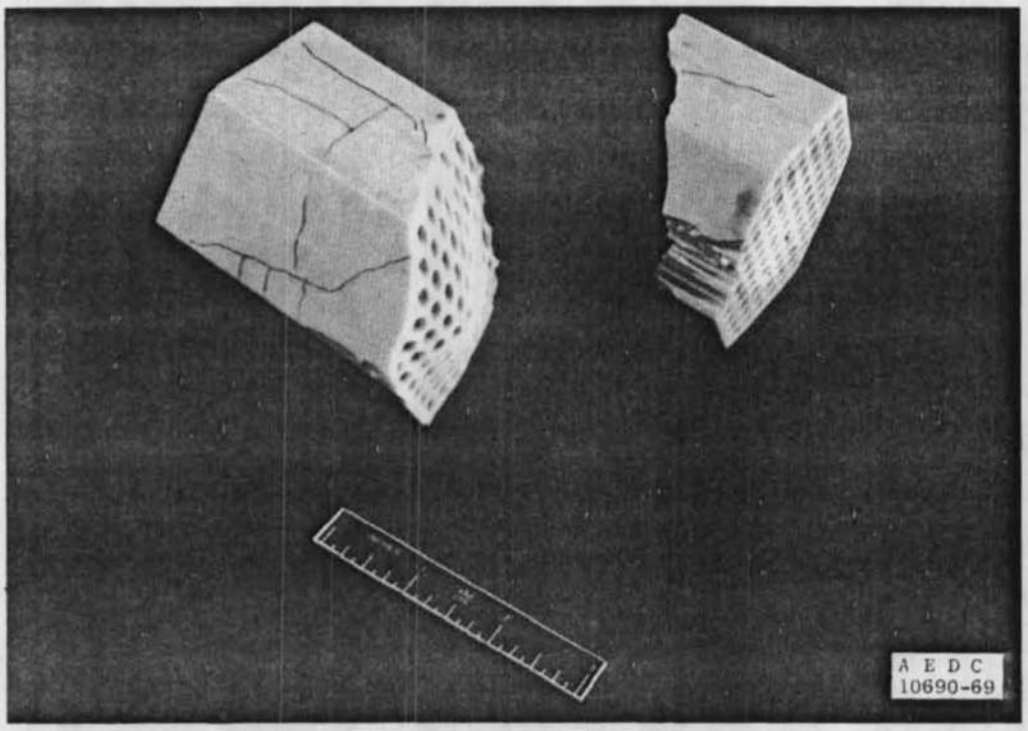

b. Brick Placed into Matrix Pre-Heat Soak, Column 1, 9.25 w/o, Coors

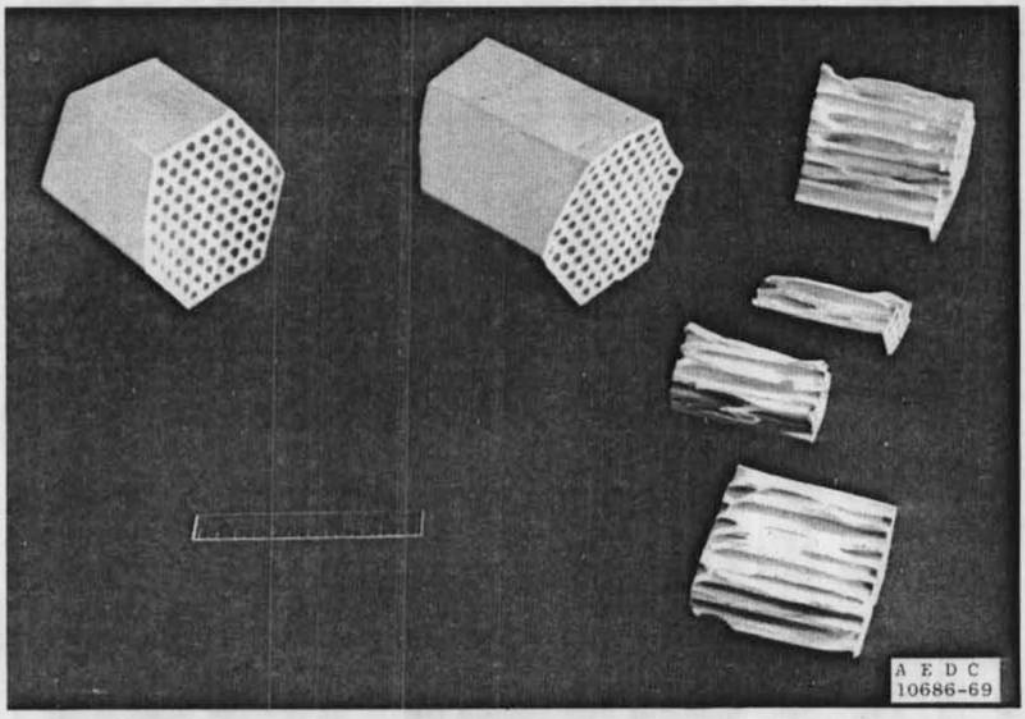

c. Brick Placed into Matrix Pre-Run 28, Column 13, 10.9 w/o, Coors
Fig. 10 Continued

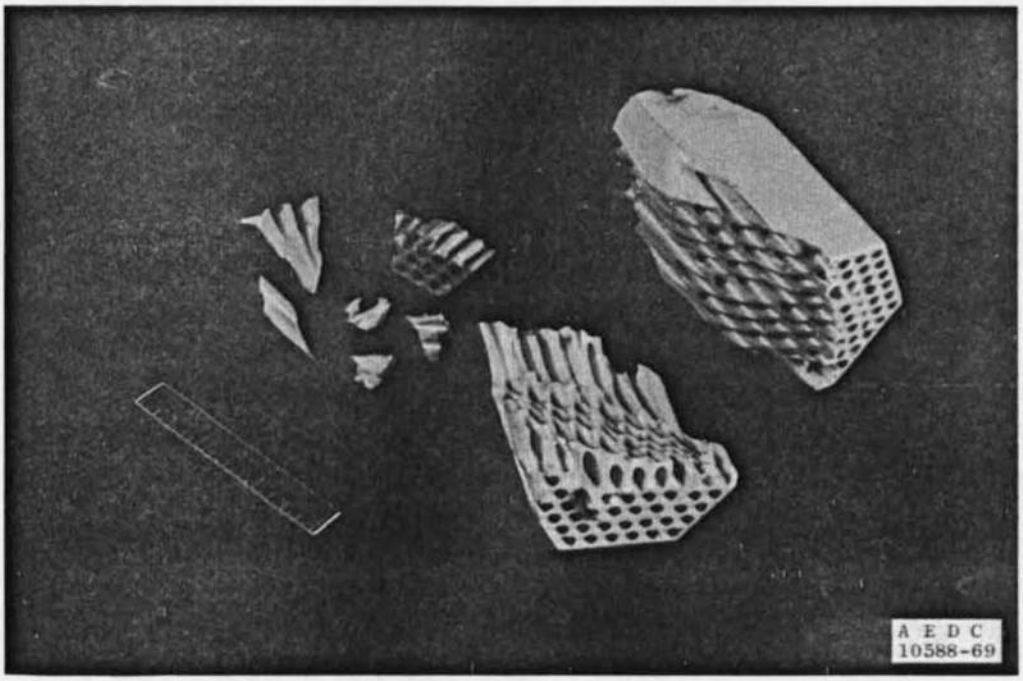

d. Brick Placed into Matrix Pre-Run 28, Column 16, 13.8 w/o, Coors

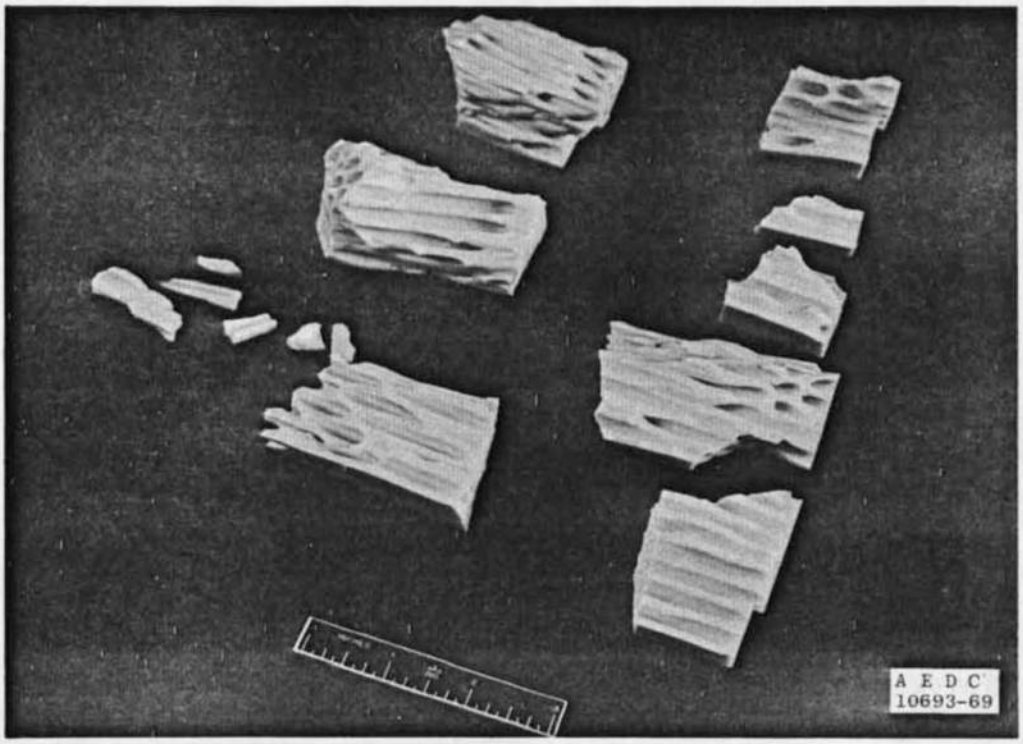

e. Original Matrix Brick, Column 17, 9.25 w/o, Coors
Fig. 10 Concluded

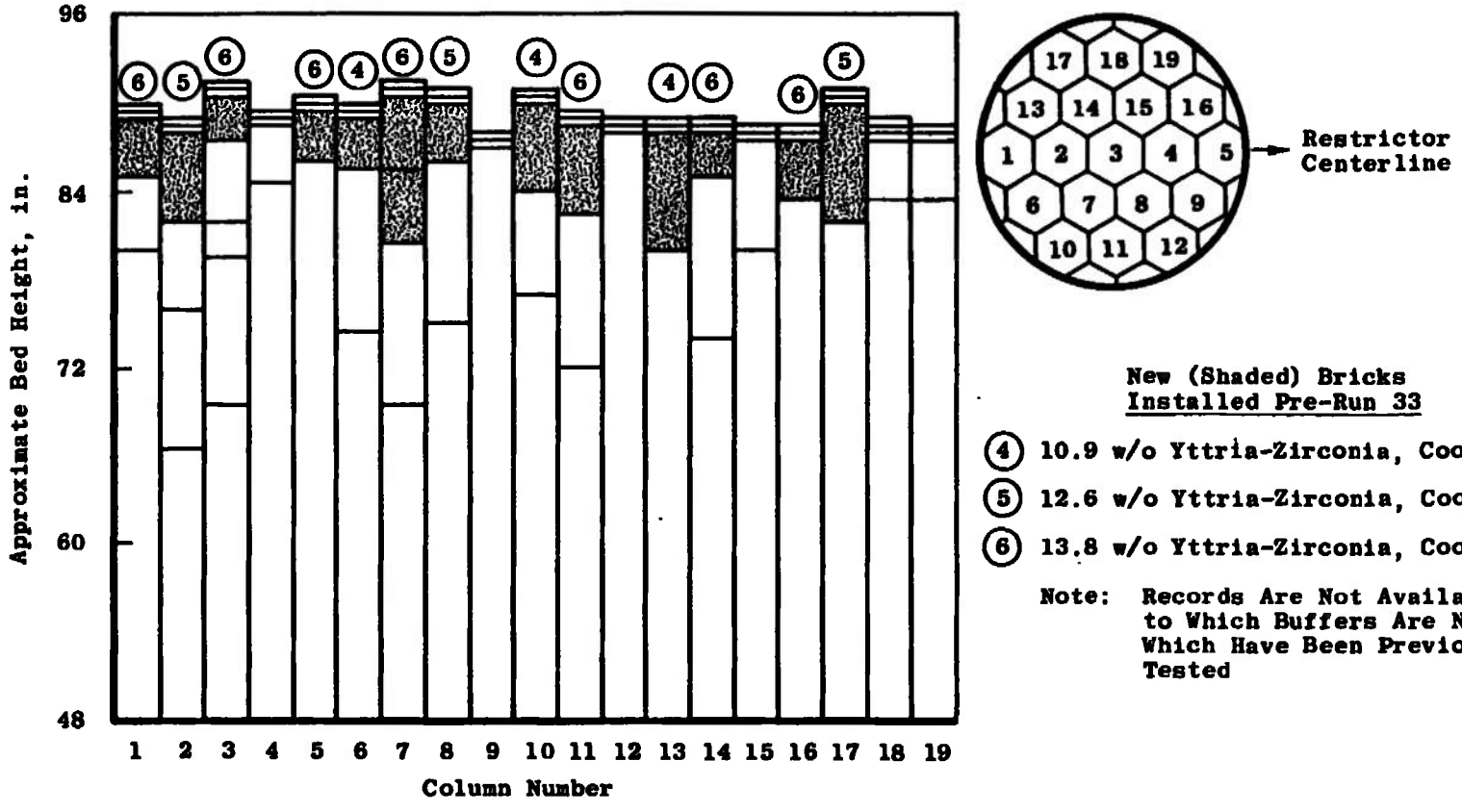

Fig. 11 Matrix Configuration, Runs 33 through 37

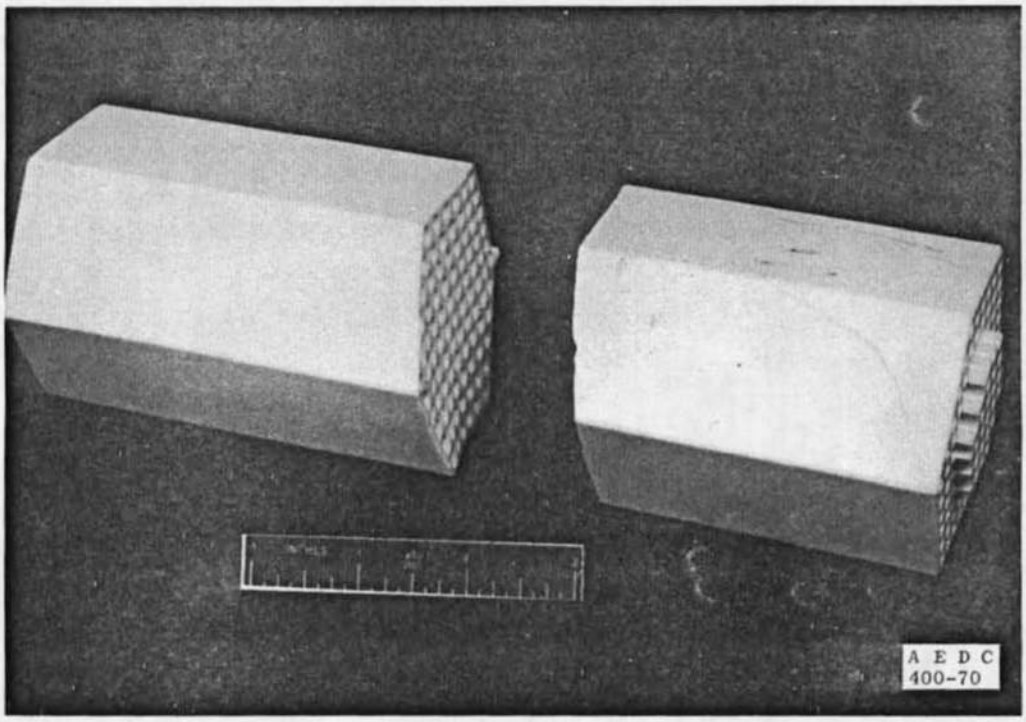

a. Column 13, 10.9 w/o, Coors

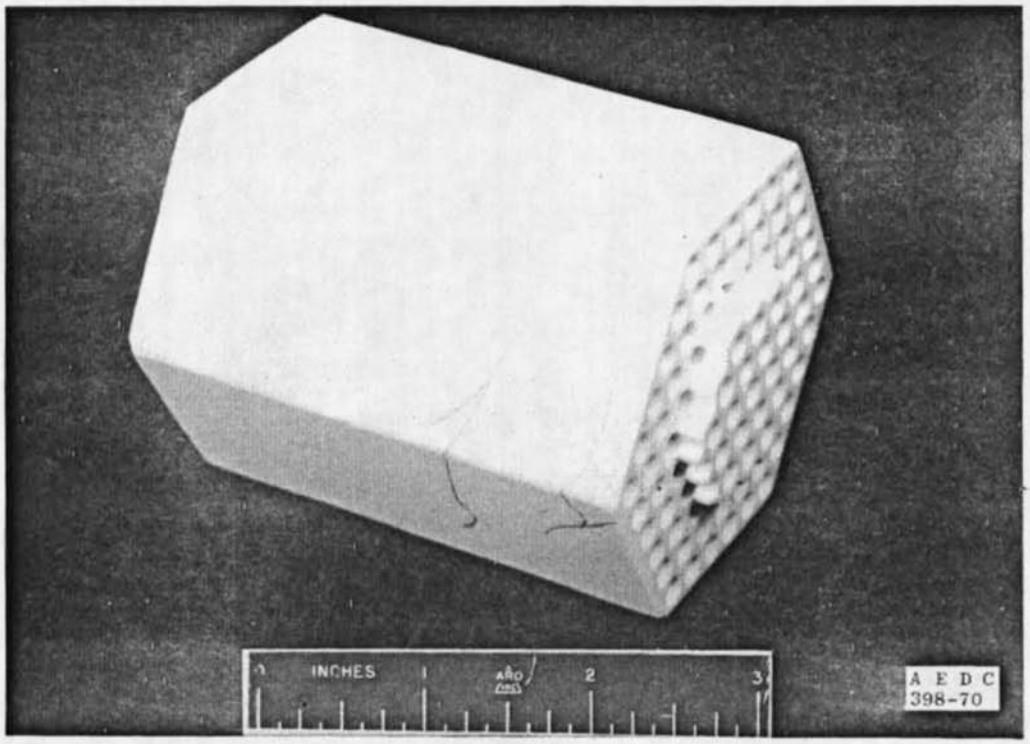

b. Column 8, 12.6 w/o, Coors

Fig. 12 Matrix Sample Bricks, Post-Run 37

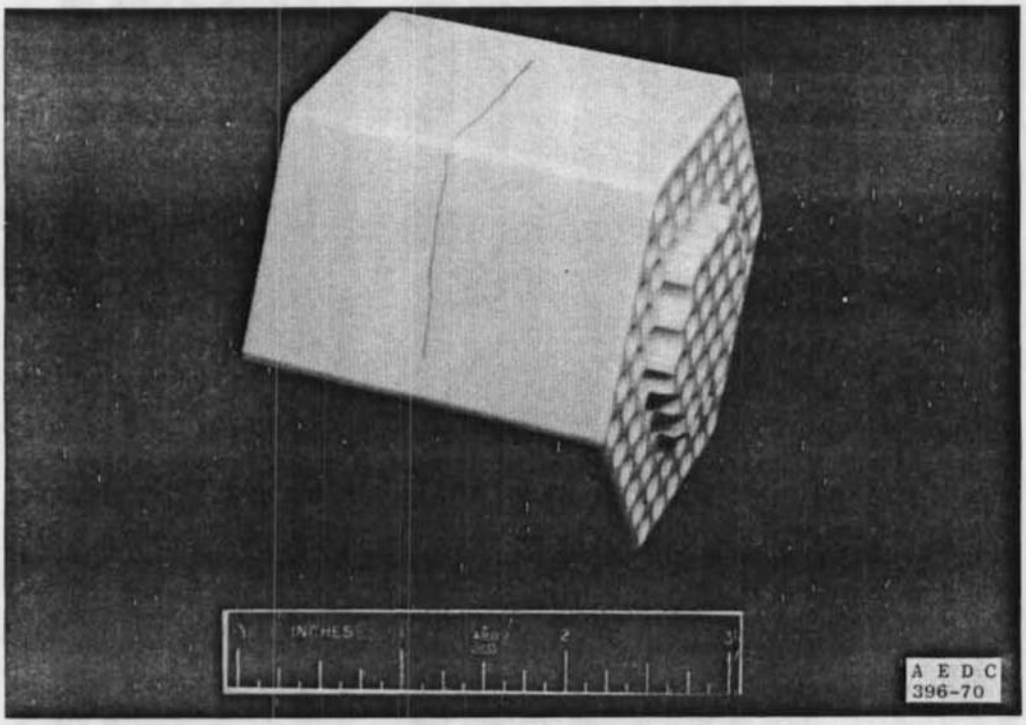

c. Column 7, 13.8 w/o, Coors
Fig. 12 Concluded

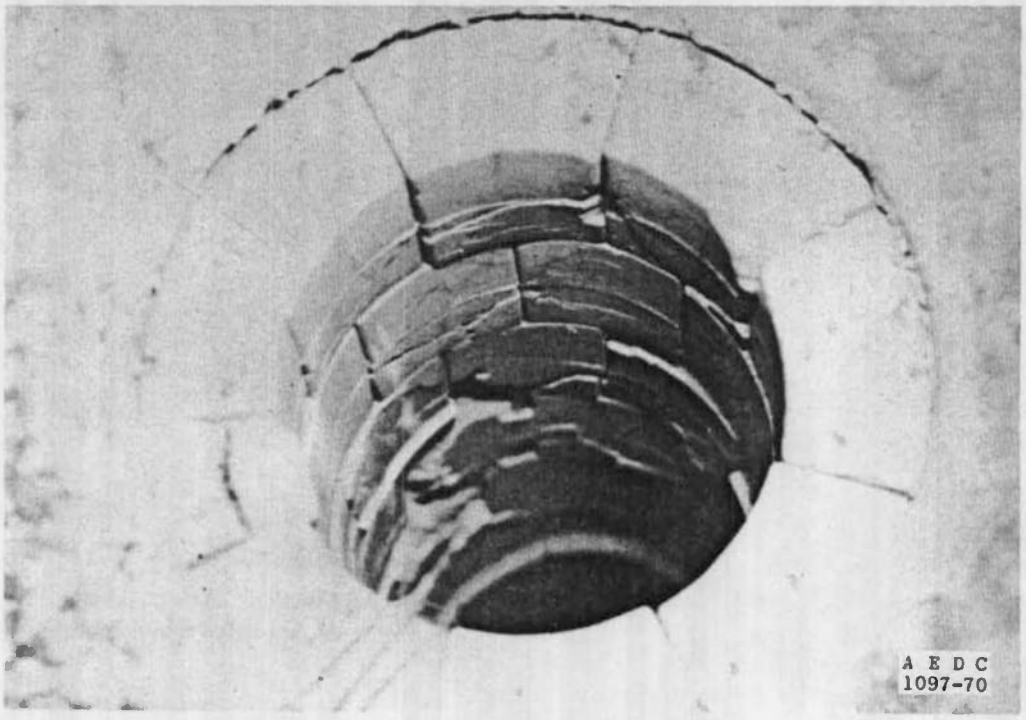

Fig. 13 Combustion Chamber Bricks, Post-Run 37

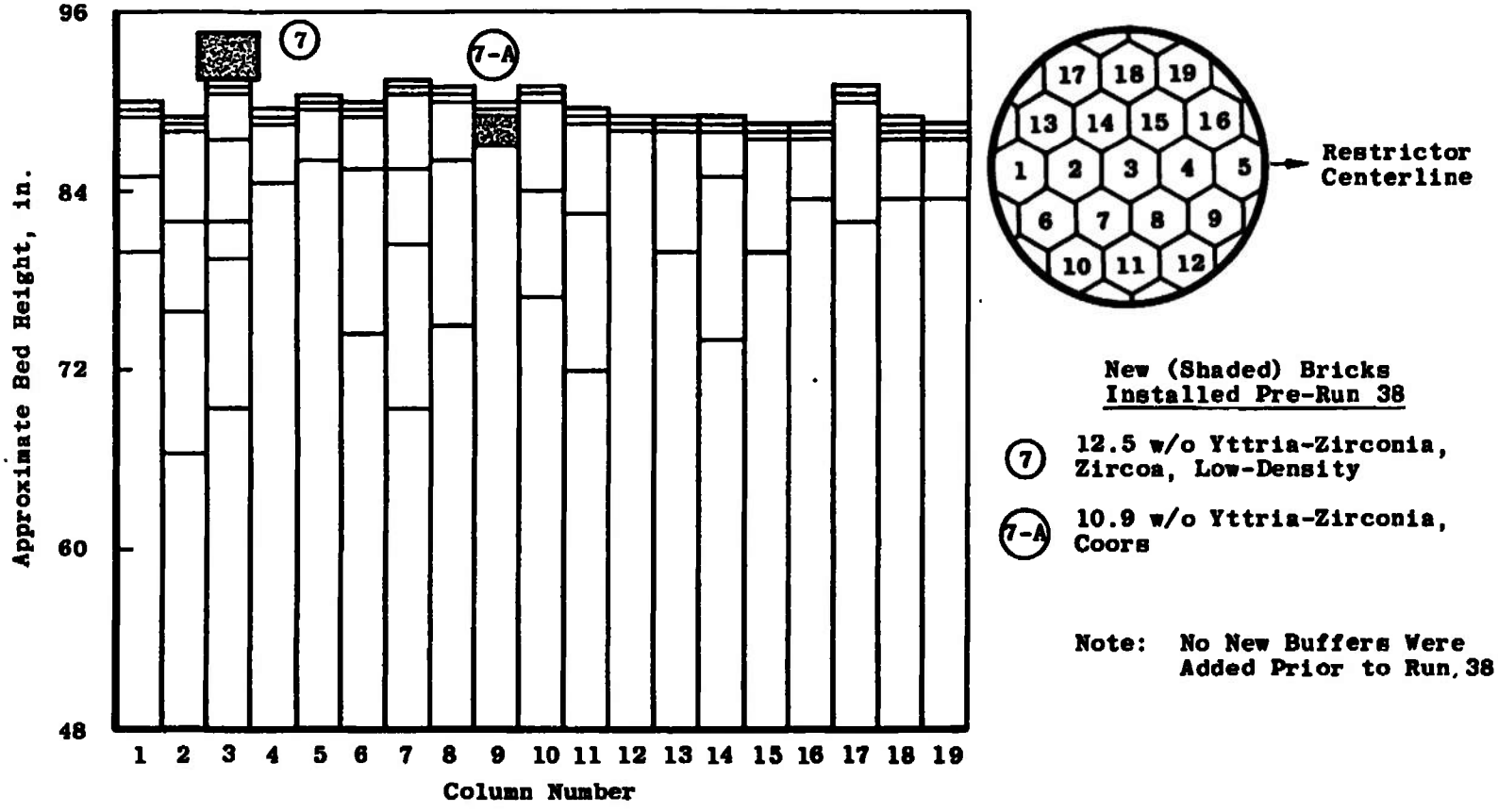

Fig. 14 Matrix Configuration, Runs 38 through 44

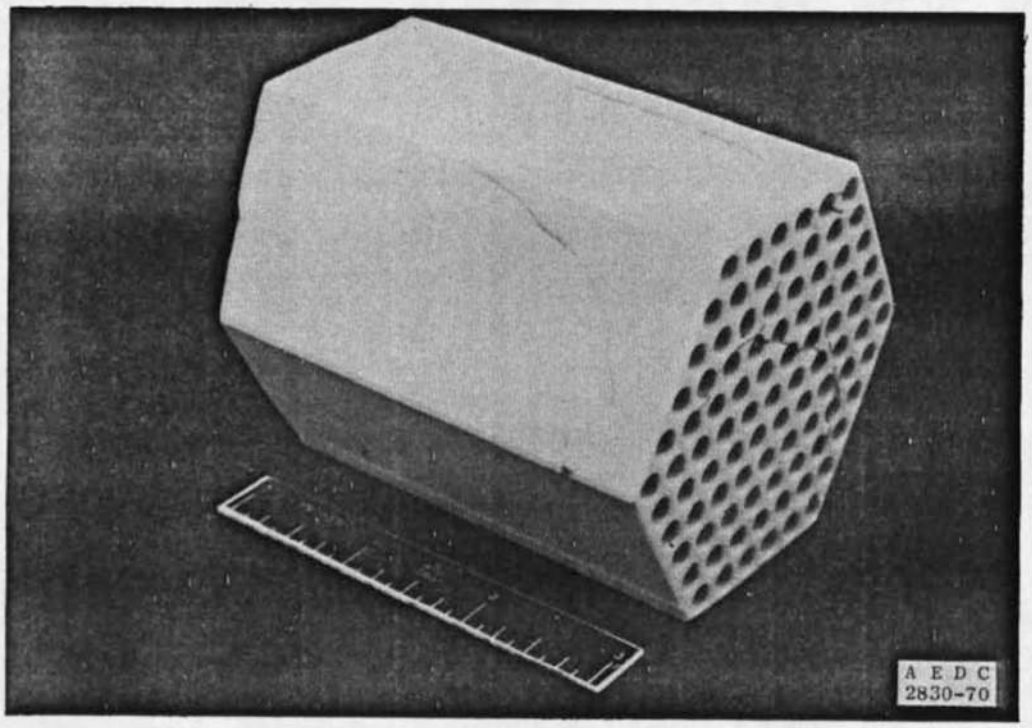

a. Column 13, 10.9 w/o, Coors

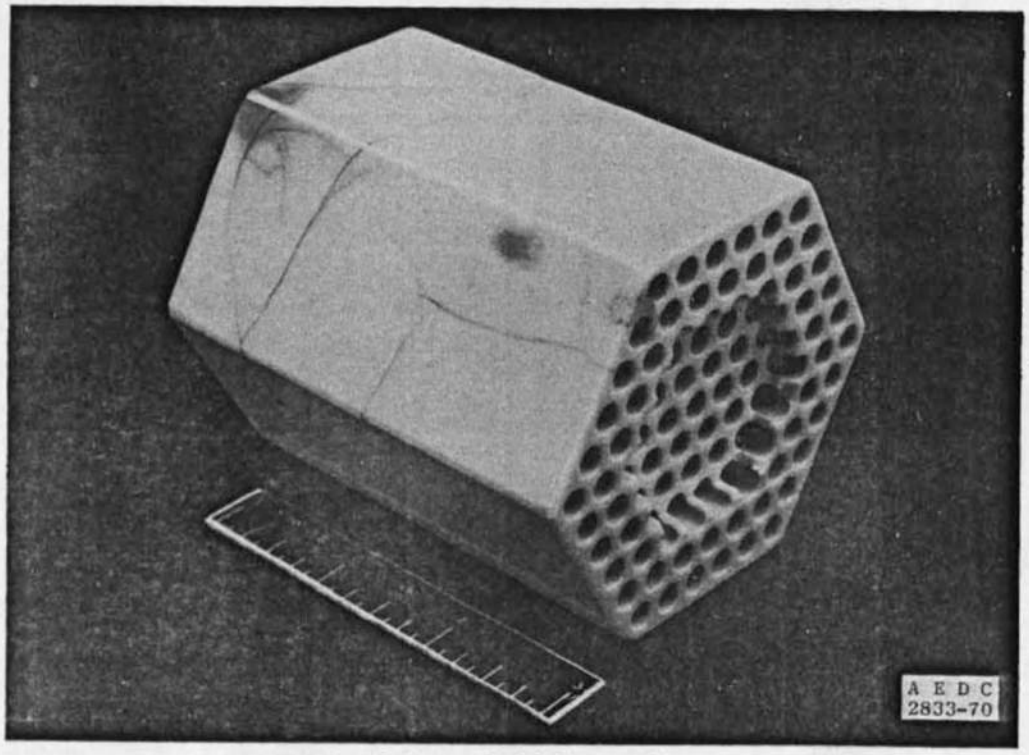

b. Column 8, 12.6 w/o, Coors

Fig. 15 Matrix Sample Bricks, Posttest 38

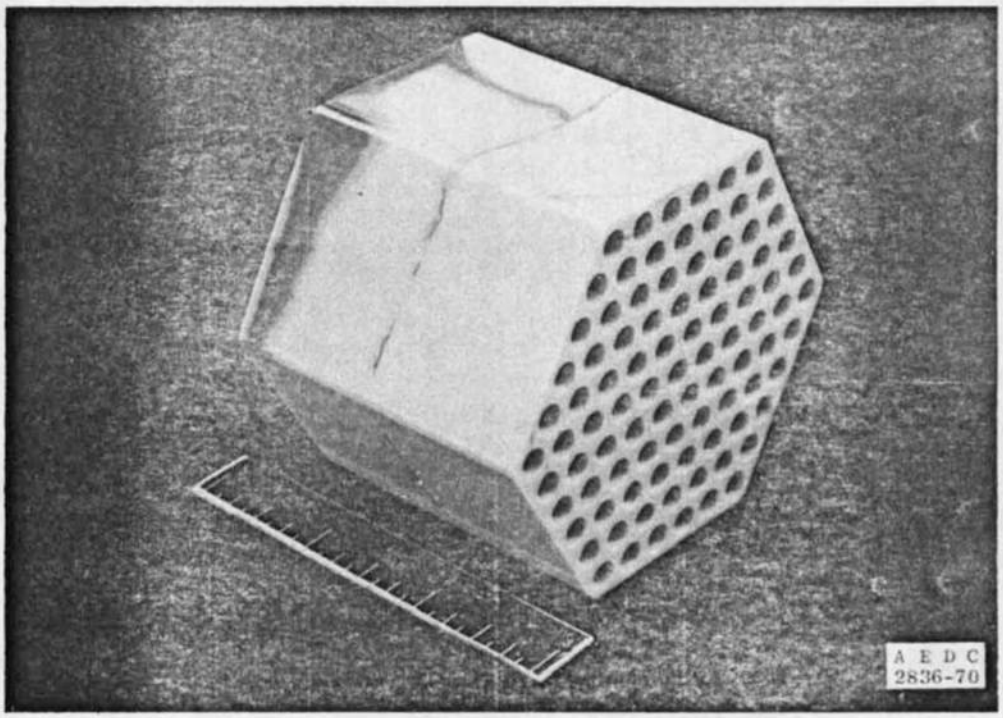

c. Column 7, 13.8 w/o, Coors

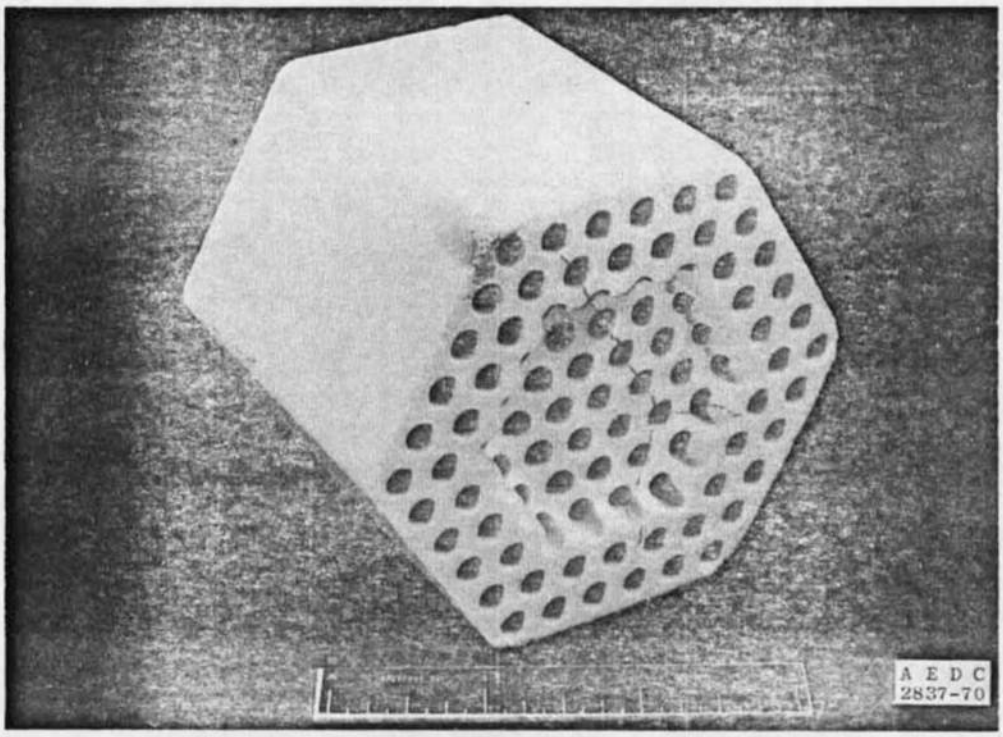

d. Zircoa, Low Density, 12.5 w/o, Posttest 38 (Upper Block)
Fig. 15 Continued

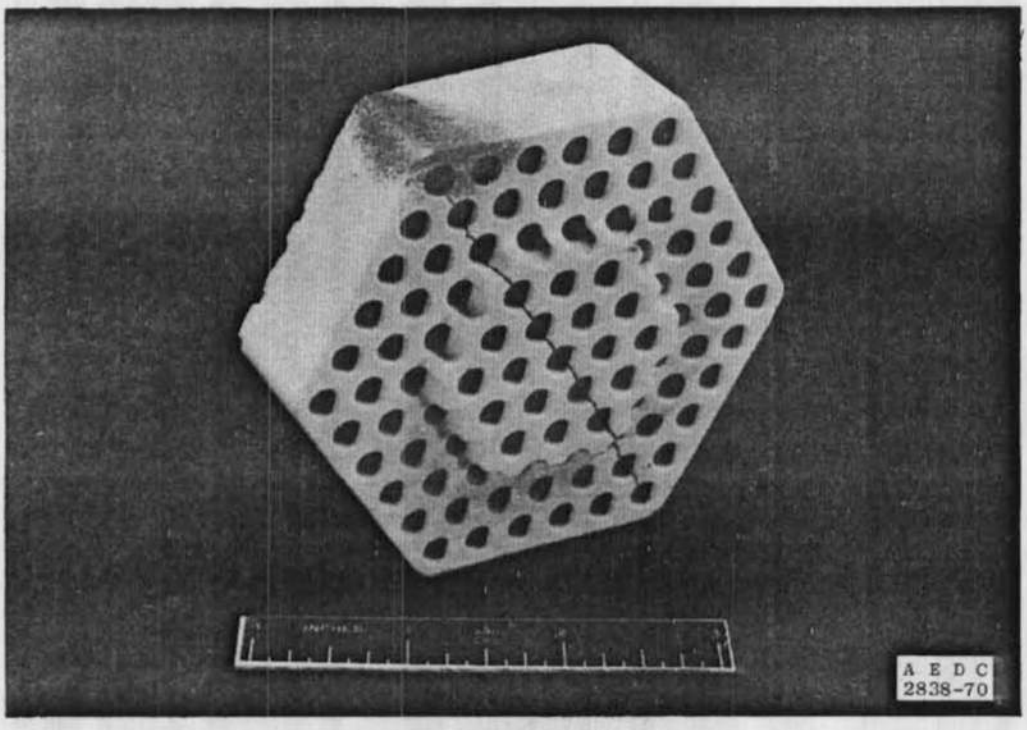

e. Lower Block
Fig. 15 Concluded

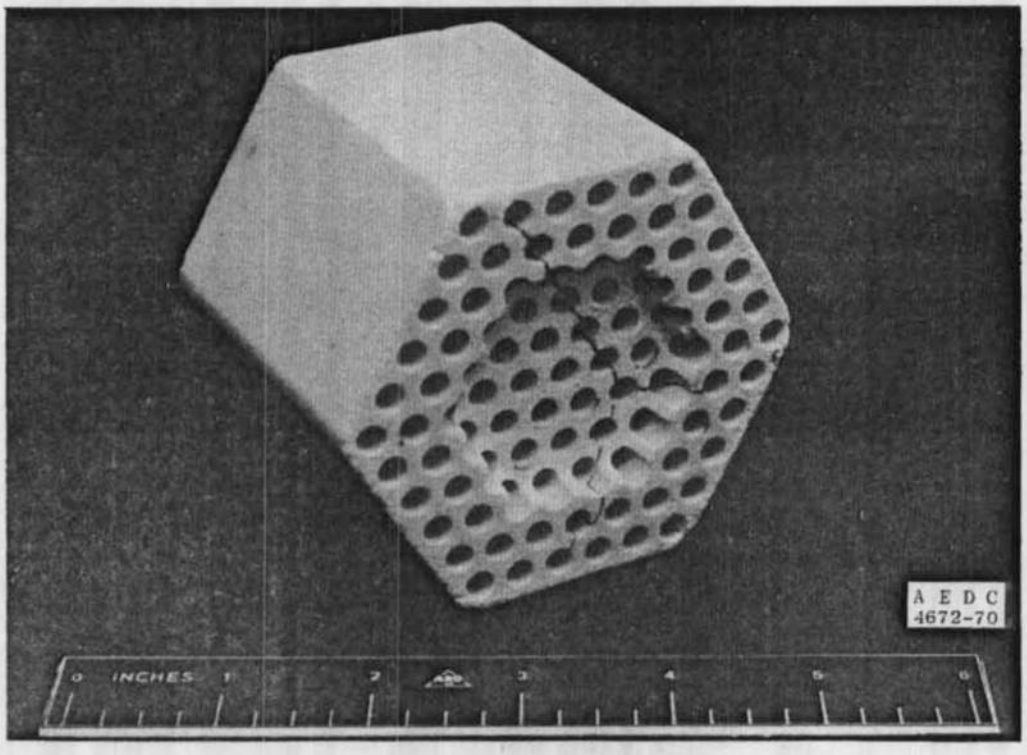

a. Zircoa, Low Density, 12.5 w/o, Upper Block
Fig. 16 Post-Run 39 Matrix Inspection

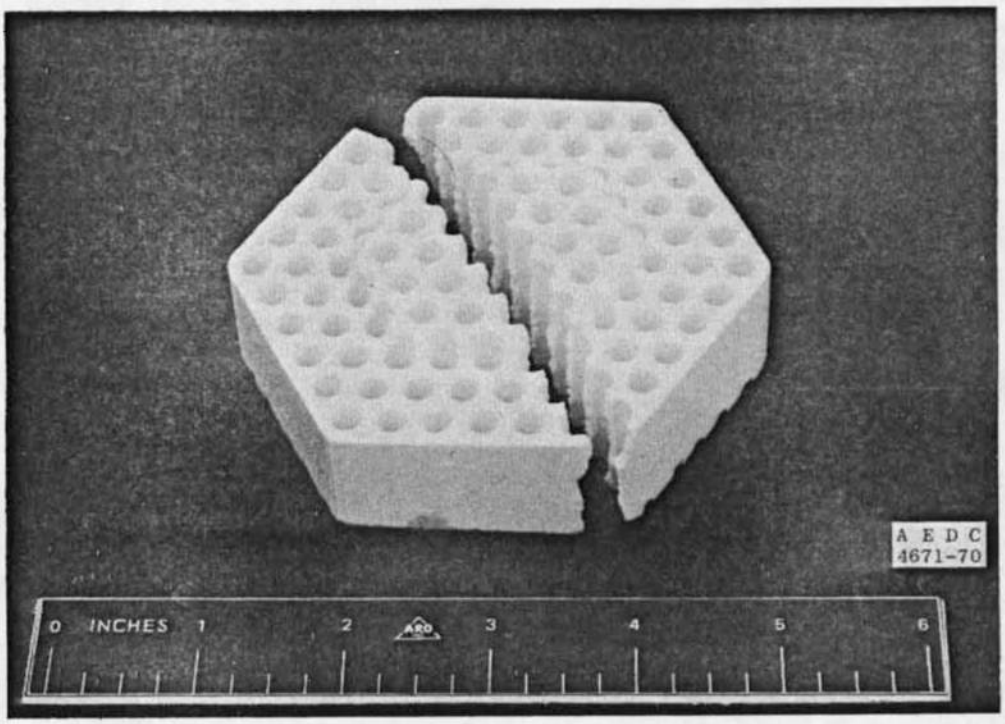

b. Zircoa, Low Density, 12.5 w/o, Lower Block

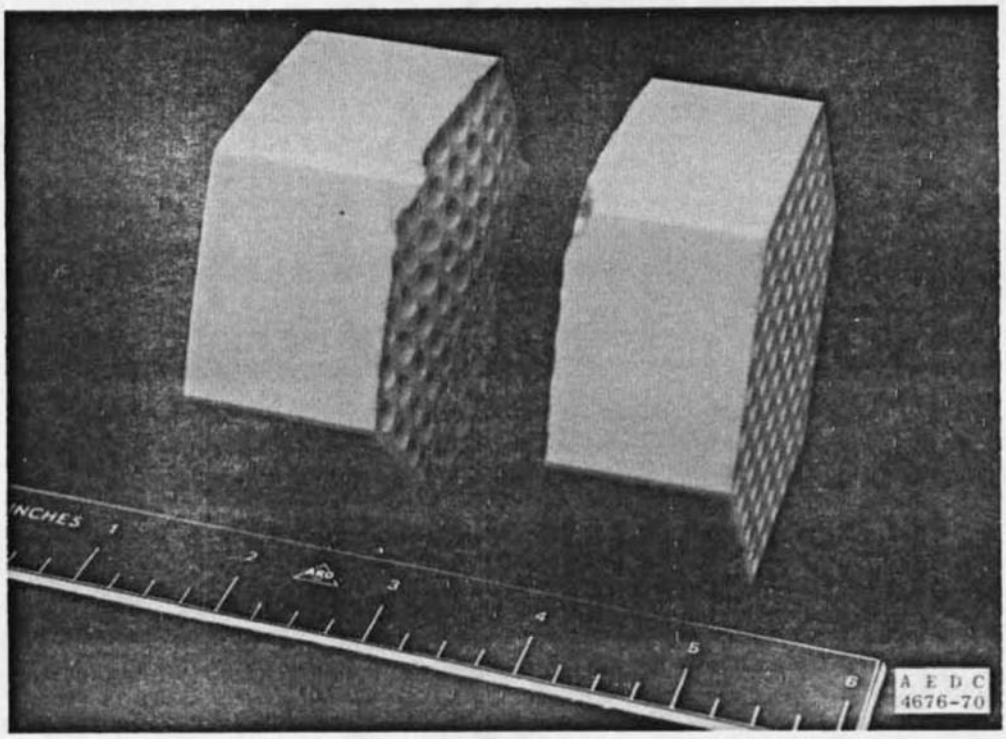

c. Column 7, 13.8 w/o, Coors
Fig. 16 Concluded

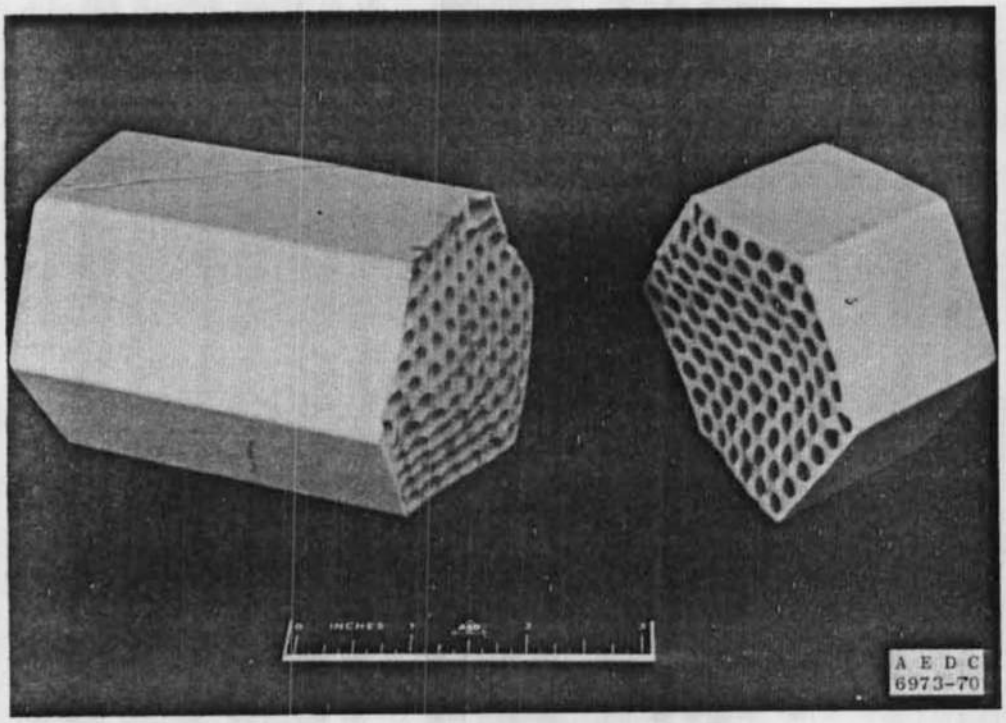

a. Column 10, 10.9 w/o, Coors

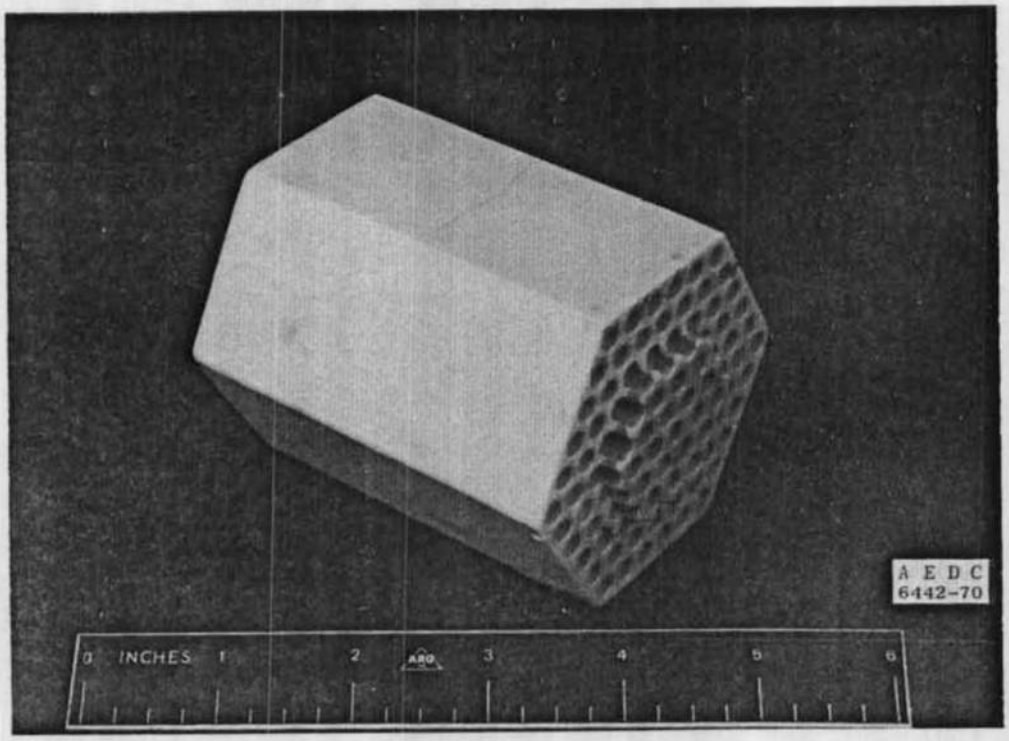

b. Column 8, 12.6 w/o, Coors

Fig. 17 Post-Run 44 Matrix Inspection

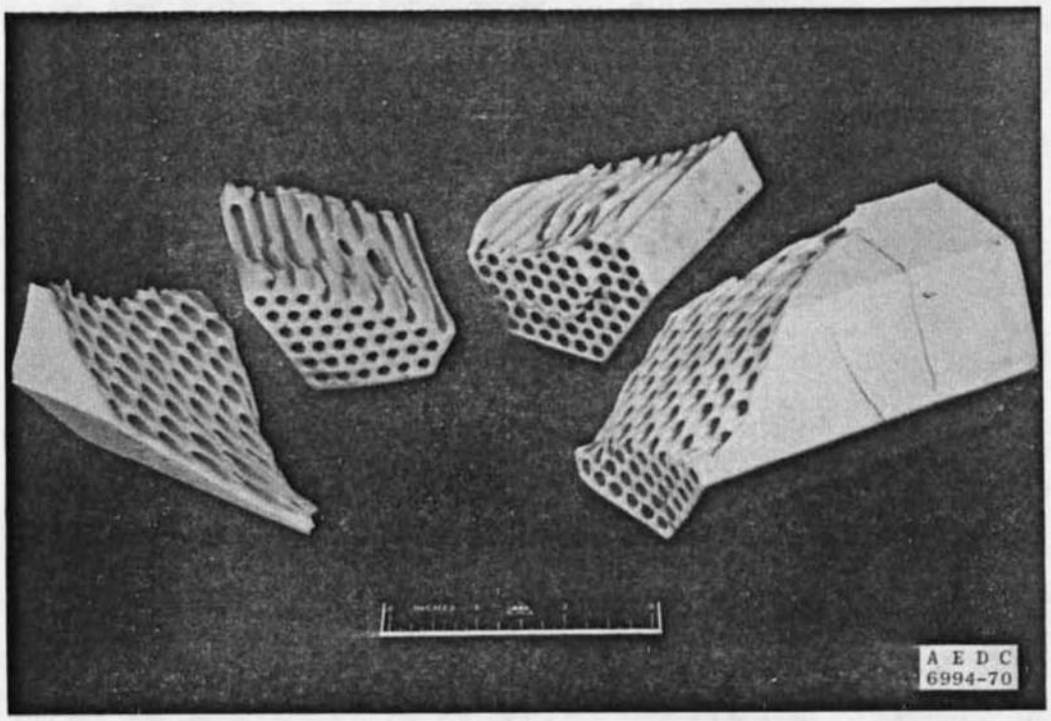

c. Column 17, 12.6 w/o, Coors

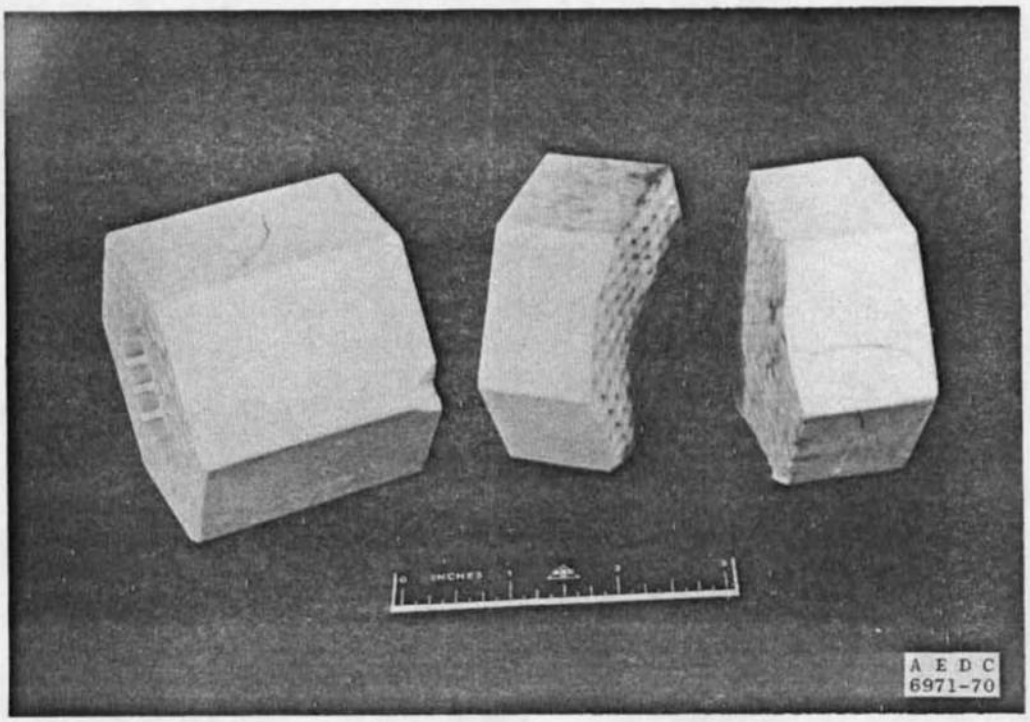

d. Column 7, 13.8 w/o, Coors
Fig. 17 Continued

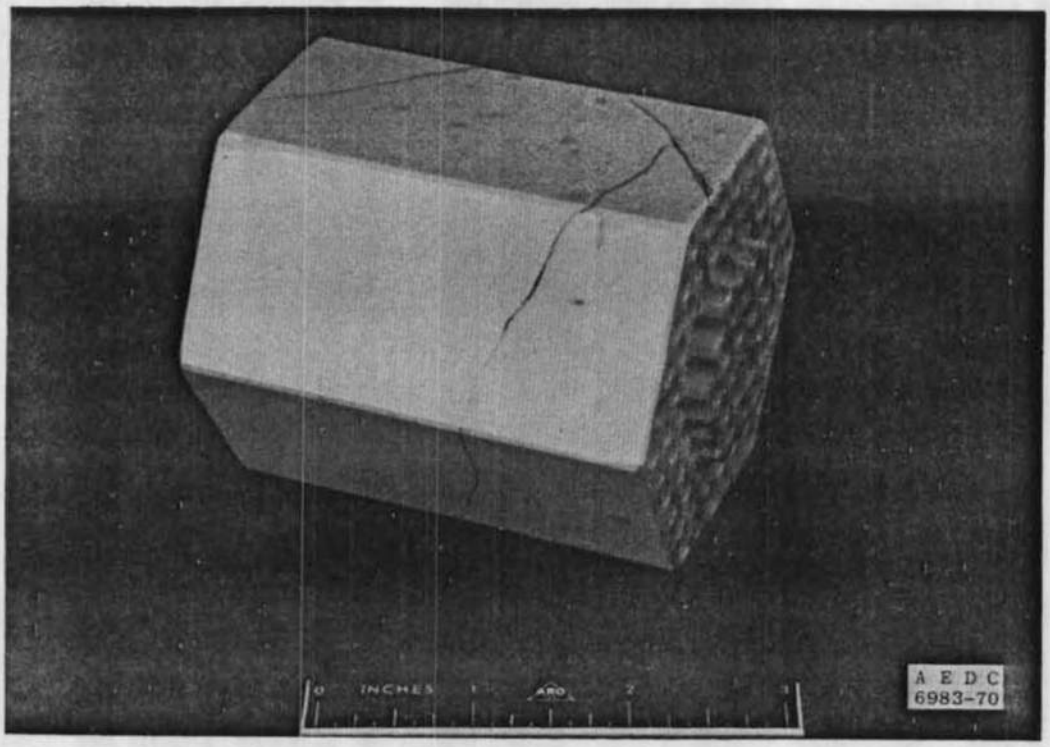

e. Column 14, 13.8 w/o, Coors

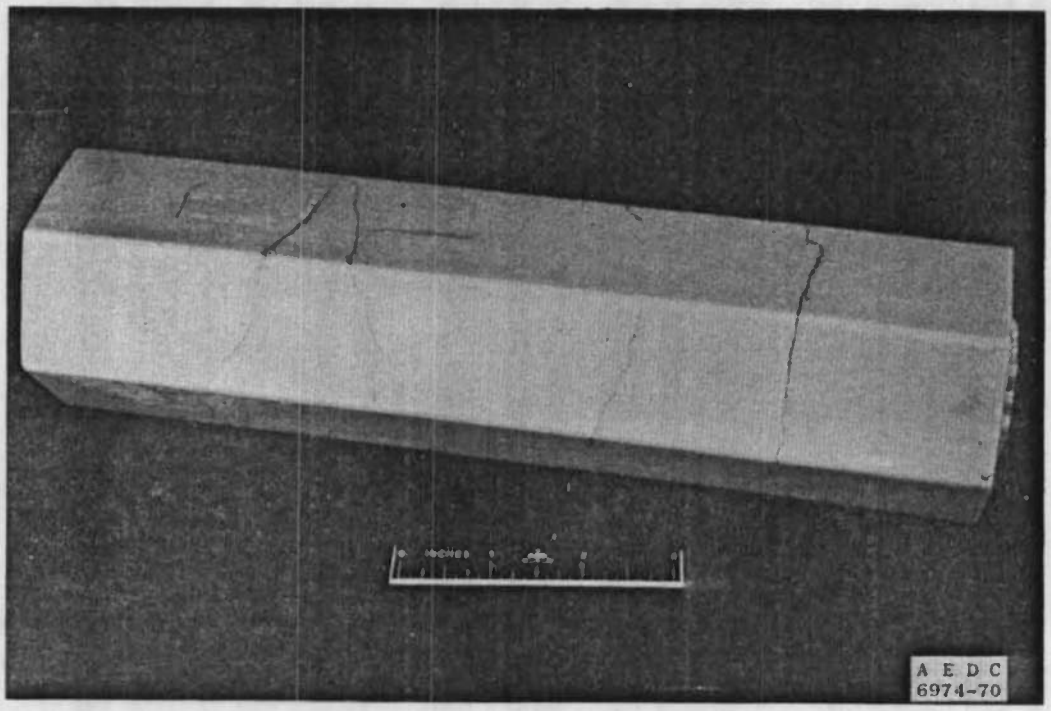

f. Column 11, 10.4 w/o, Coors
Fig. 17 Continued

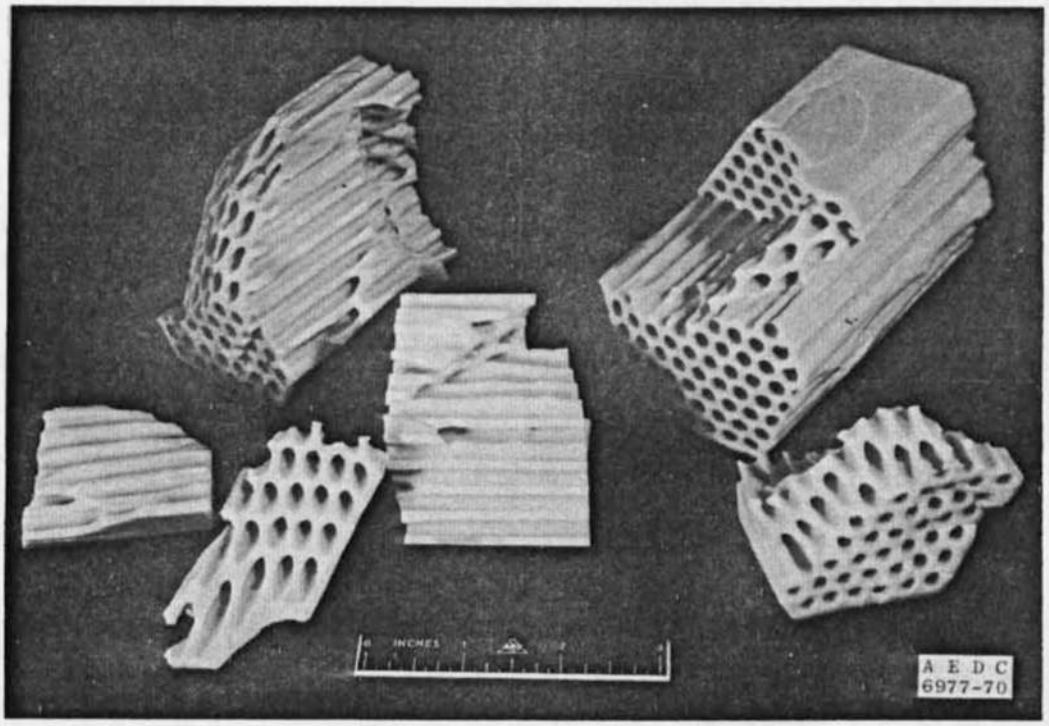

g. Column 13, 9.25 w/o, Coors

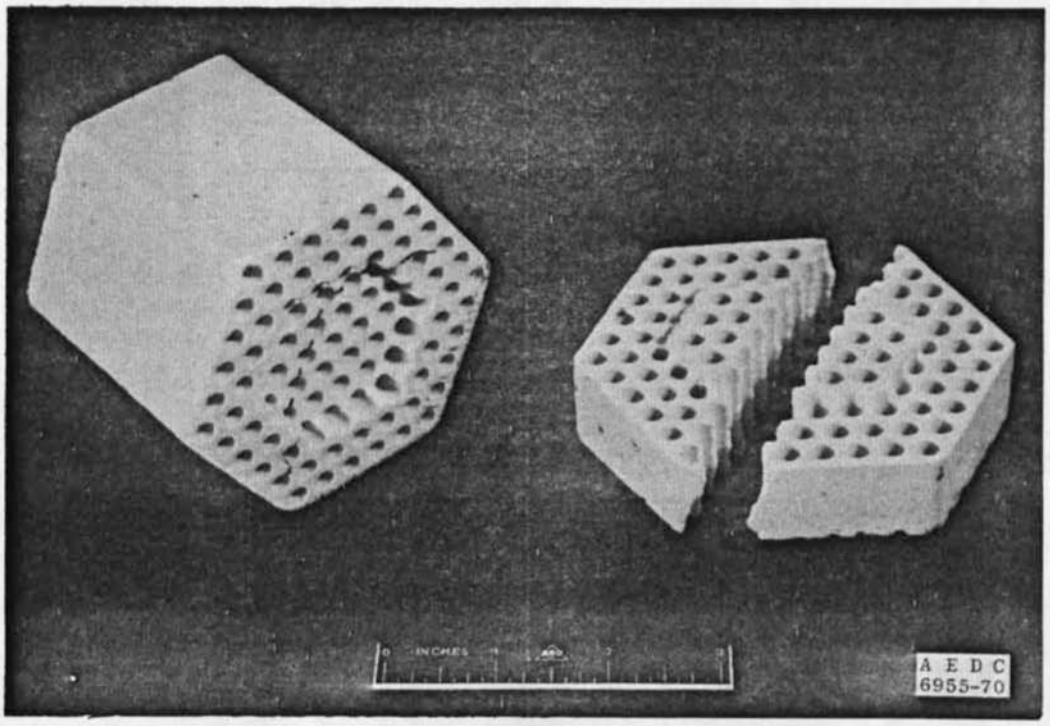

h. Zircoa, Low Density, 12.5 w/o
Fig. 17 Concluded

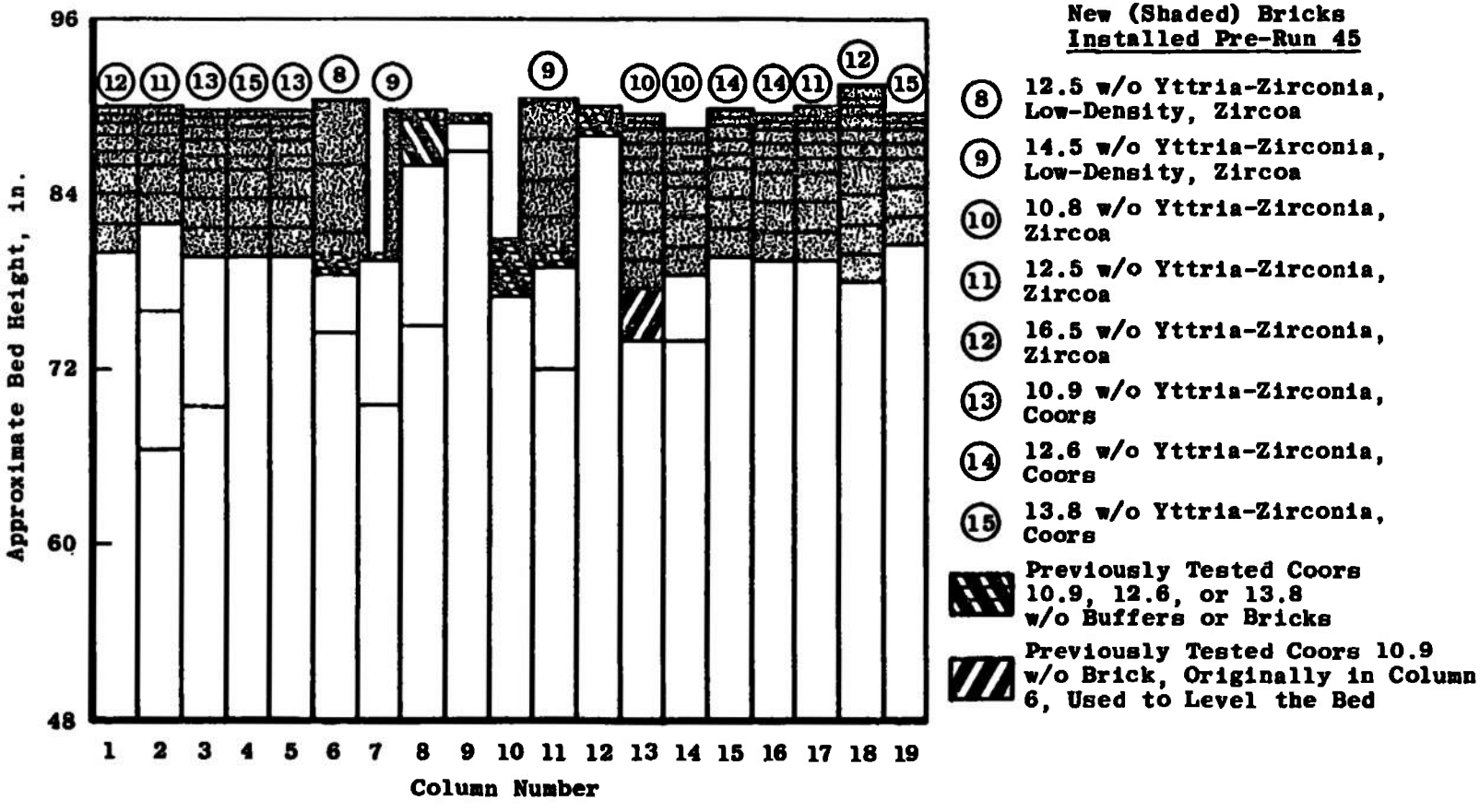

Fig. 18 Matrix Configuration, Runs 45 through 69

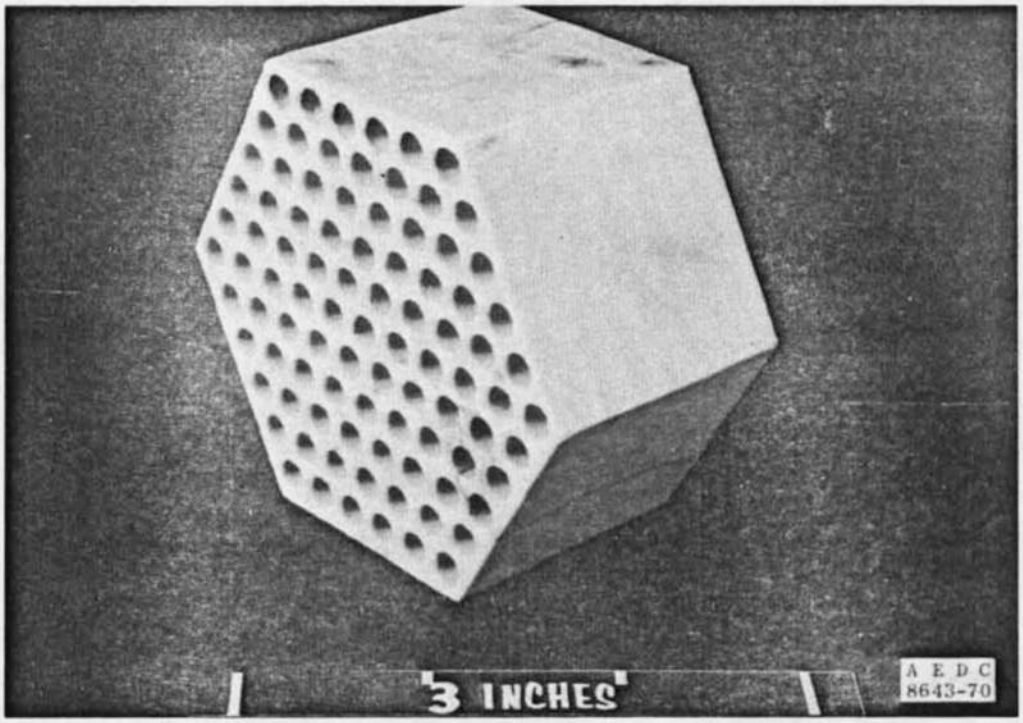

a. Coors, 12.6 w/o, Location 16-7

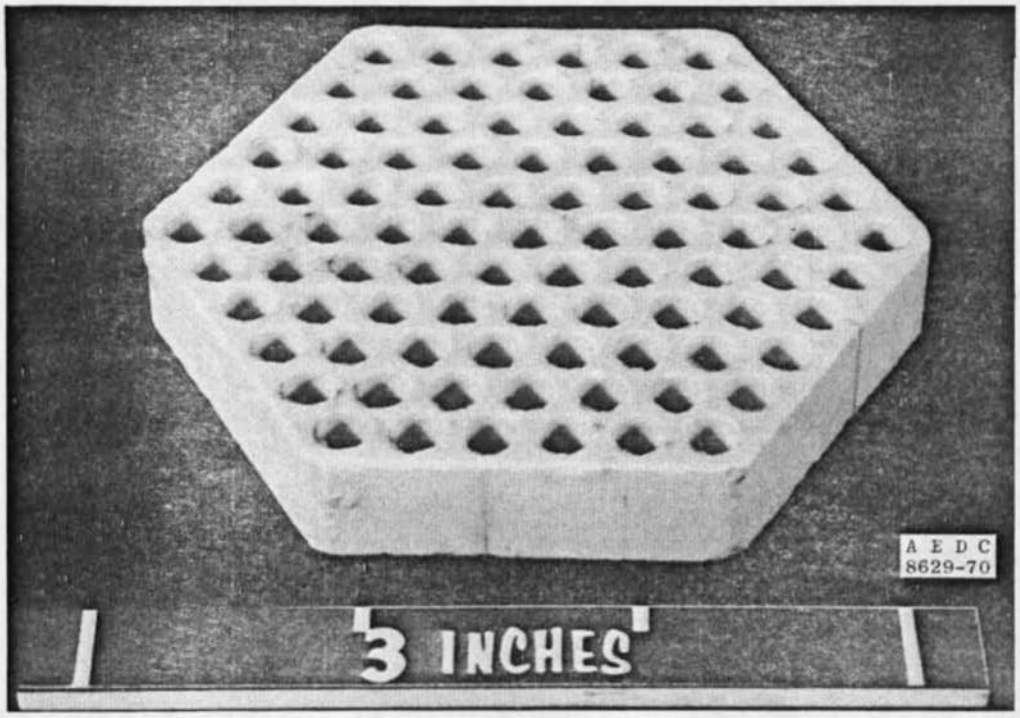

b. Coors, 13.8 w/o, Location 19-2

Fig. 19 Post-Run 69 Matrix Inspection

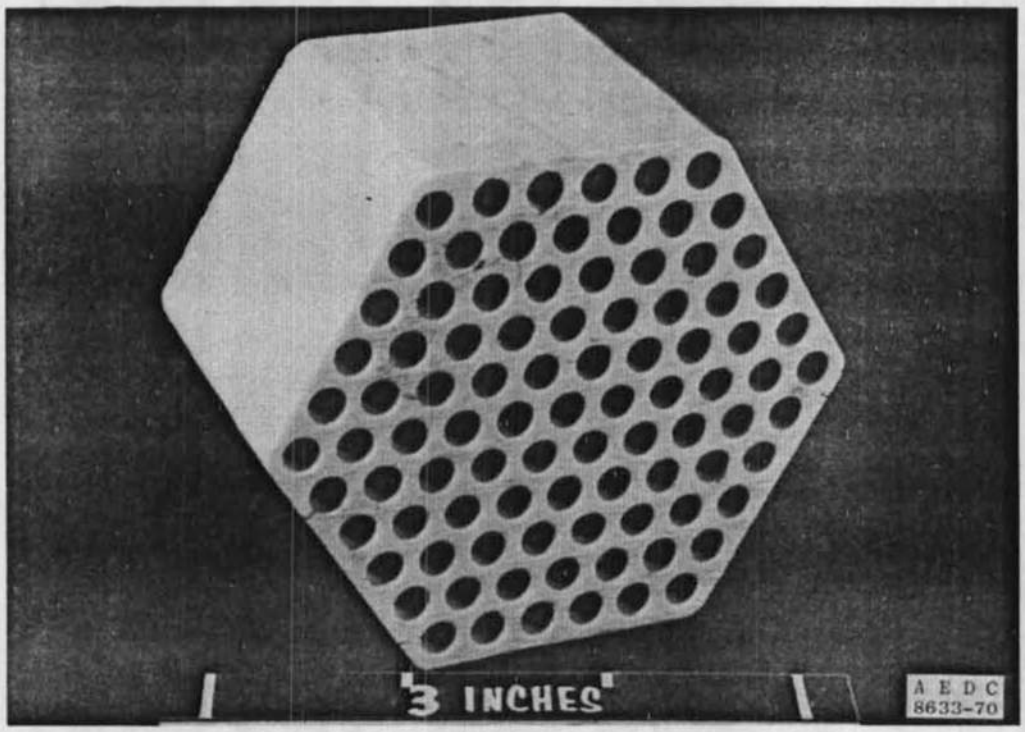

c. Coors, 13.8 w/o, Location 19-5

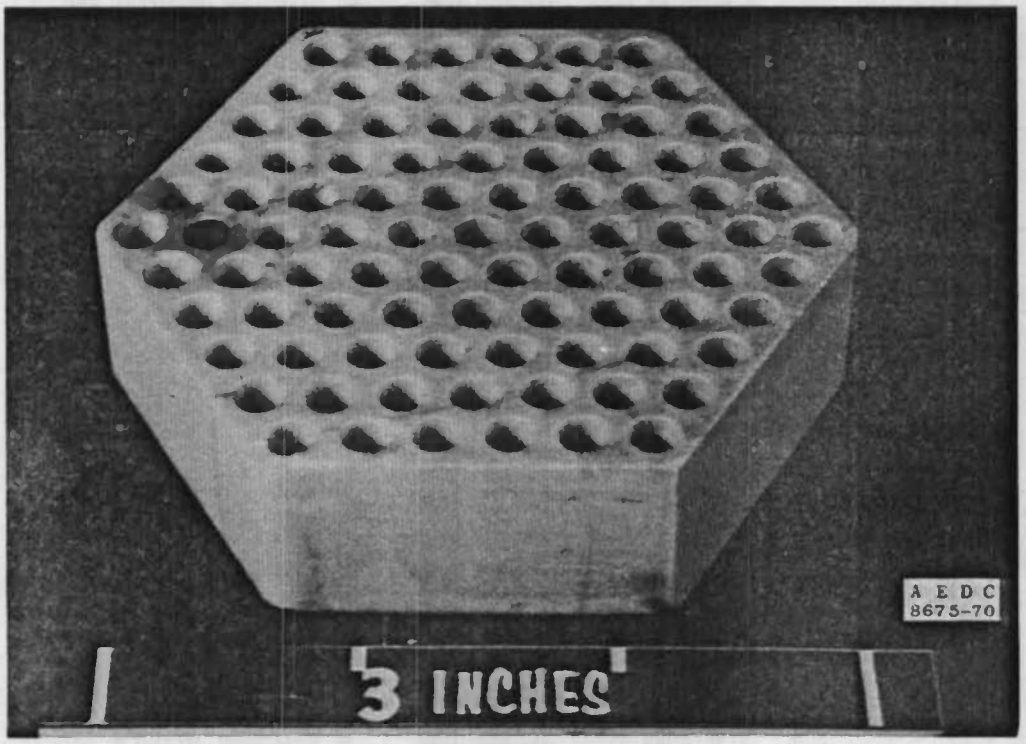

d. Zircoa, 10.8 w/o, Location 14-3
Fig. 19 Continued

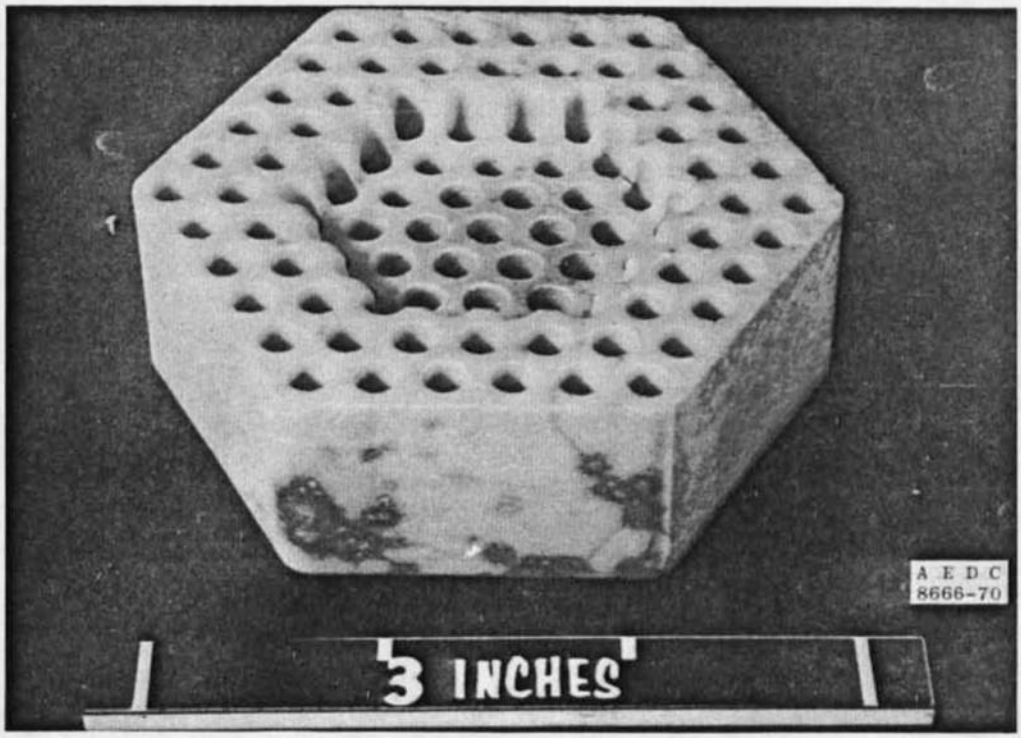

e. Zircoa, 12.5 w/o, Location 17-4

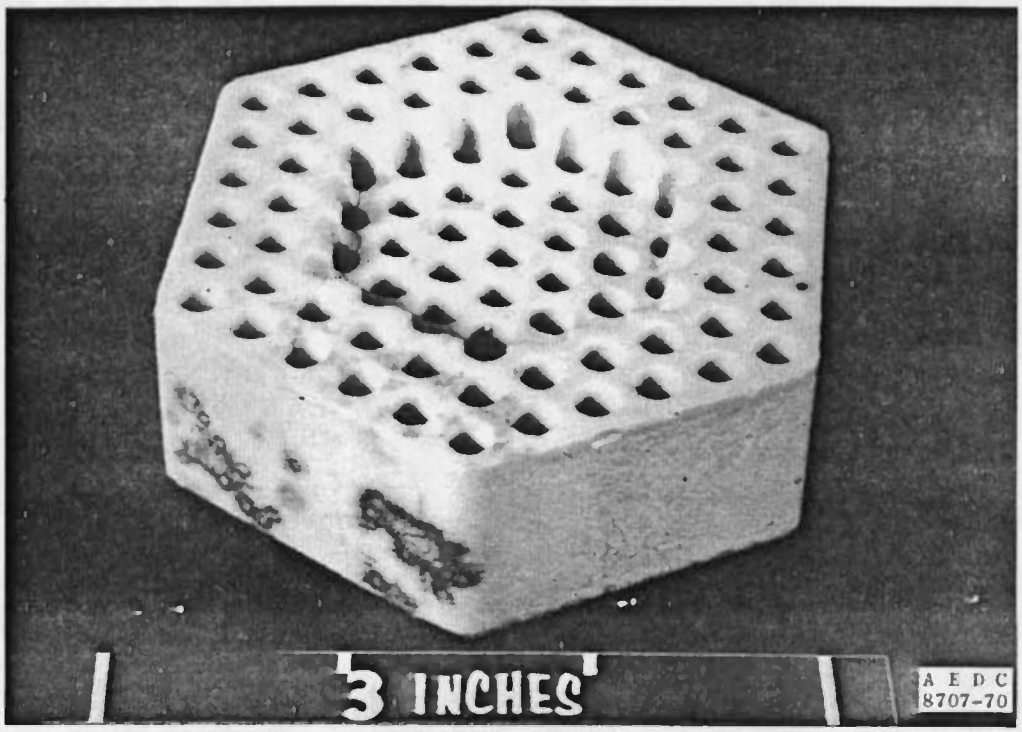

f. Zircoa, 16.5 w/o, Location 18-5
Fig. 19 Continued

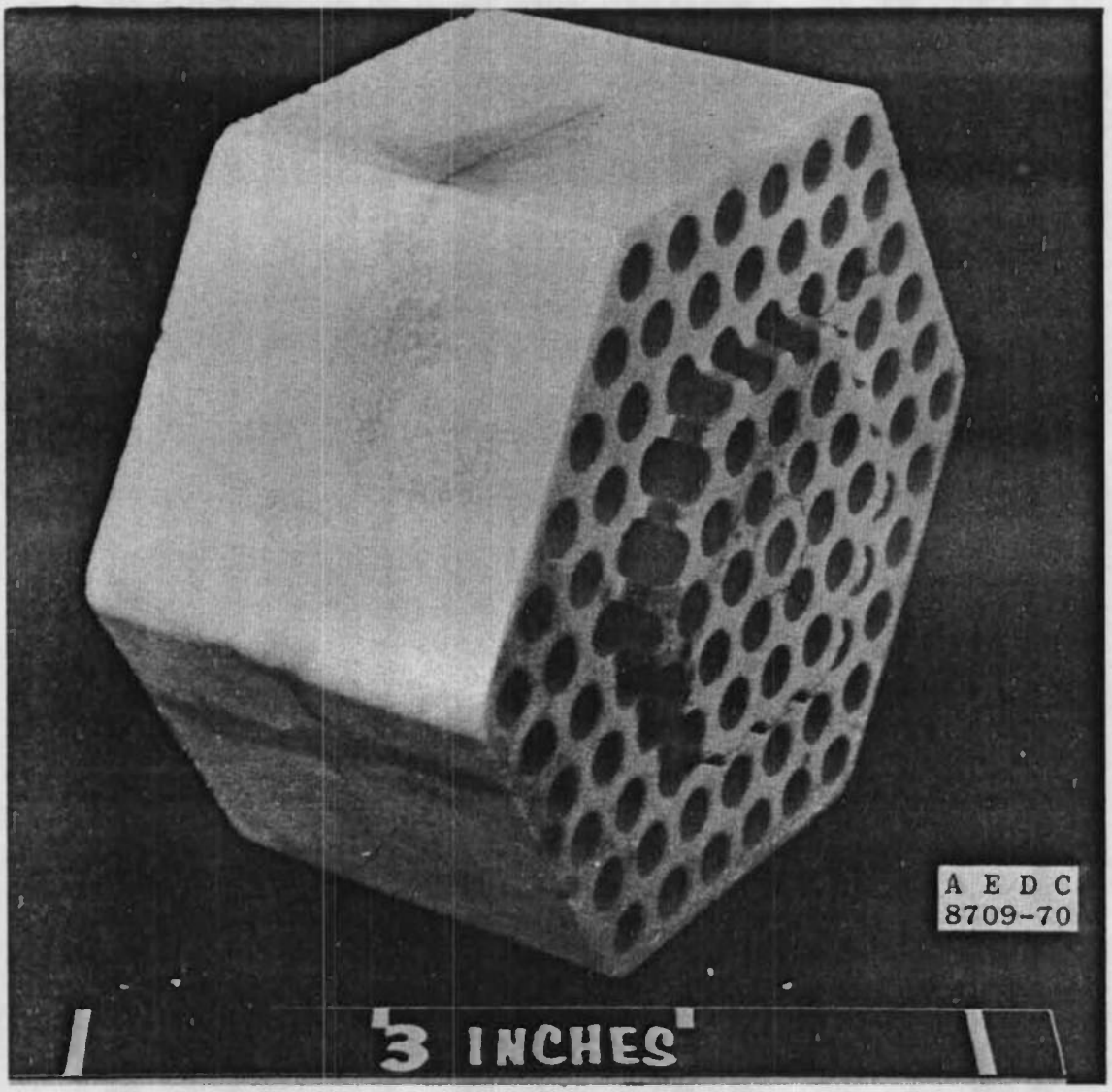

g. Zircoa, 16.5 w/o, Location 18-7
Fig. 19 Concluded

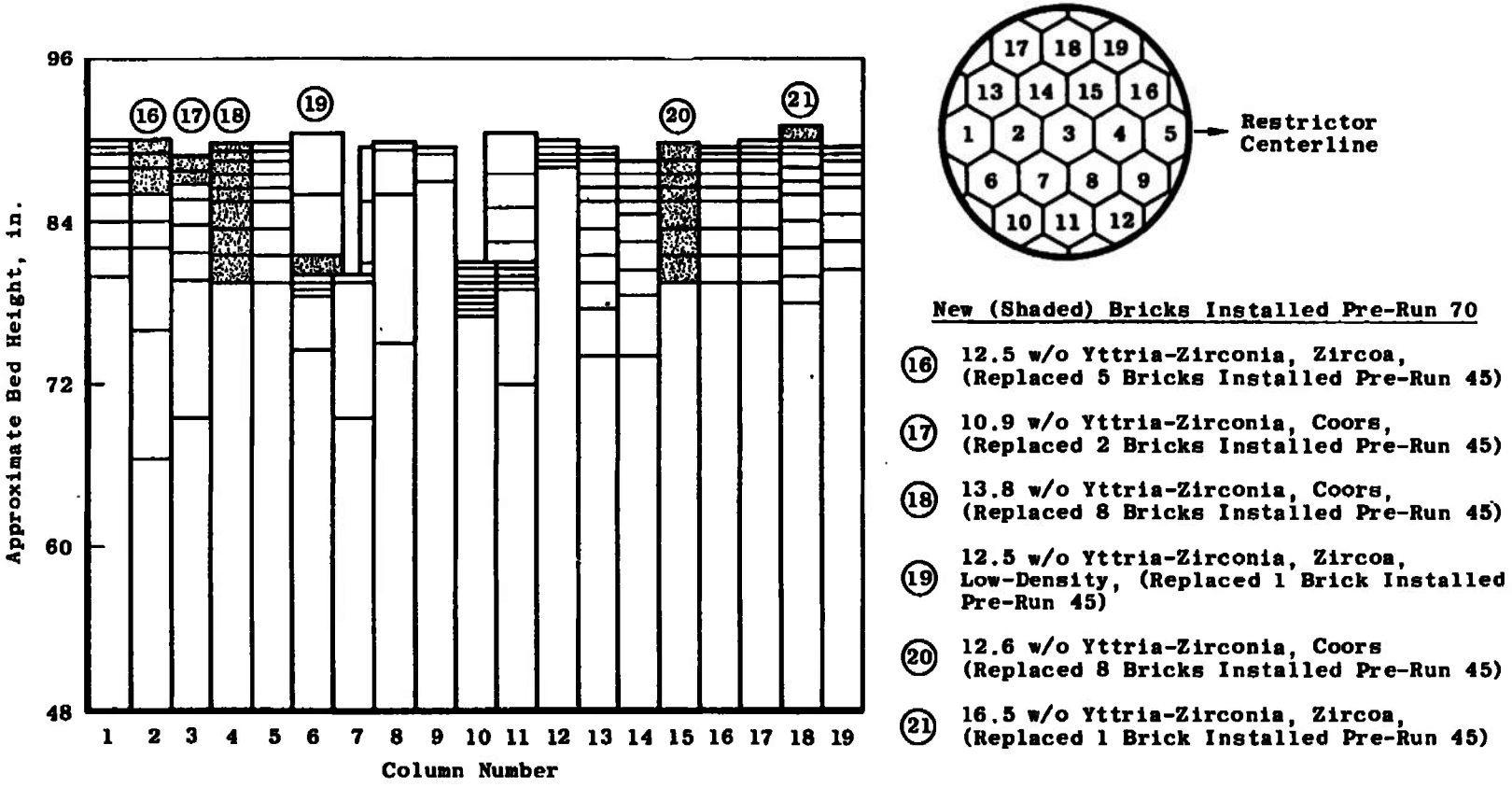

Fig. 20 Matrix Configuration, Runs 70 through 74

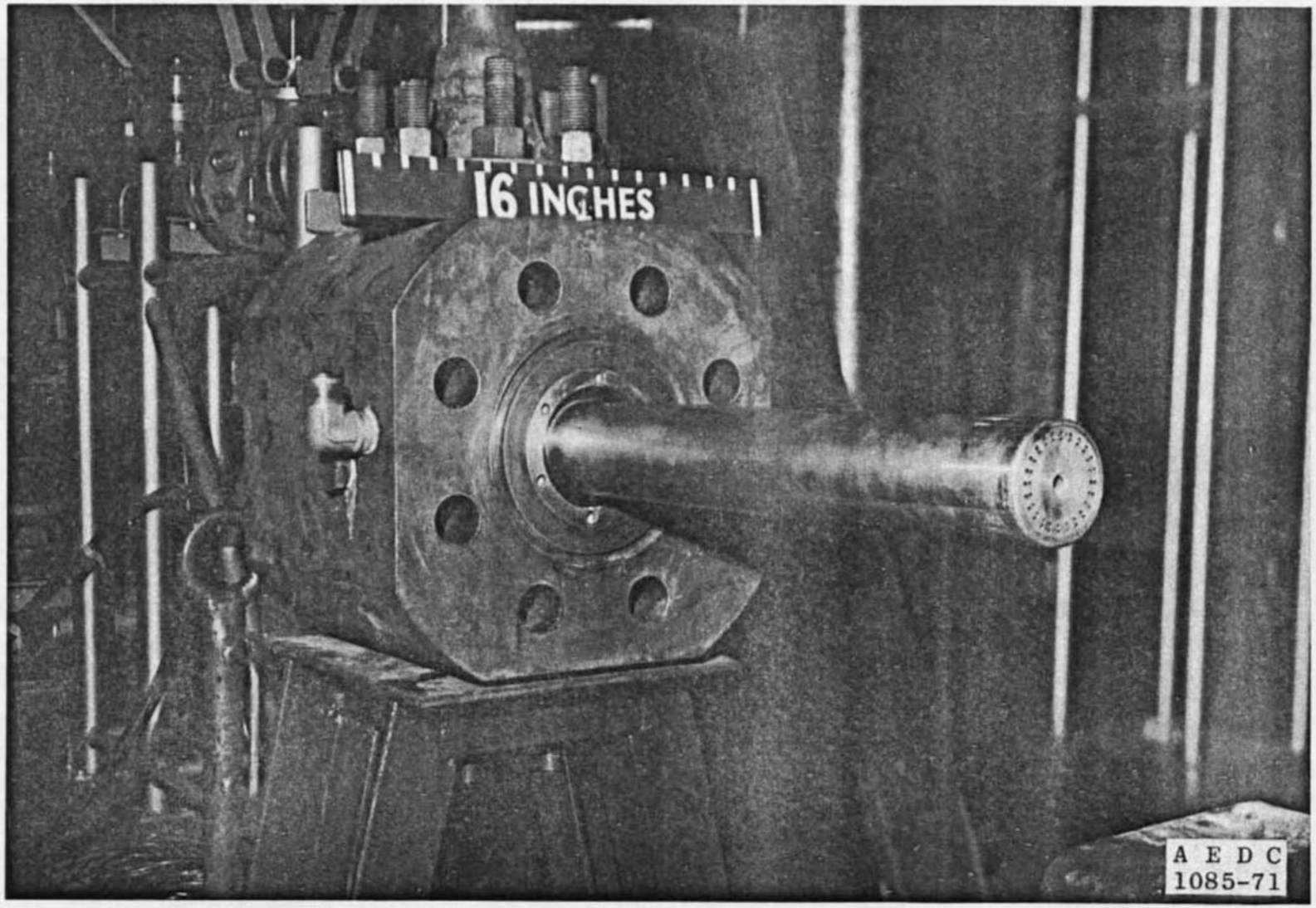

Fig. 21 Second-Generation Burner

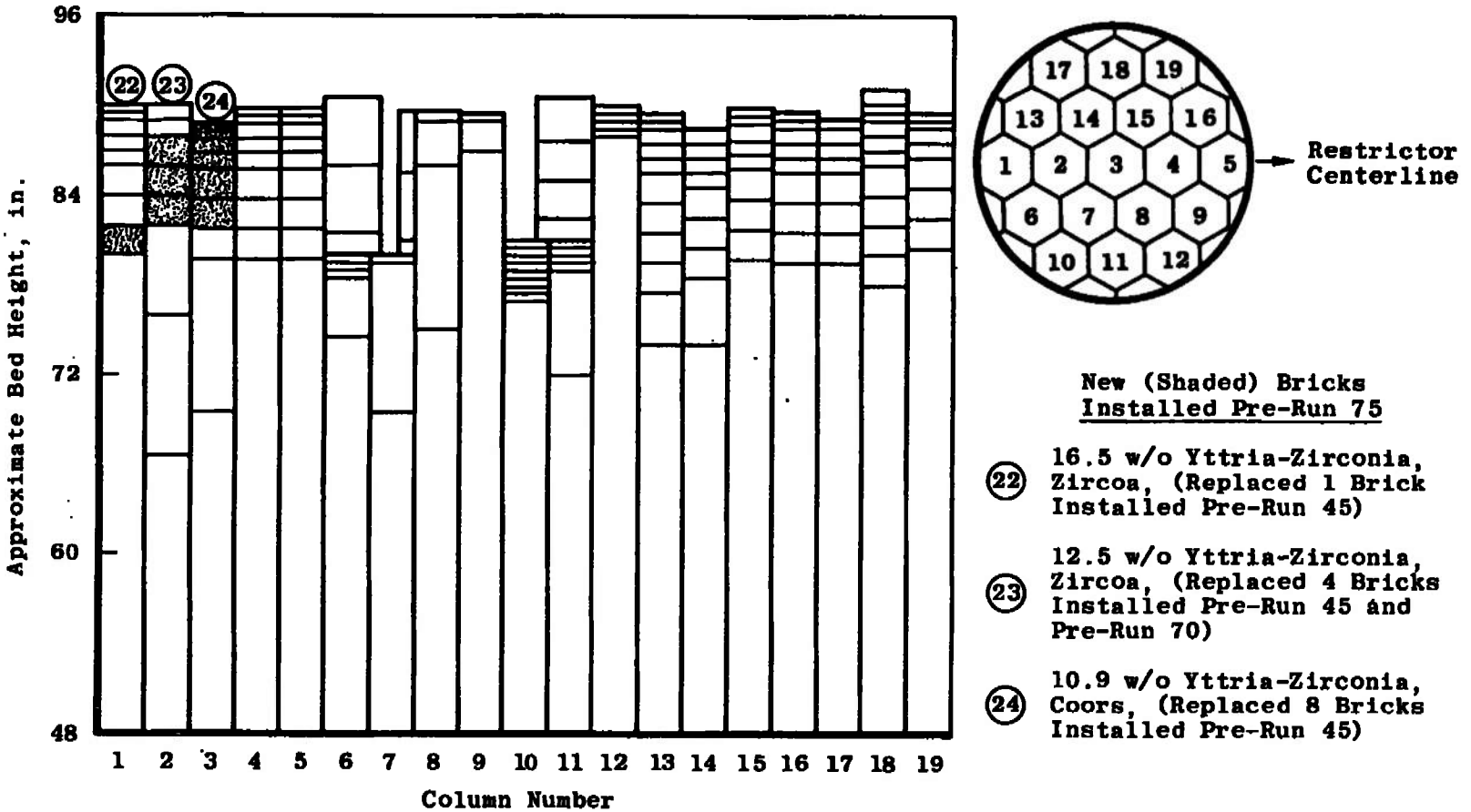

Fig. 22 Matrix Configuration, Runs 75 through 85

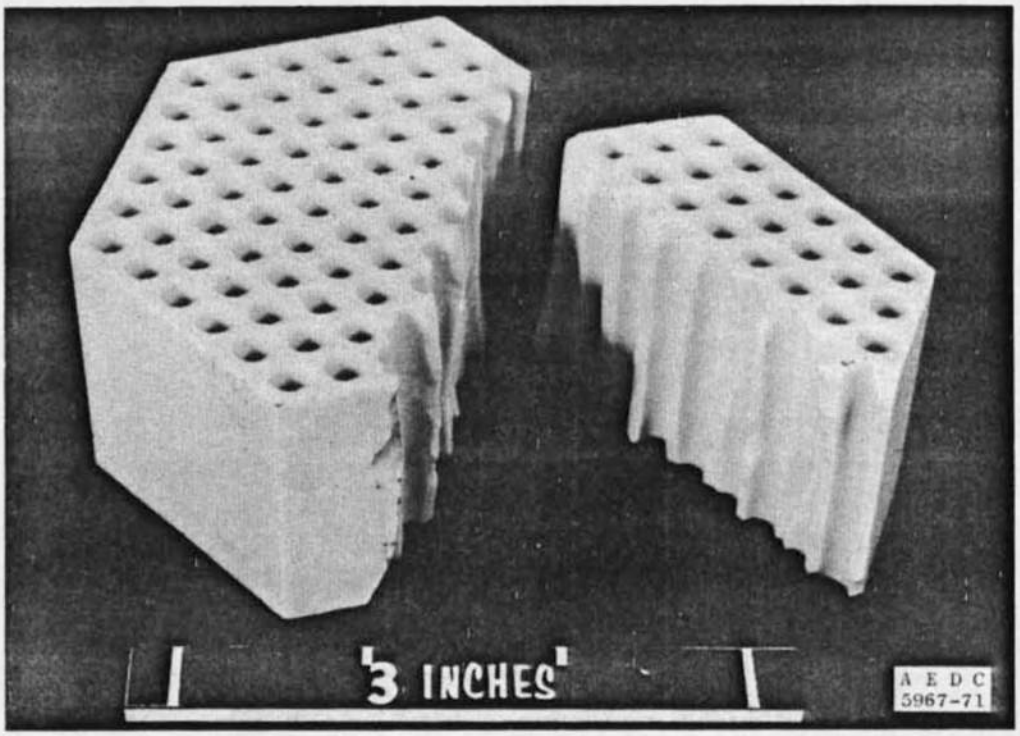

a. Coors, 12.6 w/o, Location 16-7

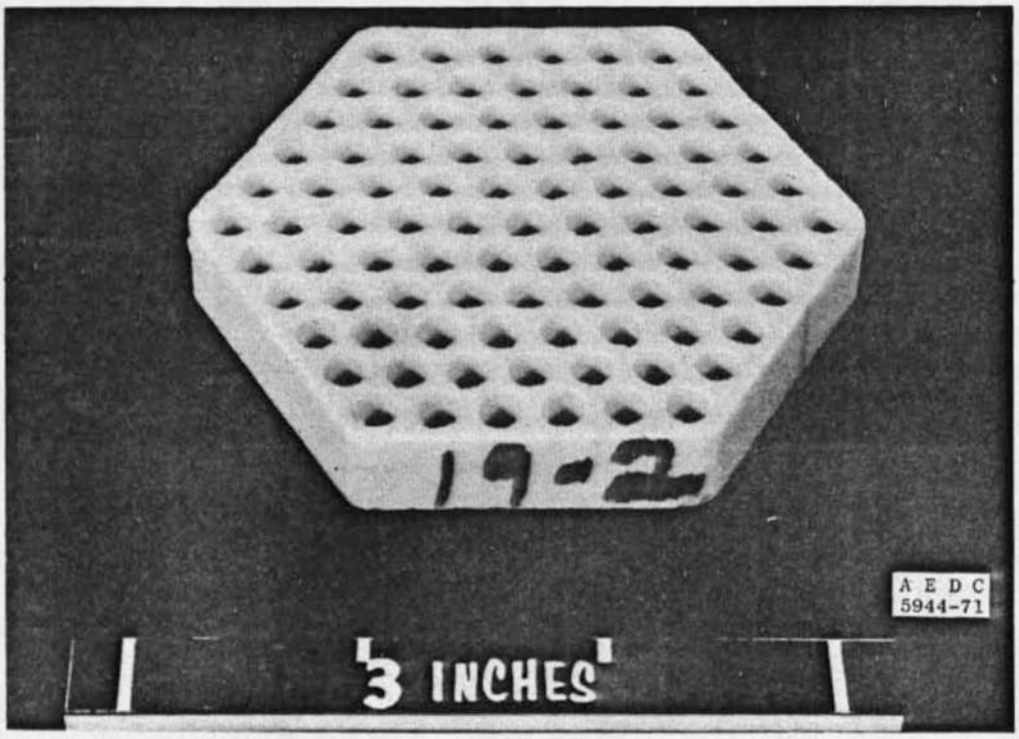

b. Coors, 13.8 w/o, Location 19-2

Fig. 23 High Density Sample Bricks, Post-Run 85

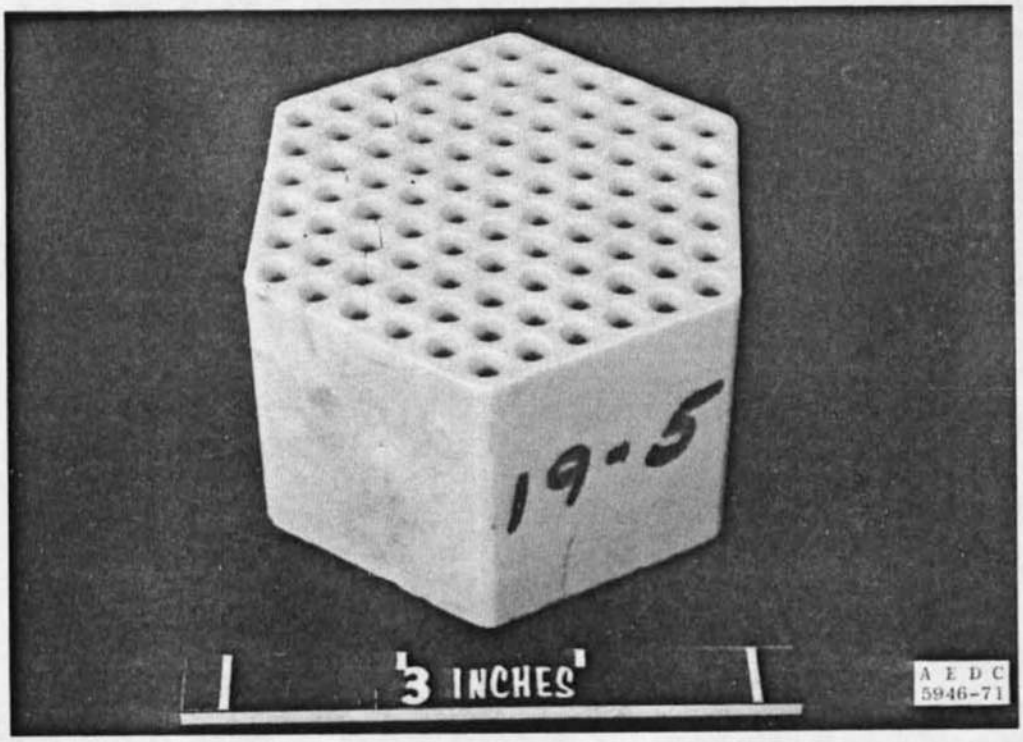

c. Coors, 13.8 w/o, Location 19-5

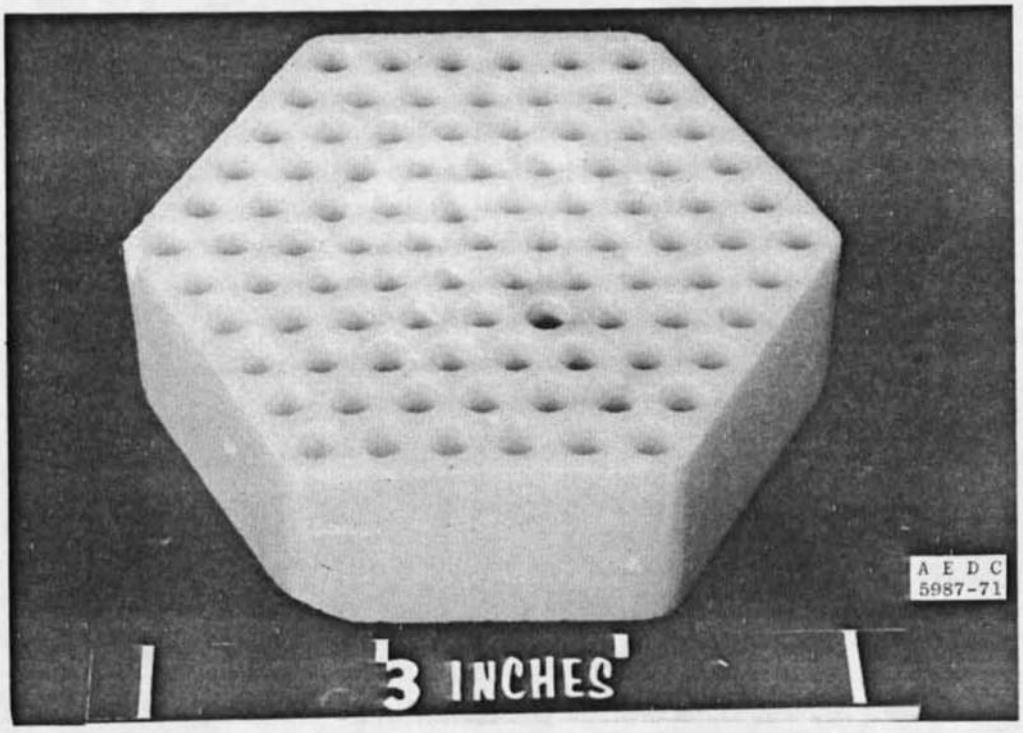

d. Zircoa, 10.8 w/o, Location 14-3
Fig. 23 Continued

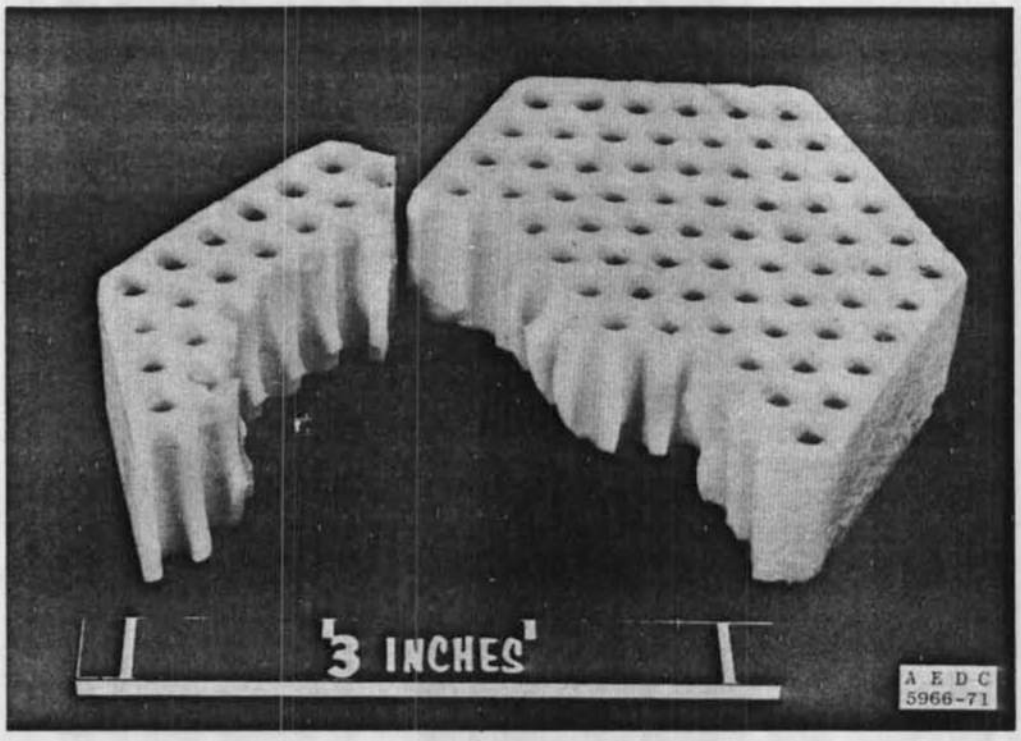

e. Zircoa, 12.5 w/o, Location 17-4

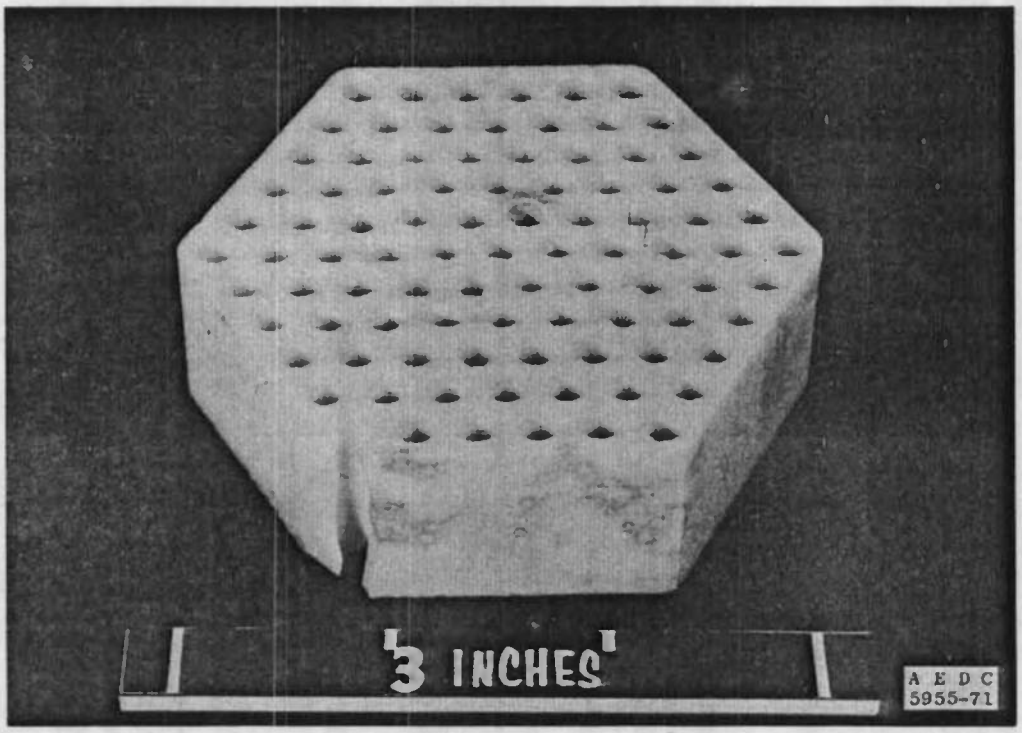

f. Zircoa, 16.5 w/o, Location 18-5
Fig. 23 Continued

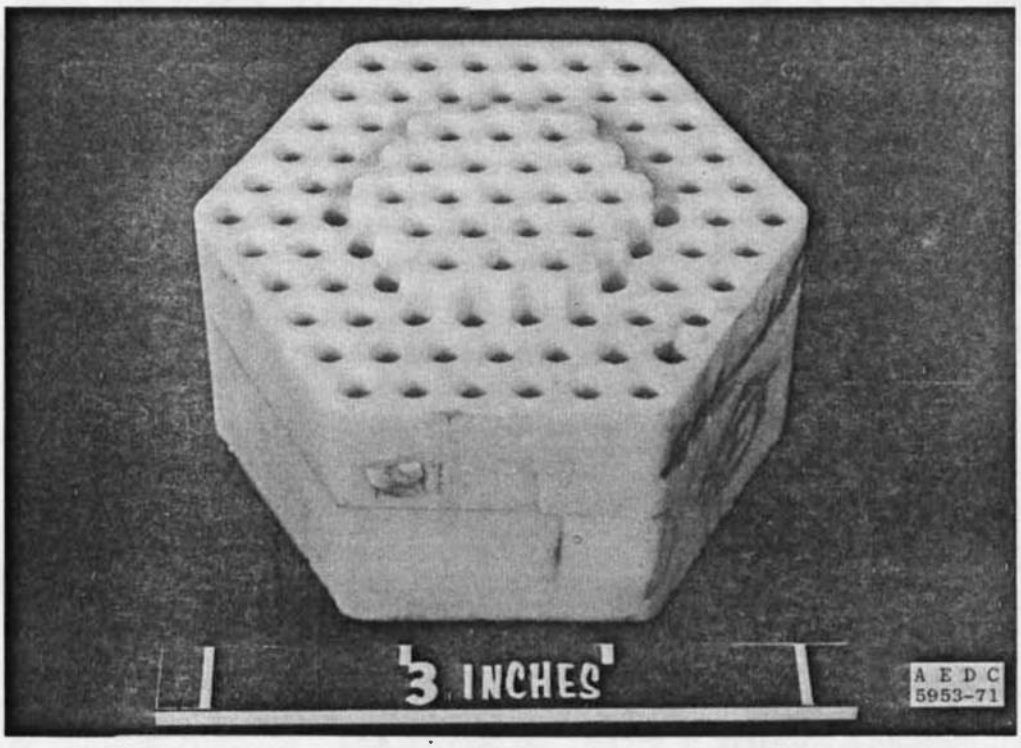

g. Zircoa, 16.5 w/o, Location 18-7

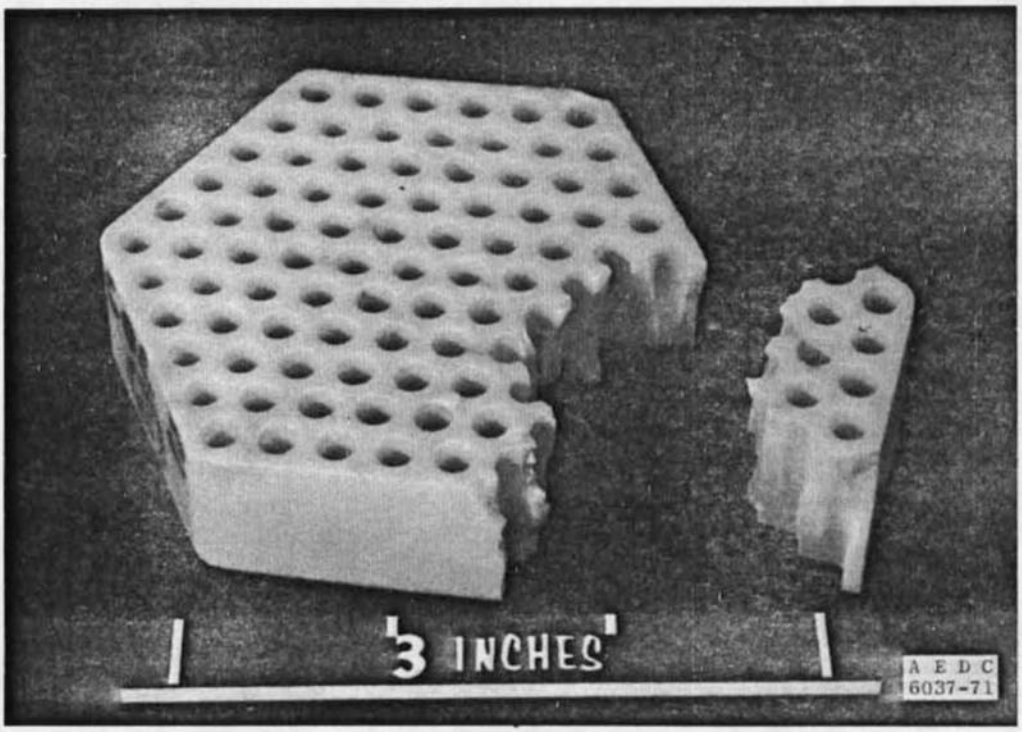

h. Zircoa, 12.5 w/o, Location 2-2
Fig. 23 Continued

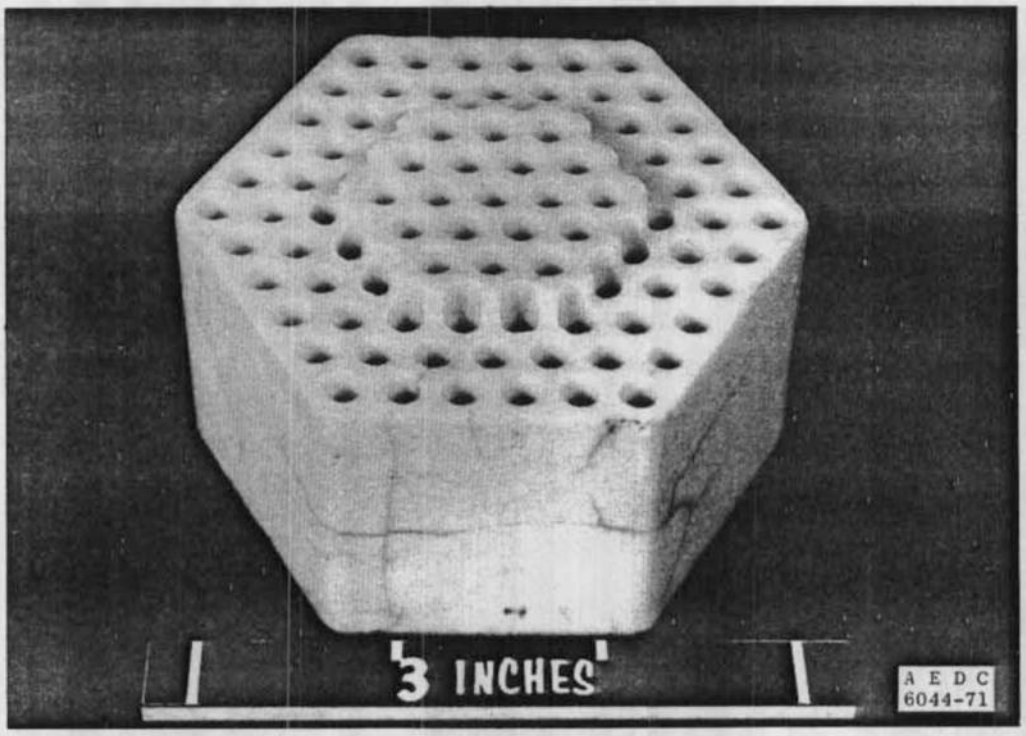

i. Zircoa, 16.5 w/o, Location 1-8
Fig. 23 Concluded

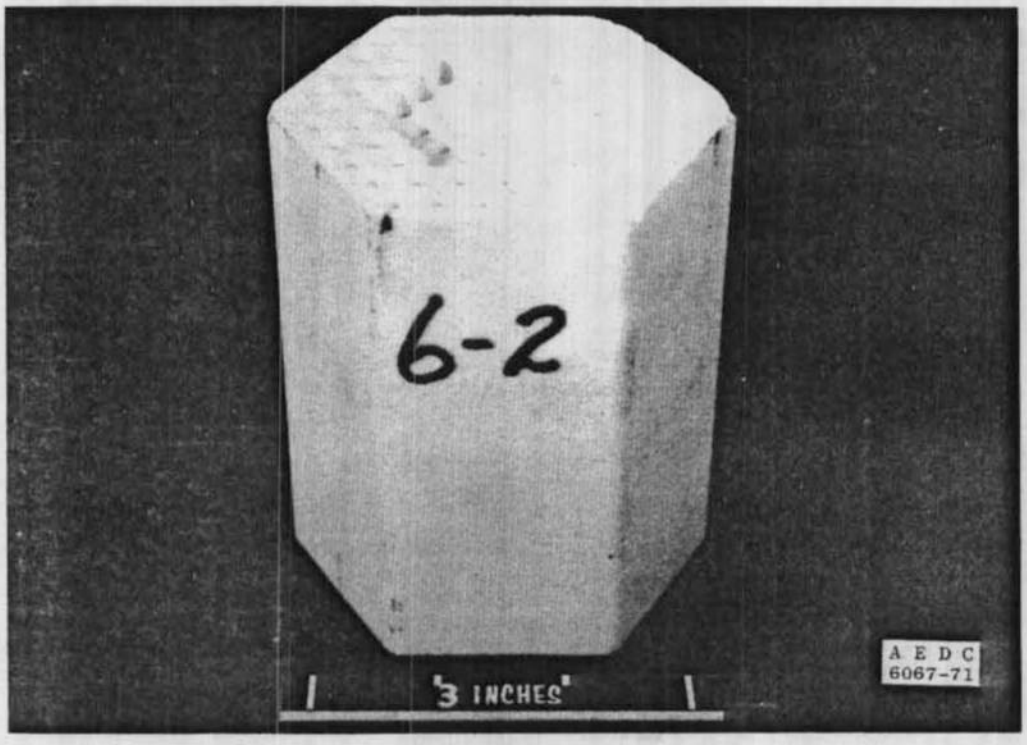

a. Zircoa, 12.5 w/o, Location 6-2
Fig. 24 Low Density Sample Bricks, Post-Run 85

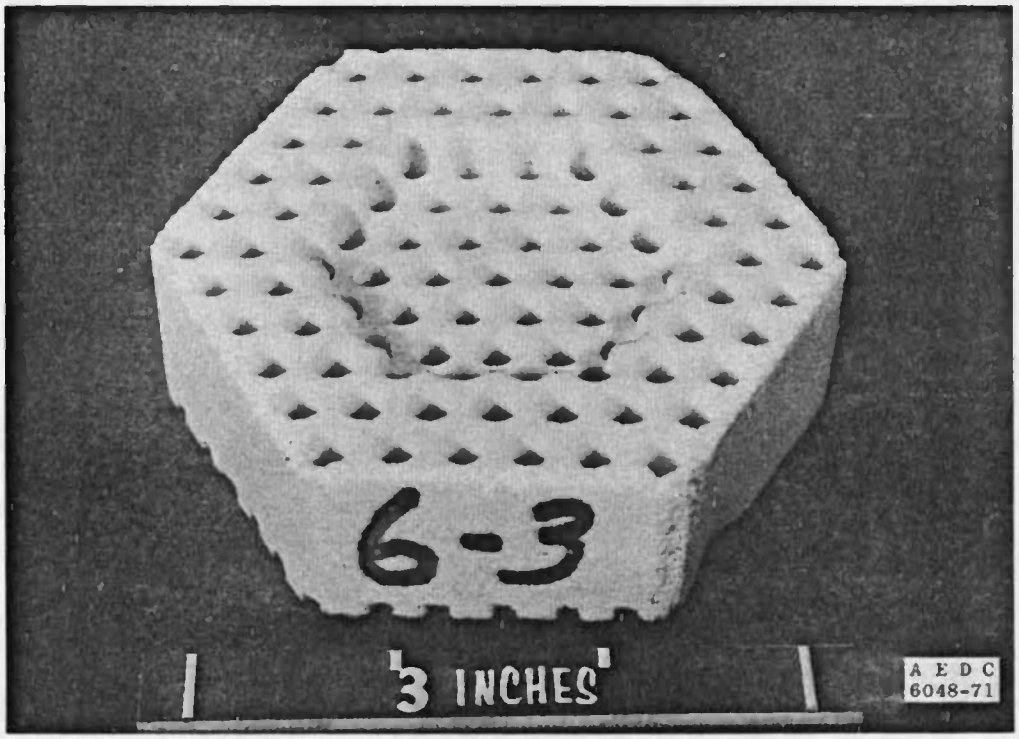

b. Zircoa, 12.5 w/o, Location 6-3

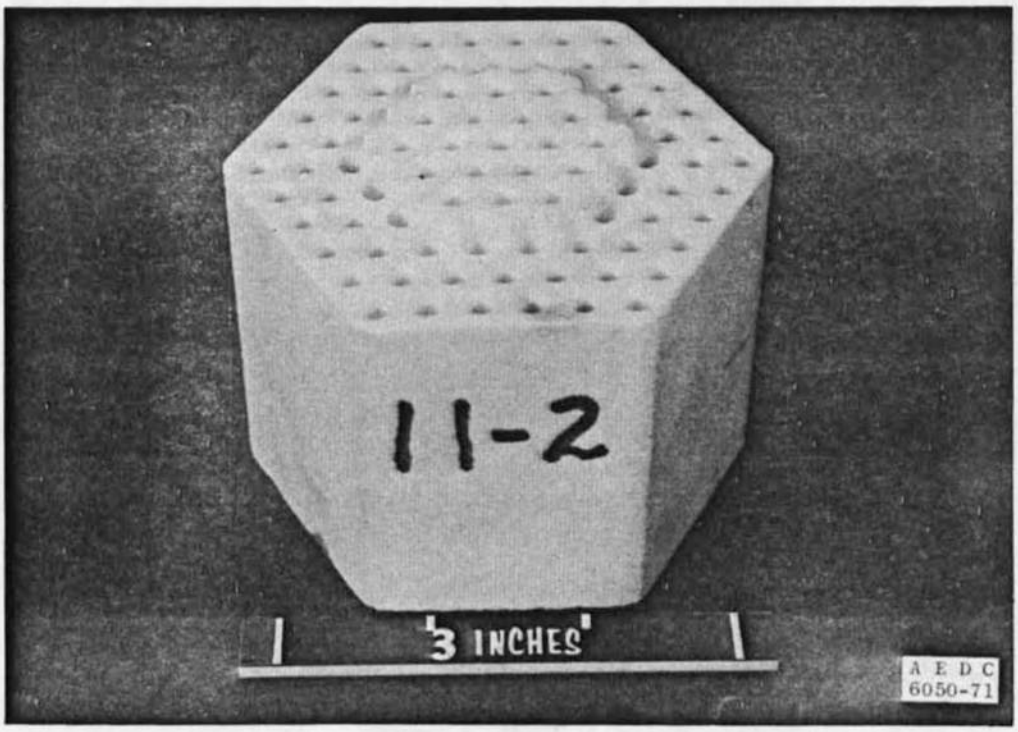

c. Zircoa, 14.5 w/o, Location 11-2
Fig. 24 Continued

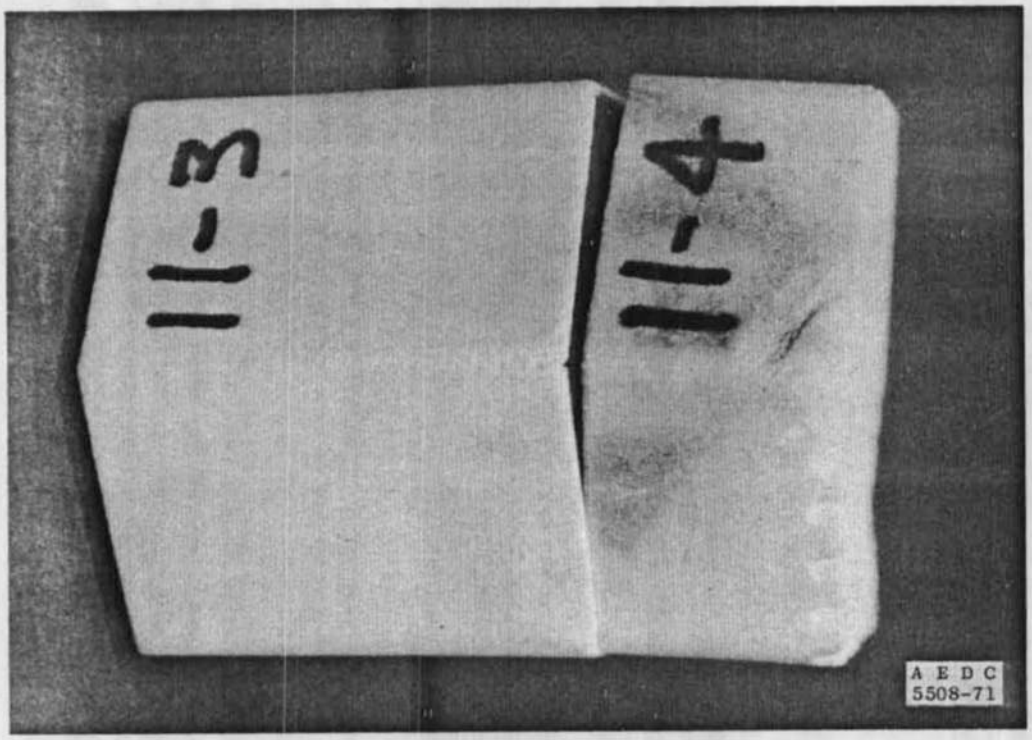

d. Zircoa, 14.5 w/o, Location 11-3 and 11-4

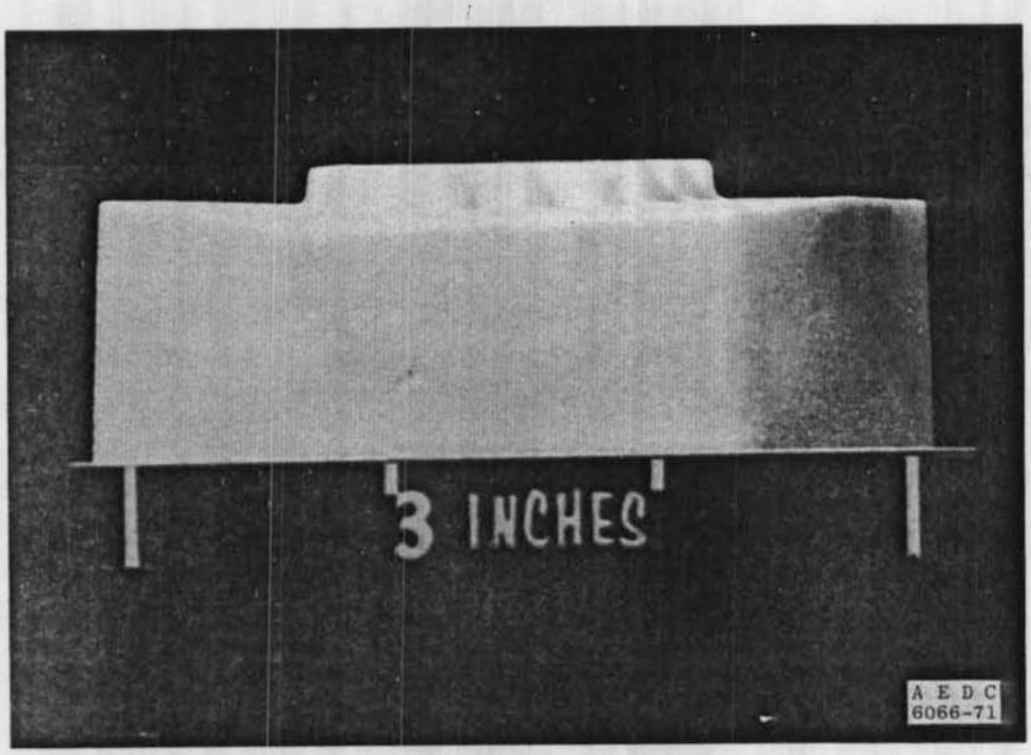

e. Zircoa, 14.5 w/o, Location 11-4
Fig. 24 Concluded

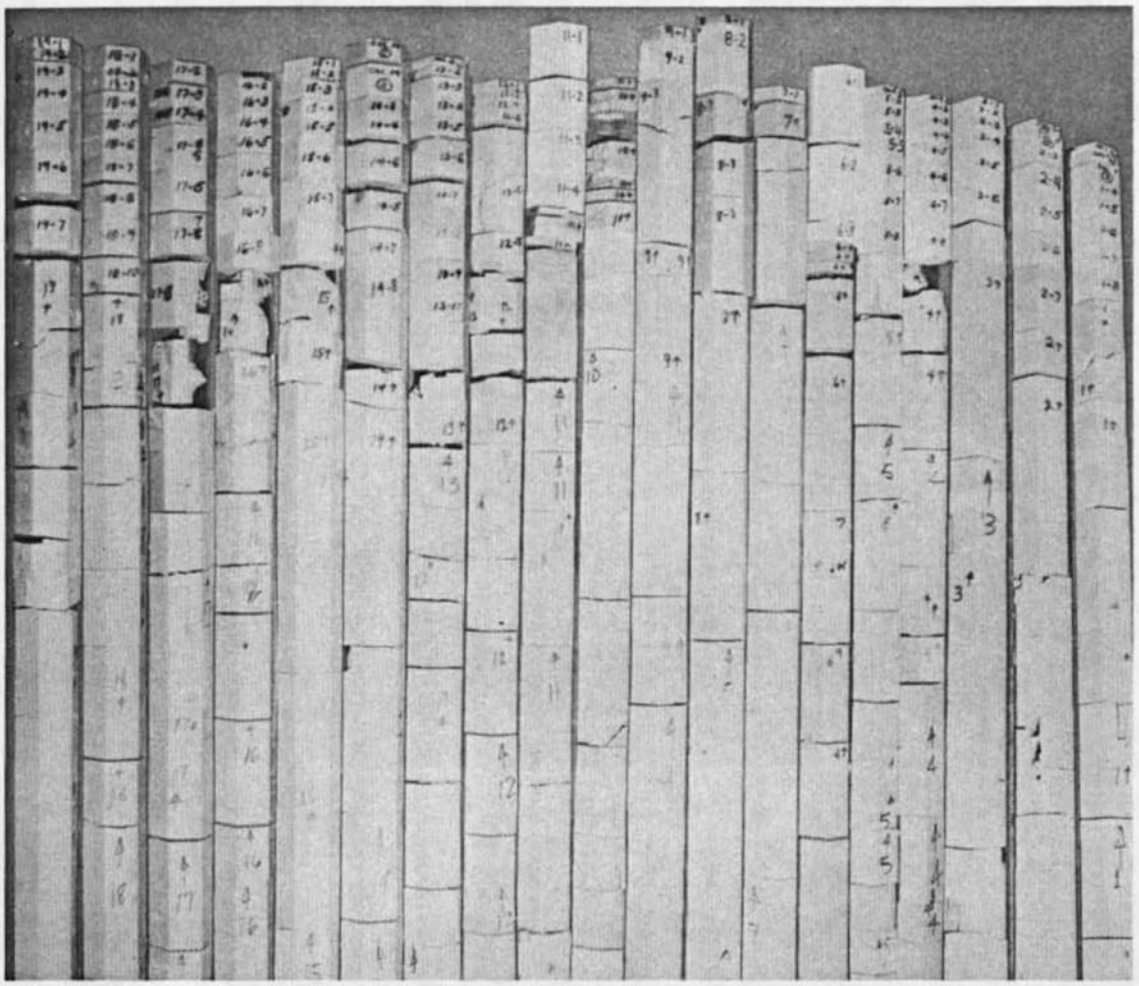

a. Upper Portion

Fig. 25 Zirconia Matrix Overall View, Post-Run 85

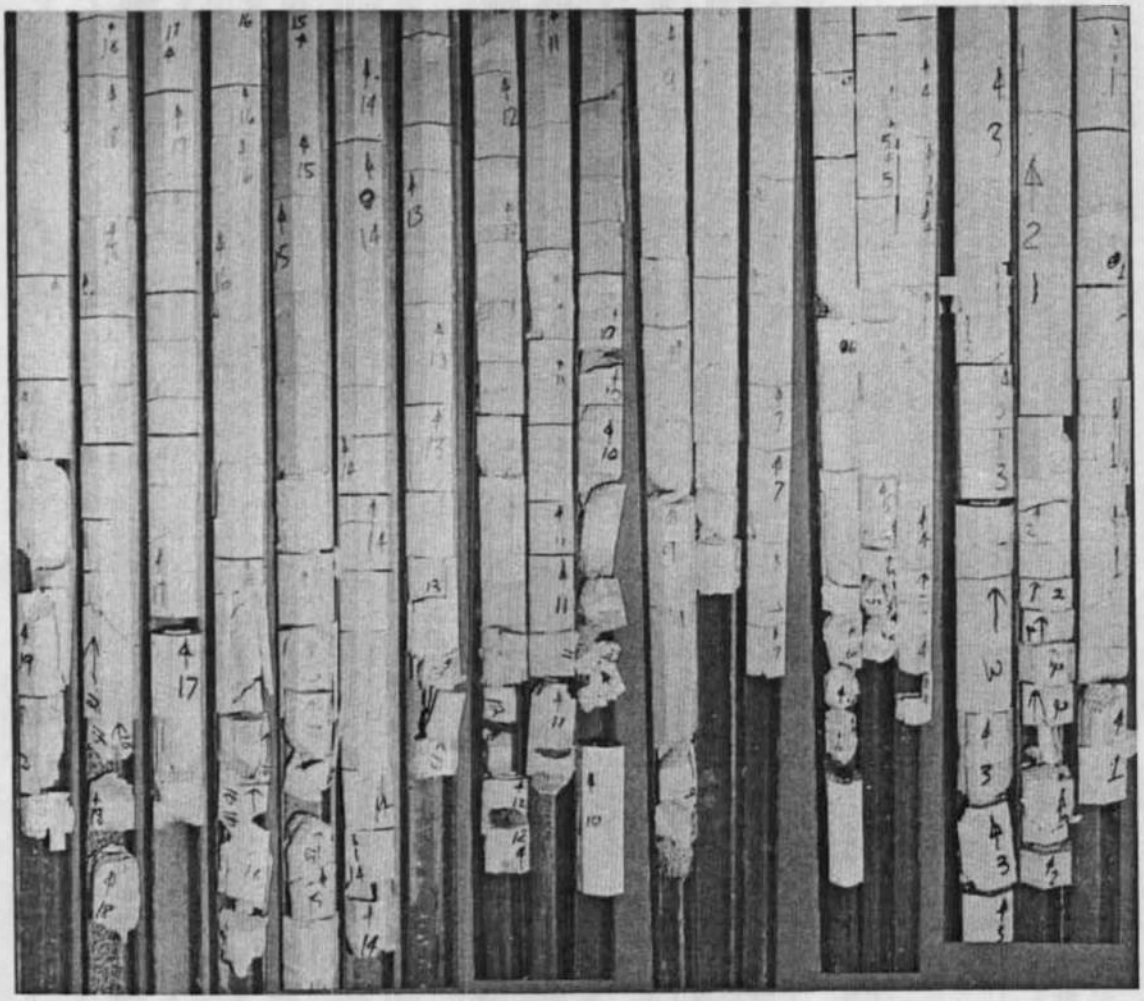

b. Lower Portion
Fig. 25 Concluded

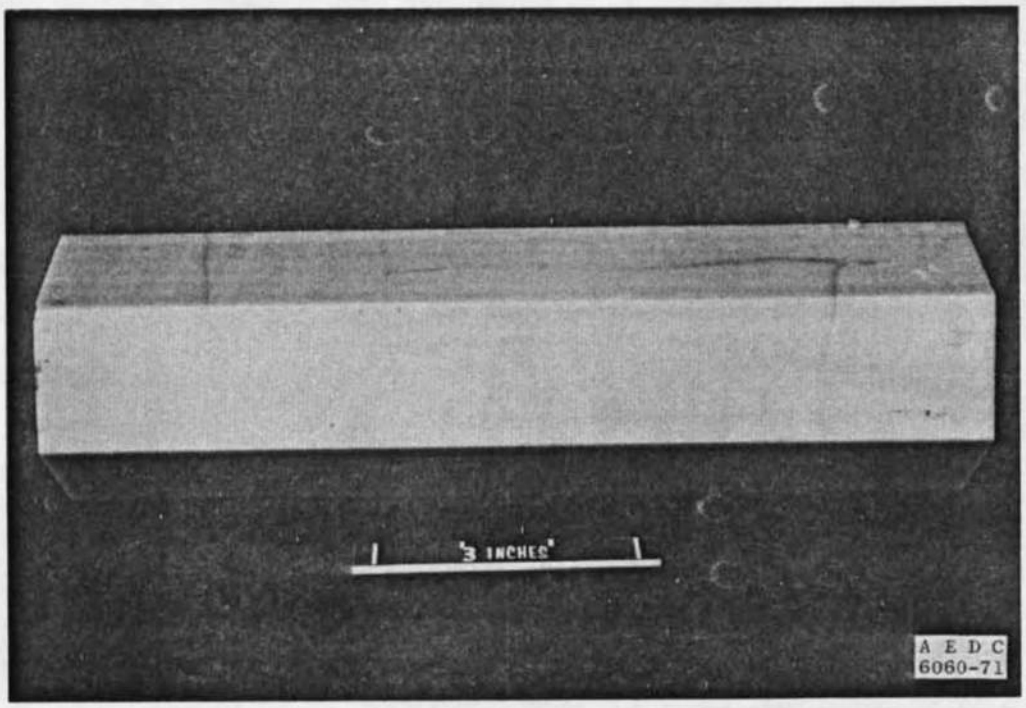

a. Coors, 9.25 w/o, Column 3, 14.5-ft Bed Level

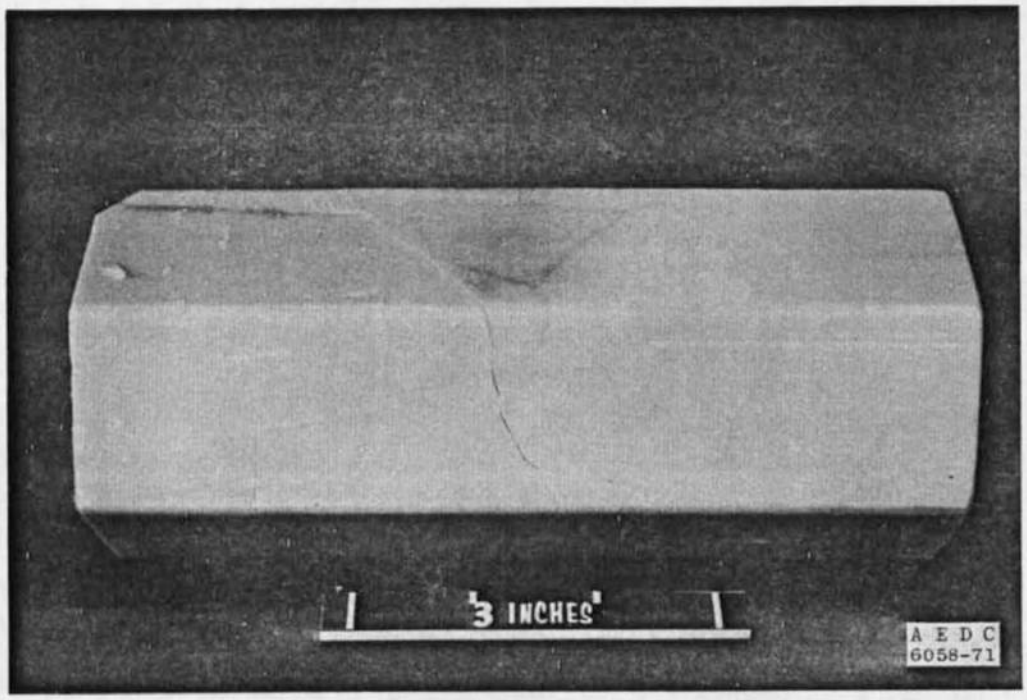

b. Coors, 10.4 w/o, Column 11, 14.5-ft Bed Level

Fig. 26 Zirconia Matrix Bricks Located Directly below Sample Bricks, Post-Run 85

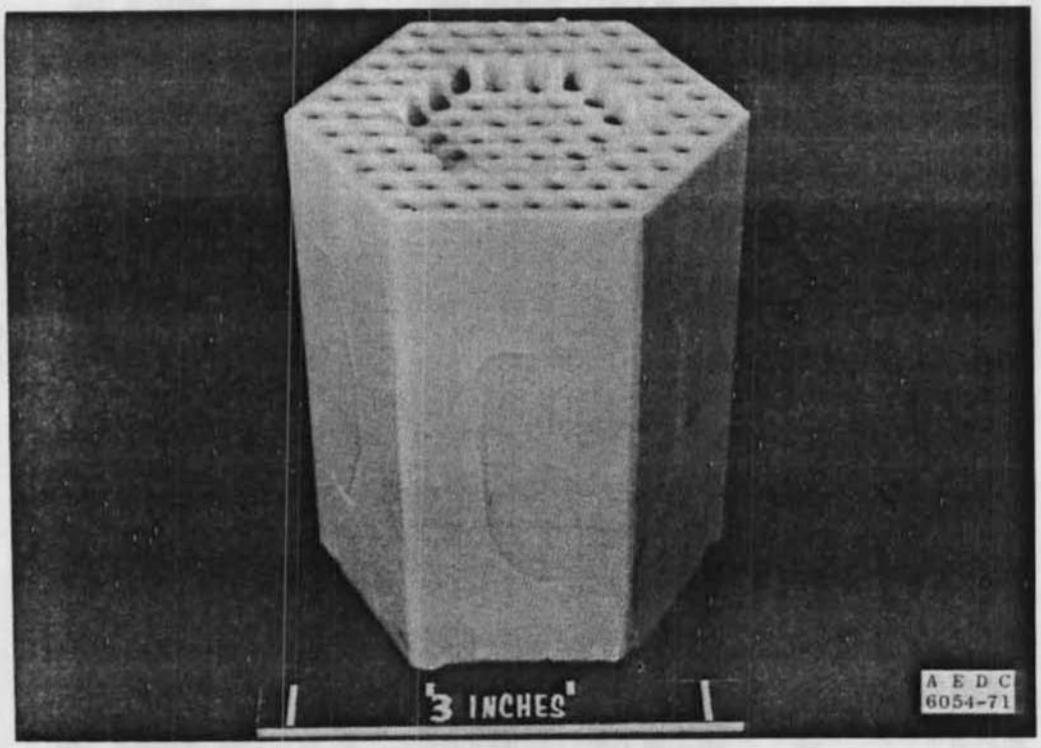

c. Coors, 9.25 w/o, Column 6, 13-ft Bed Level
Fig. 26 Concluded

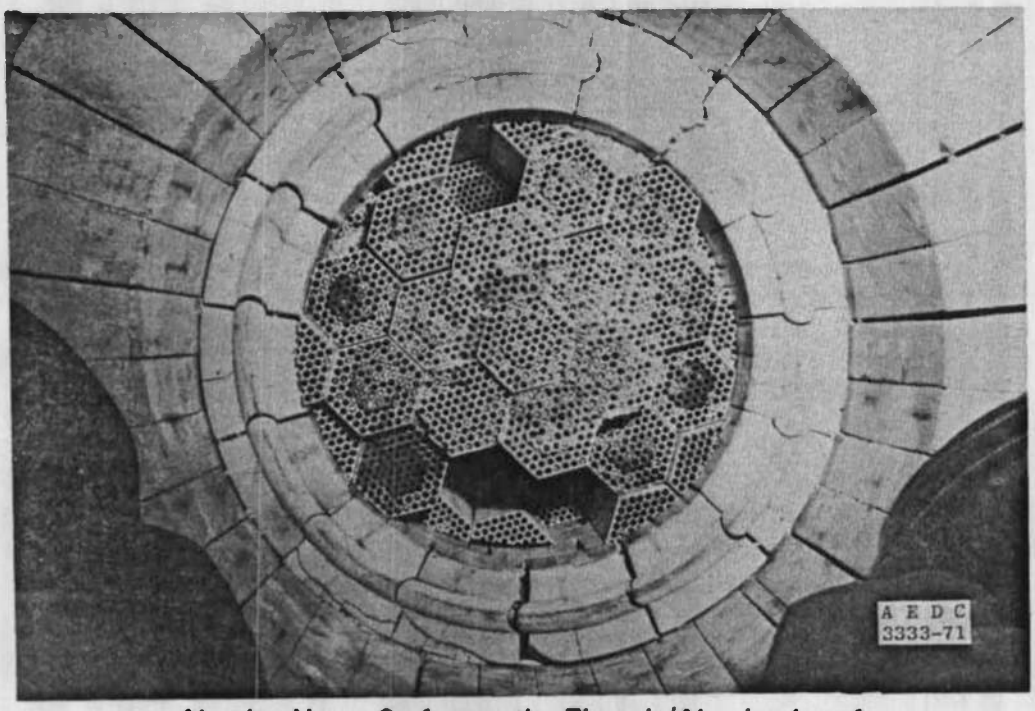

a. Alumina Upper Surface at the Zirconia/Alumina Interface
Fig. 27 Alumina Matrix, Post-Run 85

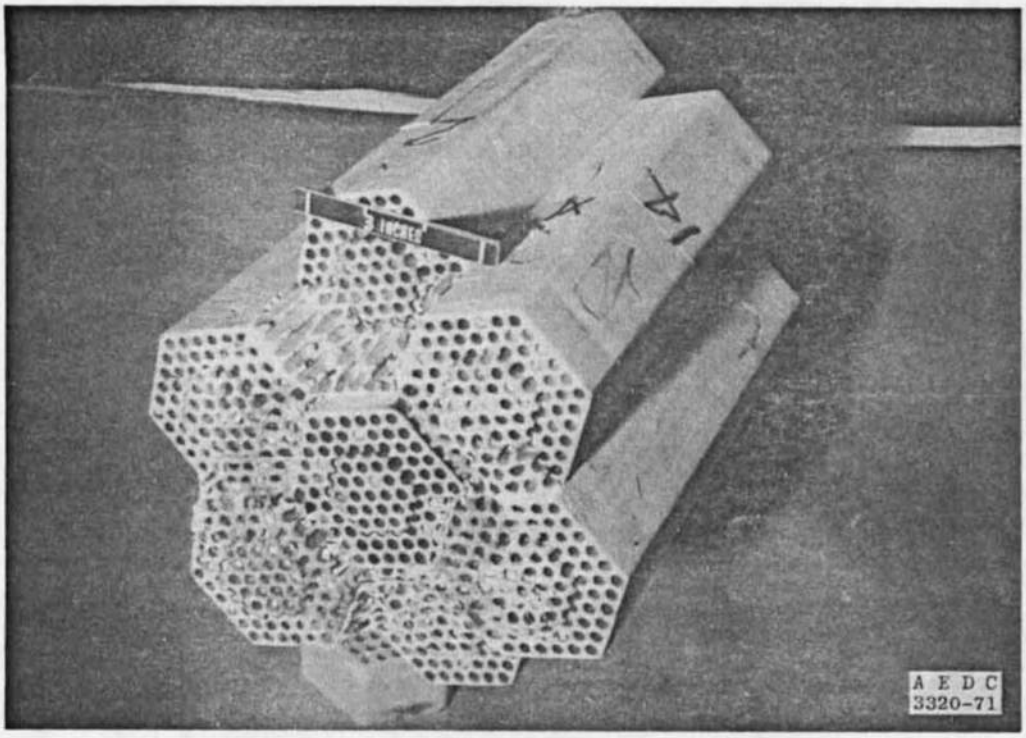

b. Center Portion of the Alumina Matrix at the Interface

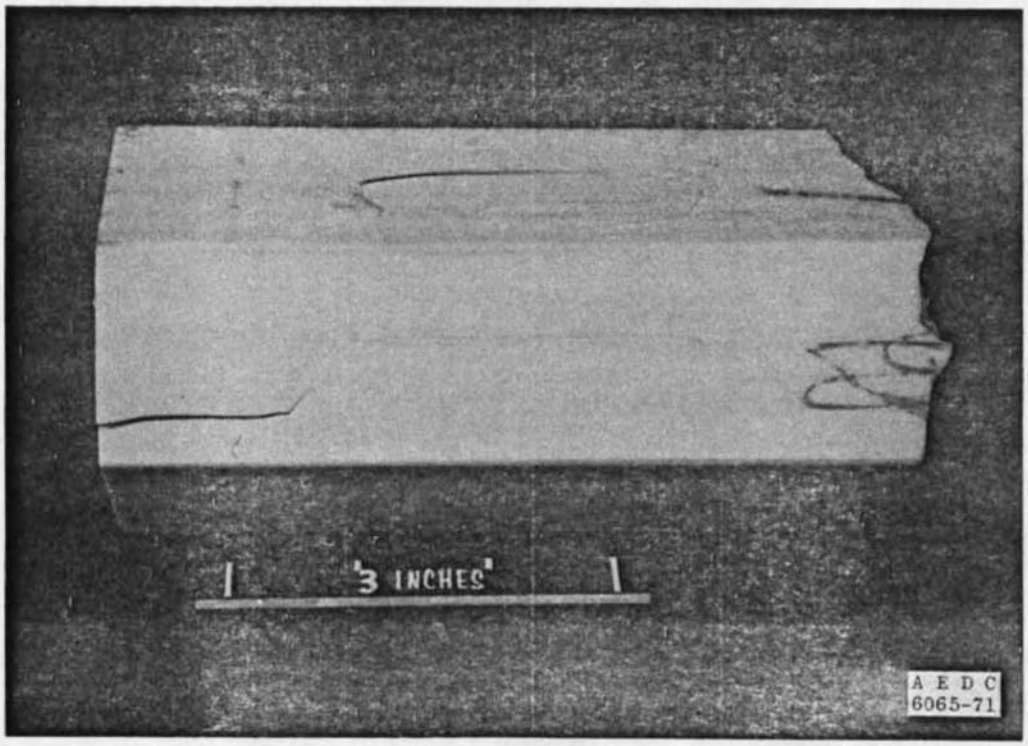

c. Lower Portion of Alumina Interface Brick from Column 7
Fig. 27 Continued

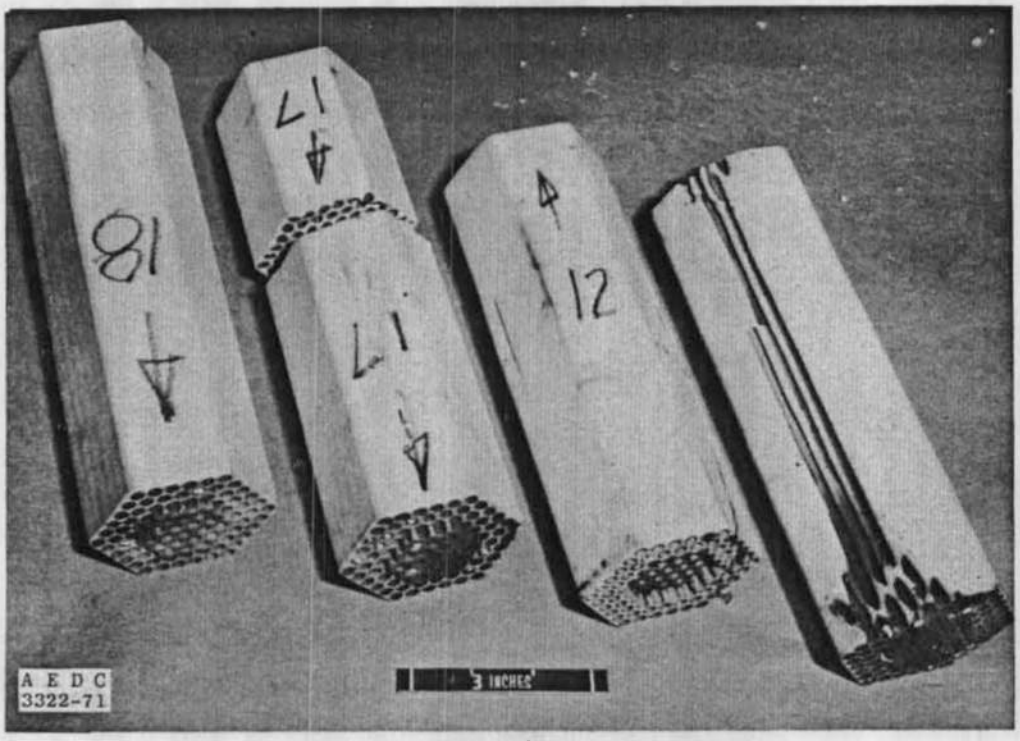

d. Alumina Bricks Located at the Interface

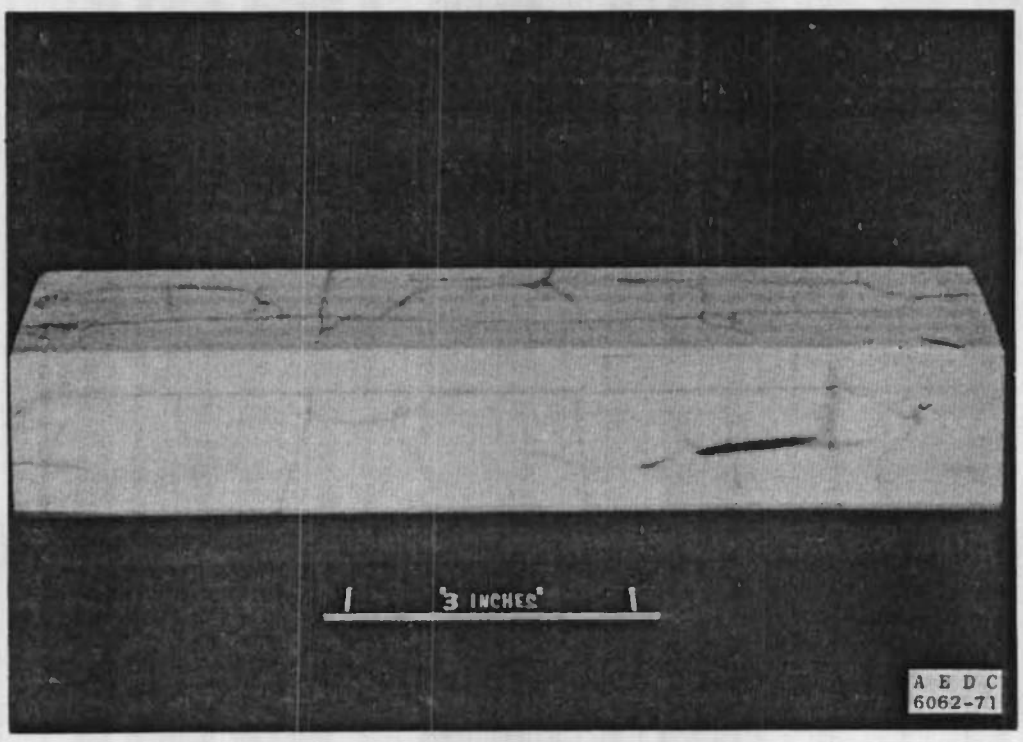

e. Alumina Brick Located at the Interface, Column 19
Fig. 27 Concluded

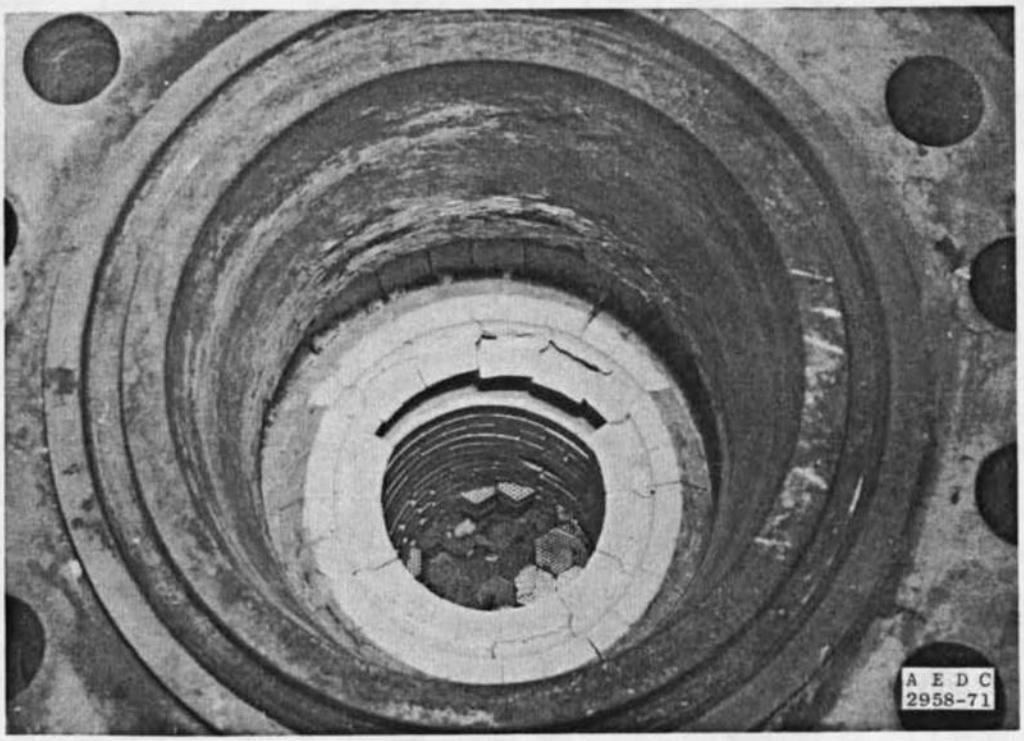

a. Dome Hot Face Liner Bricks

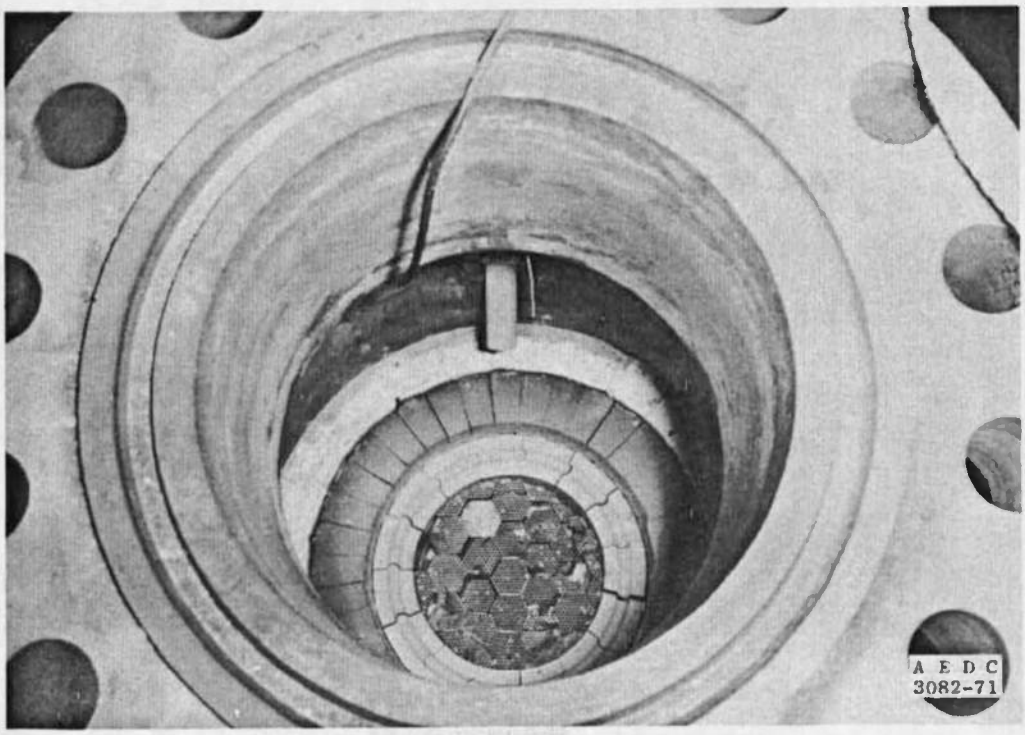

b. Heater Dome Support Shelf and Top of Matrix Refractories

Fig. 28 Various Heater Refractories, Post-Run 85

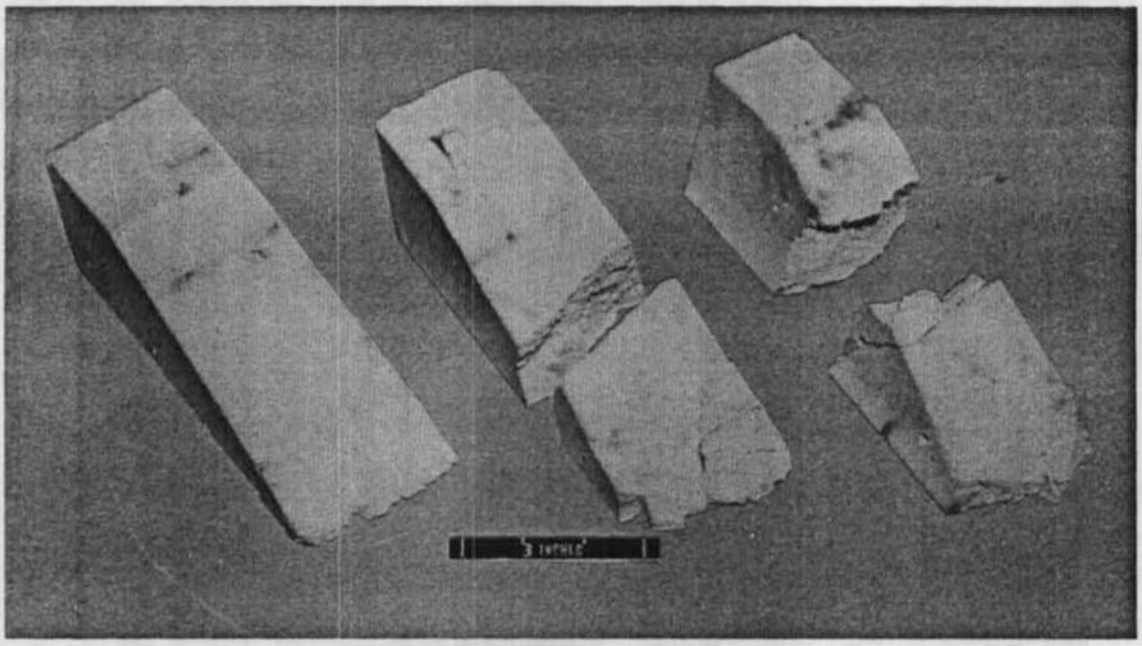

c. Typical Dome Insulation, Lightweight Fully Stabilized Calcia Zirconia

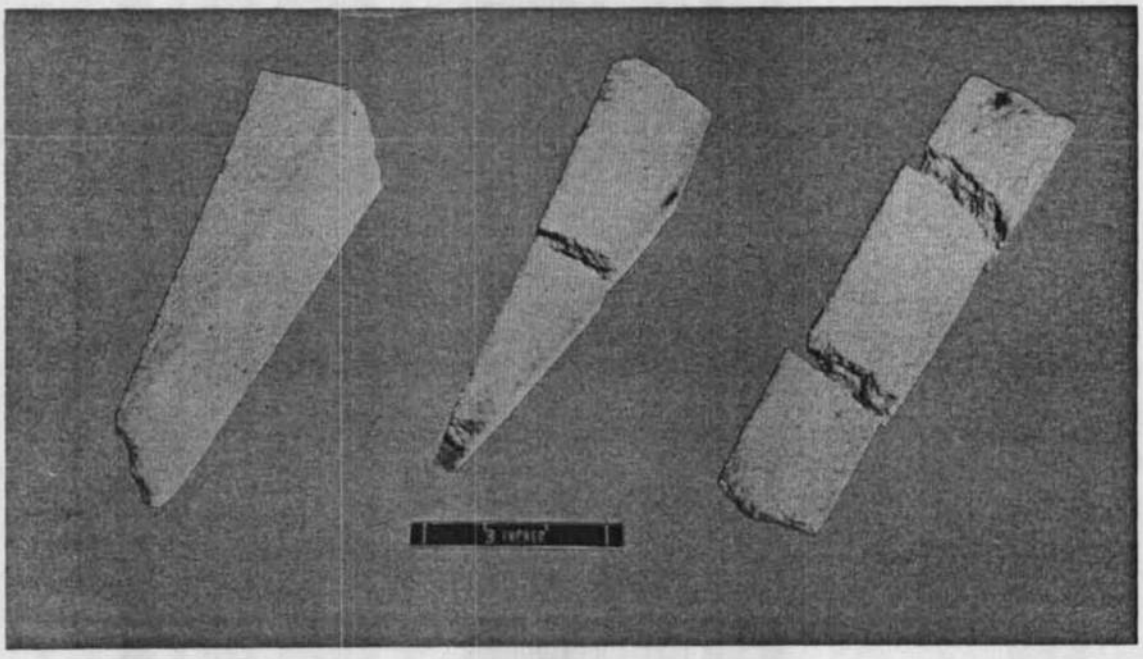

d. Typical Dome Insulation, 3250°R Firebrick
Fig. 28 Continued

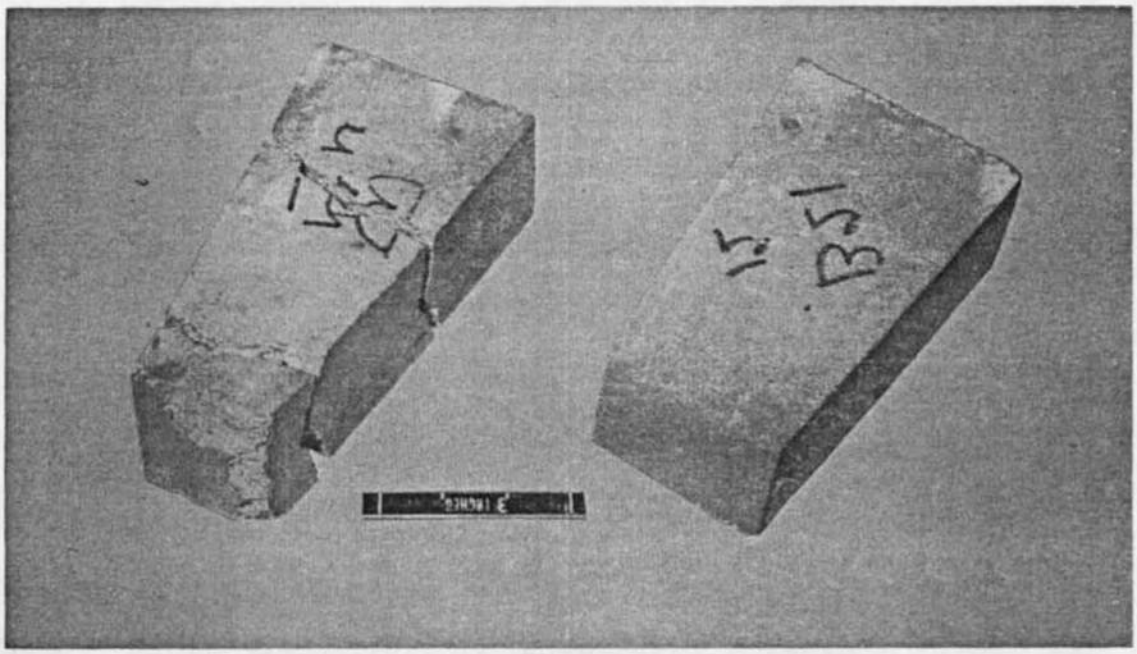

e. Typical Dome Support Shelf Insulation, Dense Fully Stabilized Calcia Zirconia

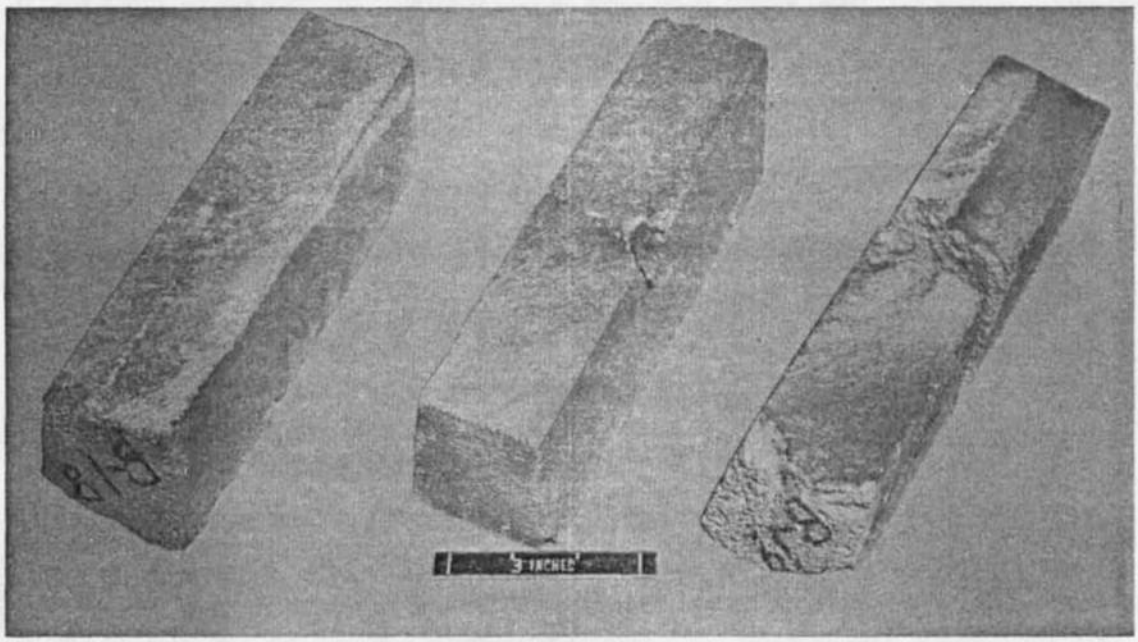

f. Outer Insulation Layer at the 15-1/2-ft Viewport, Lightweight Fully Stabilized Calcia Zirconia

Fig. 28 Continued

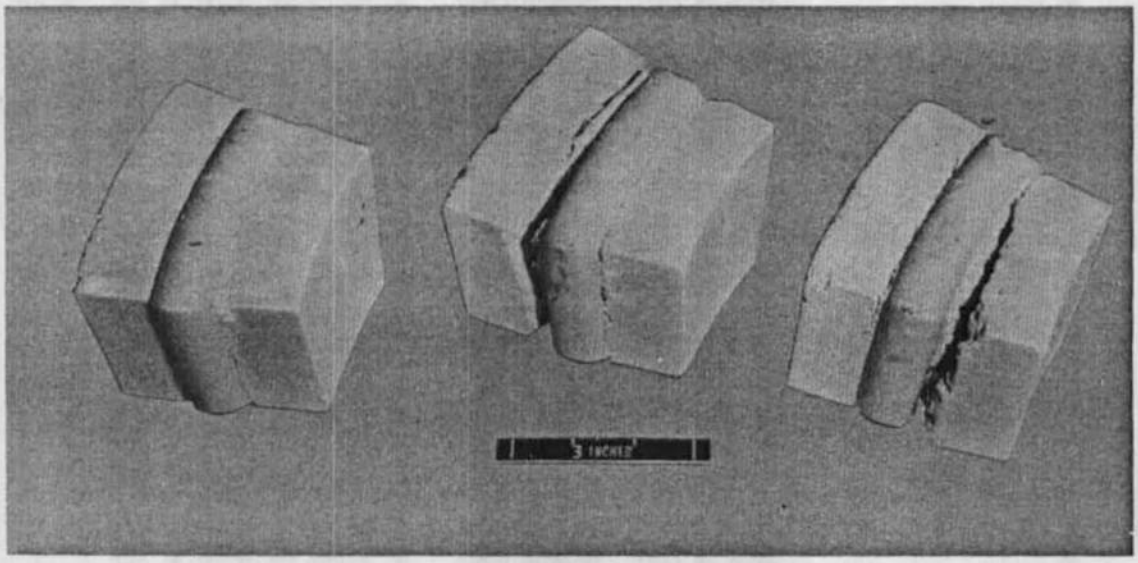

g. Typical Combustion Chamber Liner, Dense Fully Stabilized Yttria Zirconia

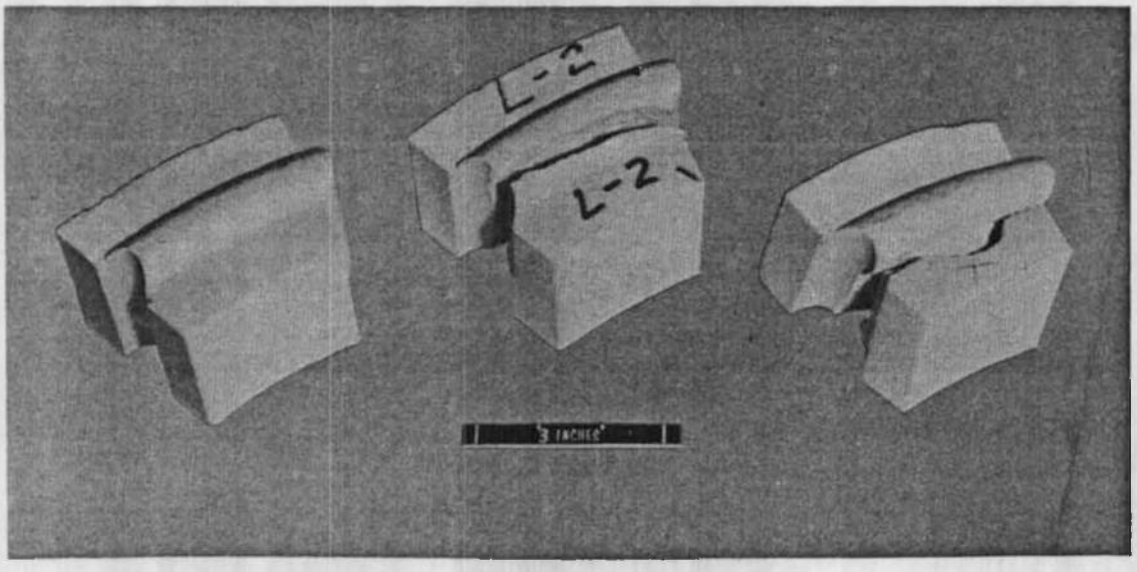

h. Typical Matrix Liner, Dense Fully Stabilized Yttria Zirconia
Fig. 28 Concluded

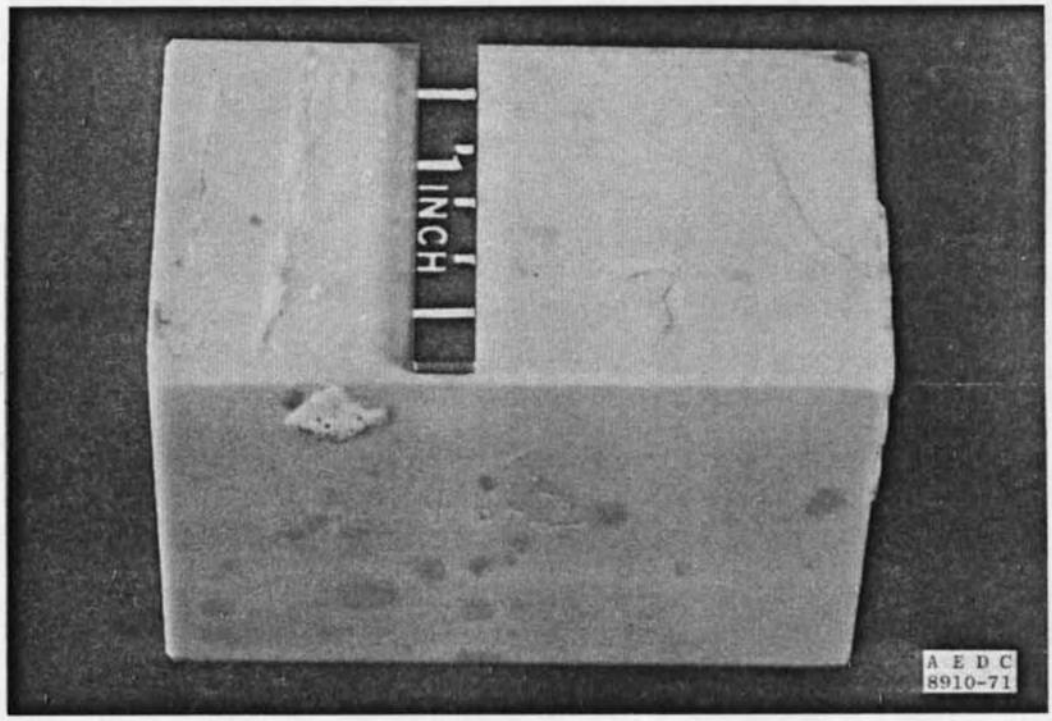

a. Side "A"

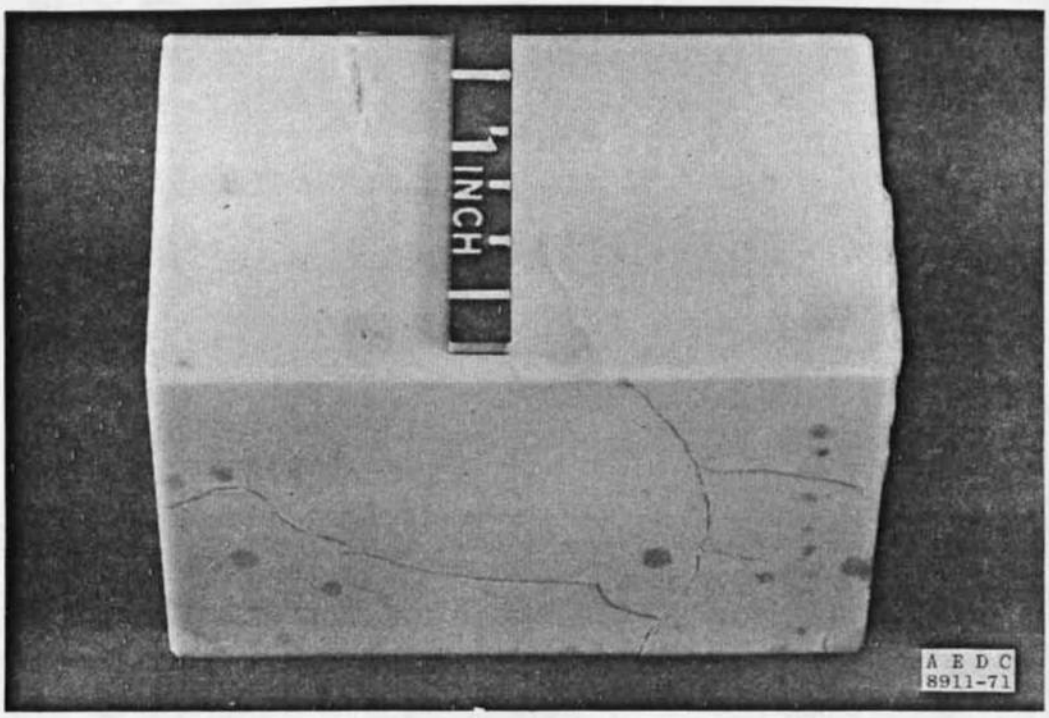

b. Side Opposite "A"

Fig. 29 Matrix Brick Exhibiting Stress Marks, Post-Run 44

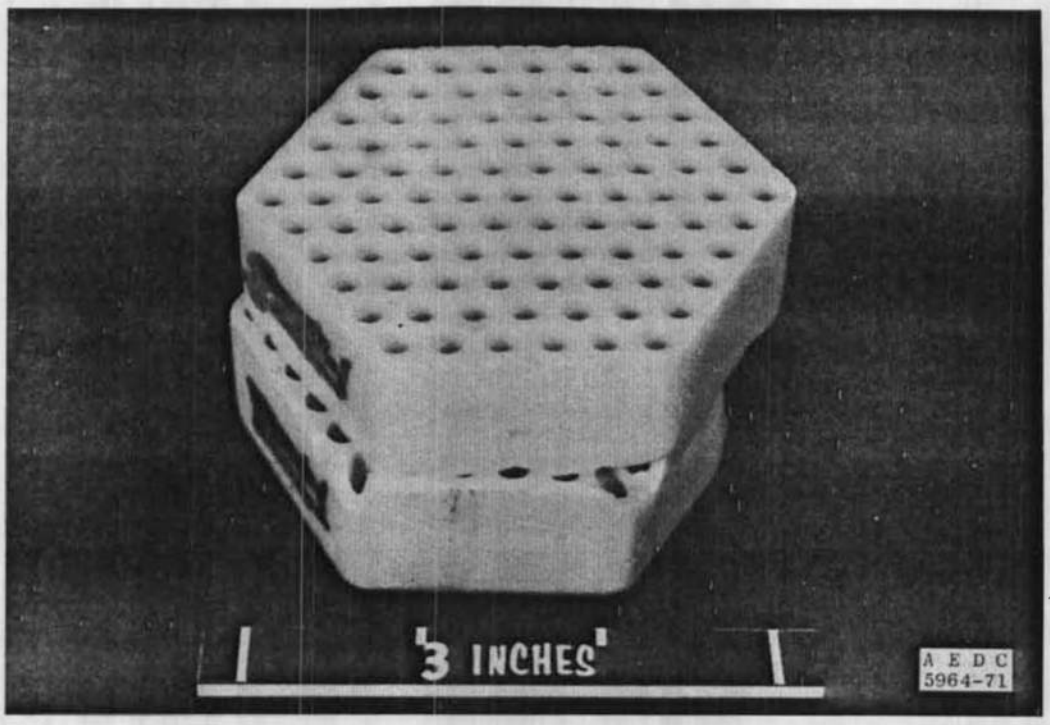

Fig. 30 Misalignment in Non-Keyed Bricks, Post-Run 85

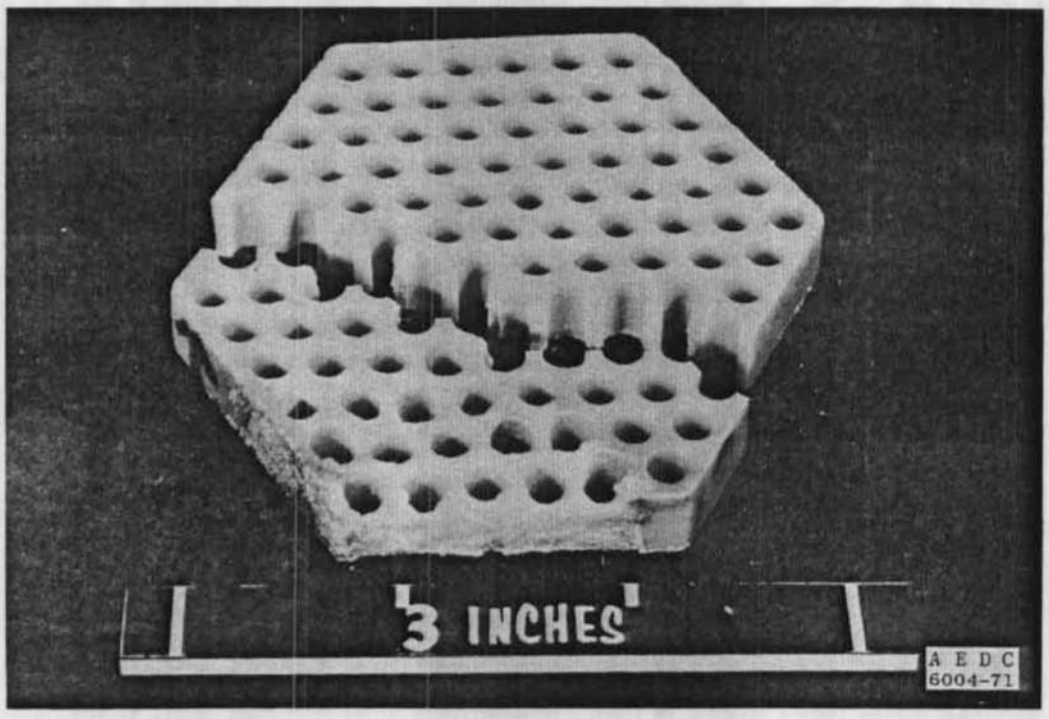

a. Coors, Buffer Brick, Column 10

Fig. 31 Bricks Exhibiting Localized Fusion and/or Material Deposits, Post-Run 85

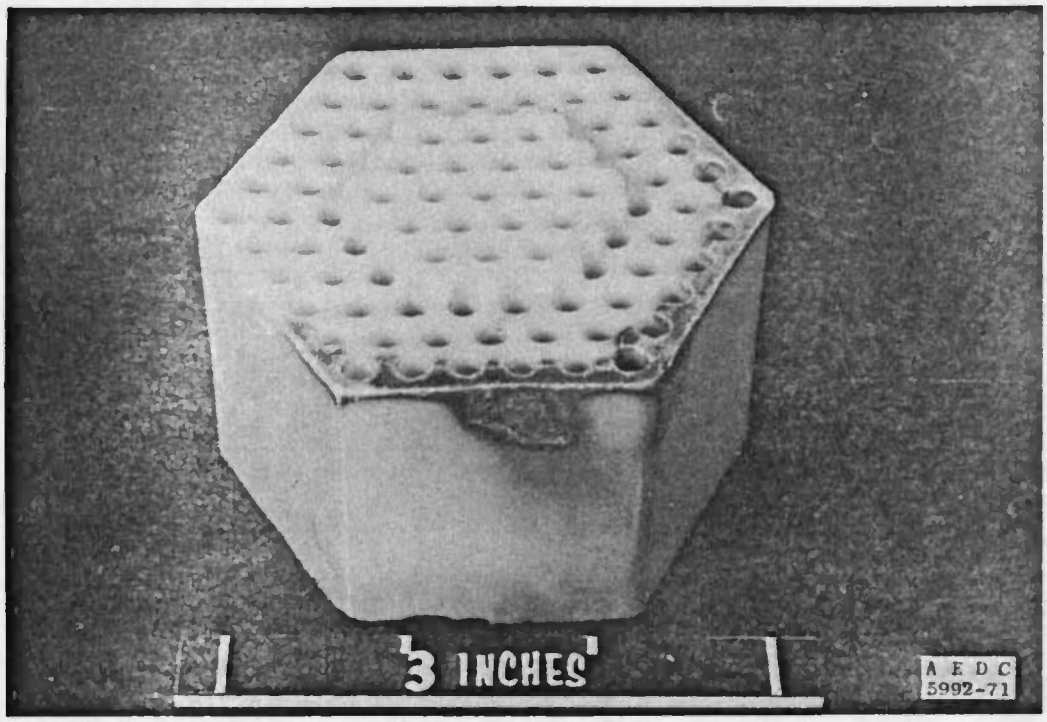

b. Zircoa, 10.8 w/o, Location 13-6

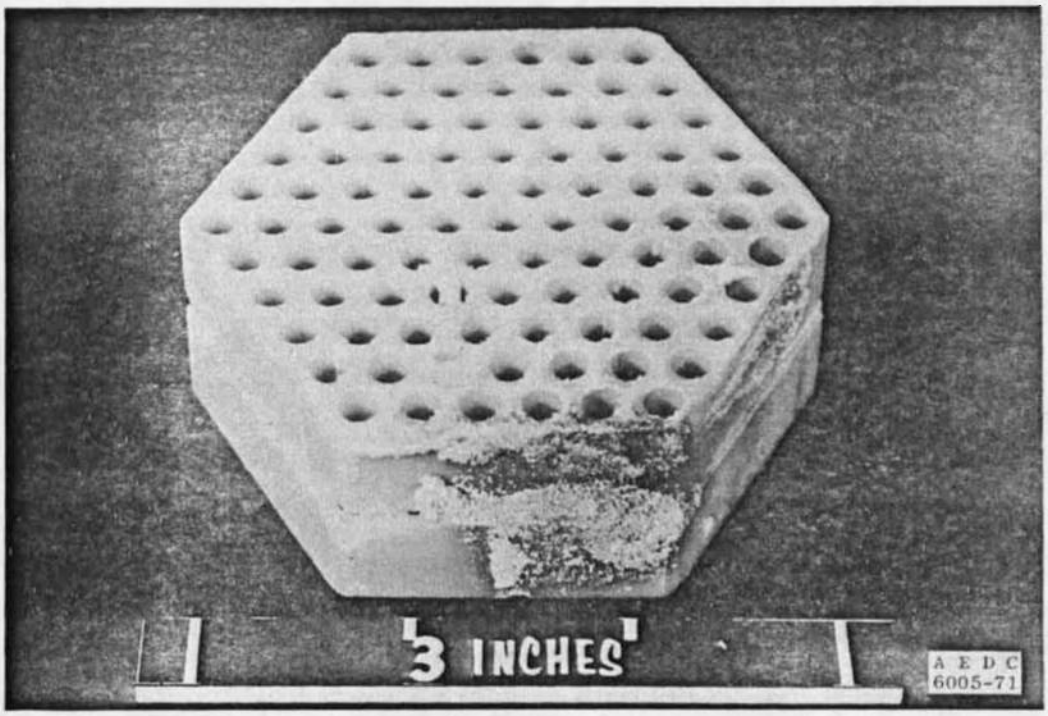

c. Coors, Buffer Bricks, Column 10
Fig. 31 Concluded

TABLE I
TYPICAL MATRIX REHEAT SCHEDULE (MAXIMUM MATRIX TEMPERATURE = 4450°R)

Step No.	Time at Setting, hr	$\dot{m}_{air}$*, lb/hr	$\dot{m}_{fuel}$, lb/hr	$\dot{m}_{O_2}$, lb/hr	$\dot{m}_{total}$*, lb/hr	$\dot{m}_{bed}$, lb/hr	$\dot{m}_{bypass}$*, lb/hr	f/o Ratio*, lb/lb	Equivalence Ratio*	Adiabatic Flame Temperature*, °R
1	3	(38.09)**	(1.91)	0	40.00	0	40.00	0.0500	0.78	3600
2	2	38.09	1.91		40.00	(40.00)	---		0.78	3600
3a	---	38.09	1.91		---	(20.00)	---		---	---
b	---	(57.14)	2.86		---	---	---		---	---
c	2	57.14	2.86		60.00	(40.00)	20.00		0.78	3600
4a	---	57.14	2.86		---	(20.00)	---		---	---
b	---	(76.19)	3.81		---	---	---		---	---
c	2	76.19	3.81		80.00	(40.00)	40.00		0.78	3600
5a	---	(95.24)	4.76		---	---	---		---	---
b	2	95.24	4.76		100.00	(60.00)	40.00	0.0500	0.78	3600
6a	---	(114.29)	5.71		---	---	---		---	---
b	1.5	114.29	5.71		120.00	(80.00)	40.00		0.78	3600
7a	---	114.29	5.71		---	(70.00)	---		---	---
b	---	(152.38)	7.62		---	---	---		---	---
c	1	152.38	7.82		160.00	(110.00)	50.00		0.78	3600
8a	---	(180.95)	9.05		---	---	---		---	---
b	1	180.95	9.05		190.00	(140.00)	50.00		0.78	3600
9a	---	(180.52)	9.03		---	---	---		---	---
b	1	180.52	(9.48)		190.00	140.00	50.00	0.0525	0.82	3730
10a	---	(179.65)	9.43		---	---	---	0.0525	---	---
b	1	179.65	(10.35)		190.00	140.00	50.00	0.0576	0.90	3900
11a	---	179.65	10.50	(5.50)	---	---	---	0.0576	---	---
b	---	(173.04)	10.28	5.50	---	---	---	0.0576	---	---
c	---	173.04	(11.46)	5.50	---	---	---	0.0642	---	---
d	1	173.04	11.46	5.50	190.00	(140.00)	50.00	0.0642	0.907	4130
12a	---	173.04	11.79	(10.60)	---	---	---	0.0642	---	---
b	---	(167.00)	11.40	10.60	---	---	---	0.0642	---	---
c	---	167.00	(12.40)	10.60	---	---	---	0.0698	---	---
d	1	167.00	12.40	10.60	190.00	(140.00)	50.00	0.0698	0.907	4260
13a	---	167.00	12.40	10.60	---	(130.00)	---	0.0698	---	---
b	---	167.00	12.82	(16.60)	---	---	---	0.0698	---	---
c	---	(150.48)	11.66	16.60	---	---	---	0.0698	---	---
d	---	150.48	(12.92)	16.60	---	---	---	0.0773	---	---
e	1	150.48	12.92	16.60	180.00	(130.00)	50.00	0.0773	0.907	4430
14a	---	150.48	12.92	16.60	---	(120.00)	---	0.0773	---	---
b	---	150.48	13.36	(22.40)	---	---	---	0.0773	---	---
c	---	(134.17)	12.10	22.40	---	---	---	0.0773	---	---
d	---	134.17	(13.43)	22.40	---	---	---	0.0858	---	---
e	1	134.17	13.43	22.40	170.00	(120.00)	50.00	0.0858	0.907	4590

TABLE I (Concluded)

Step No.	Time at Setting, hr	$\dot{m}_{air}$*, lb/hr	$\dot{m}_{fuel}$, lb/hr	$\dot{m}_{O_2}$, lb/hr	$\dot{m}_{total}$*, lb/hr	$\dot{m}_{bed}$, lb/hr	$\dot{m}_{bypass}$*, lb/hr	f/o Ratio*, lb/lb	Equivalence Ratio*	Adiabatic Flame Temperature*, °R
15a	---	134.17	13.43	22.40	---	(110.00)	---	0.0858	---	---
b	---	134.17	13.90	(27.80)	---	---	---	0.0858	---	---
c	---	(118.33)	12.54	27.80	---	---	---	0.0858	---	---
d	---	118.33	(13.87)		---	---	---	0.0949	---	---
e	1		13.87		160.00	(110.00)	50.00		0.907	4720
16a	---		13.87		---	(100.00)	---		---	---
b	---		14.29	(32.20)	---	---	---		---	---
c	---	(103.67)	12.89	32.20	---	---	---		---	---
d	---	103.87	(14.13)		---	---	---	0.1040	---	---
e	1		14.13		150.00	(100.00)	50.00		0.907	4830
17a	---		14.13		---	(90.00)	---		---	---
b	---		14.52	(35.90)	---	---	---		---	---
c	---	(89.85)	13.08	35.90	---	---	---		---	---
d	---	89.85	(14.25)		---	---	---	0.1133	---	---
e	1		14.25		140.00	(90.00)	50.00		0.907	4900
18a	---		14.25		---	(82.00)	---		---	---
b	---		14.66	(39.50)	---	---	---		---	---
c	---	(78.05)	13.32	39.50	---	---	---		---	---
d	---	78.05	(14.45)	39.50	---	---	---	0.1229	---	---
e	1	78.05	14.45	39.50	132.00	(82.00)	50.00		0.907	5000
19a	---	78.05	16.24	(54.05)	---	---	---		---	---
b	---	(77.81)	16.21	54.05	---	---	---		---	---
c	---	77.81	(18.14)		---	---	---	0.1376	---	---
d	52		18.14		150.00	(100.00)	50.00	0.1376	0.907	5100
20a	---		(13.23)		---	---	---	0.1003	---	---
b	---		17.73	(98.91)	---	---	---		---	---
c	---	(355.51)	45.58	98.91	---	---	---		---	---
d	***	355.51	45.58	98.91	500.00	(450.00	50.00		0.907	4800

*Does not include burner tube exterior air purge (5.46 lb/hr).

**Control adjustments are denoted by parentheses.

***Hold last step until desired plateau length is formed.

Note: After completing each step, make final corrections to reactant flow rates and flow through the bed as required to obtain the correct final settings.

CAUTION:
1. Do not allow zirconia-alumina interface to exceed 3450°R.
2. Do not allow grate to exceed 1650°R.
3. As the temperature of the matrix and outlet ceramics increases at any one setting, the pressure drop through them will vary. Consequently, the bypass valve will have to be periodically checked and adjusted.
4. Minimum zirconia-alumina interface temperature during blowdown will be 1950°R.

TABLE II
RUN SUMMARY FOR INITIAL SHAKEDOWN RUNS AND HEAT SOAK

Run No.	Date	Description of Run
1		Cold bed, low pressure (shakedown)
2	2/21/69	2300°R to room temperature at 430 psi
3	3/14/66	2300°R to room temperature at 400 psi
4	3/27/66	2600°R to room temperature at 450 psi
5	4/4/66	2900 to 2300°R at 700 psi
6	4/6/69	3320 to 2080°R (no blowdown - burner off approximately 12 hr due to an electrical difficulty)
7	4/7/69	3460 to 2790°R at 800 psi
8	4/8/69	3400 to 2760°R at 650 psi
9	4/8/69	3350 to 2600°R at 550 psi
10	4/10/66	3370 to 2770°R at 790 psi
11	4/10/69	3350 to 2800°R (no steady pressure obtained)
12	4/11/66	3380 to 2630°R at 450 psi (heater allowed to cool to ambient)

VISUAL INSPECTION OF CERAMICS

1. Hot face insulation, heater combustion chamber, and air outlet excellent.
2. Top surface buffers cracked and fractured.
3. No ceramic deterioration noted through viewports.

PRETEST 13 PREPARATION

1. No changes made to matrix.

13a	4/30/66	3450 to 2660°R (no steady pressure obtained)
b	4/30/66	3450 to 2790°R at 1360 psi
14	5/1/66	3450 to 2770°R at 1440 psi
15	5/1/69	3400 to 2760°R at 1300 psi
16	5/2/66	3440 to 2960°R at 1260 psi
17	5/2/69	3450 to 2630°R at 1270 psi
18a	5/2/66	3280°F to room temperature at 200 to 300 psi (breakdown of Roots blower)
b	5/10/69	3450 to 2650°R at 1180 psi (low film flow setting)
c	5/10/69	3440 to 2750°R at 1650 psi
19	5/11/69	3450 to 2730°R at 1600 psi
20	5/12/66	3450 to 2950°R at 1550 psi
21	5/12/69	3450 to 2750°R at 1670 psi
22a	5/13/66	3450 to 3150°R (no blowdown due to malfunctioning control valve)
b	5/13/69	3450 to 2800°R at approximately 1600 psi
23	5/14/69	3430 to 2950°R at 1990 psi maximum (long pressurization prevented obtaining steady-state conditions)
24	5/14/69	3440 to 2800°R at 1920 psi
25	5/15/66	3470 to 2840°R at 2000 psi
26	5/15/66	3430 to 2850°R at 2020 psi
27	5/16/69	3450 to 2750°R at 2080 psi (heater allowed to cool to ambient)

POST-TEST 27 INSPECTION

1. Additional fracturing of matrix top surface buffers.
2. Sample buffers removed. Found to be friable, indicating destabilization.
3. Tests at Wright-Patterson revealed 10 to 15 percent monoclinic, confirming destabilization.
4. All buffers and some matrix bricks then removed.
5. Bricks categorized as (A) chalky white and (B) gray with distinct white regions randomly located or, in some cases, outlining cracks. All chalky white were weak and friable. All gray were comparatively strong. However, the white areas areas were also friable. Tests revealed white regions 10 to 11 percent monoclinic and gray regions 4 to 5 percent monoclinic.
6. Ceramics at 9-ft viewport still hard.
7. Combustion chamber bricks fractured and spalled.
8. Remaining hot face insulation showed some cracks.

PRE-HEAT SOAK PREPARATION

1. Additional bricks placed in matrix to replace those removed.

Heat Soak	9/25/69 through 10/3/69	Maximum matrix temperature of 4550°R held for 94 hr.

POST-HEAT SOAK PREPARATION

1. Original 9.25 w/o matrix bricks were hard, strong, and gray.
2. 9.25 w/o and 10.4 w/o bricks installed pre-heat soak were strong and hard.
3. Partial fusing between adjacent bricks noted.
4. Small destabilized samples inserted pre-heat soak through viewport holes also inspected. Those located on matrix bricks were hard, strong, and gray. Those located on cooler bed liner remained weak, friable, and gray-white.
5. Heater combustion chamber basically unchanged.
6. Arch bricks (adjacent to dome skew bricks) showed deterioration.
7. Remaining insulation refractories in this region were basically in good condition.

TABLE III
RUN SUMMARY FOR RUNS 28 THROUGH 85

Test Number	Test Date	Pressure, psig		Temperature, °R	Steady-State Run Time, sec	Interface Temperature, °R	Comments
		Desired	Actual				
PRE-TEST 28 PREPARATION 1. Installed 6 Coors 10.9, 12.6, and 13.8 w/o yttria bricks into the heater to level top of bed. 2. Propane flow anomaly occurred during bed generation (dropped top of bed temperature from 3220 to 2400°R).							
28	12-11-68	500	~500*	3450	30	2130	Run accomplished on fourth attempt. Problem was high pressure air leak into oxidizer system. Replaced valve after third attempt.
29	12-11-69	500	~500*		74	2120	
30	12-11-69	1000	~1000*		50	1920	
31	12-12-68	1000	~1000*		44	2040	Run accomplished on third attempt. Same valve problem as run 28. Replaced valve seat after second attempt.
32	12-12-69	1000	~1000*		46	1980	
POST-TEST 32 INSPECTION 1. Bricks showed no destabilization. 2. Excessive cracking and fracturing of matrix bricks. 3. All Coors 10.9, 12.6, and 13.8 w/o bricks placed into matrix pre-run 28 severly cracked. Some fractured into pieces. 4. Bricks installed pre-heat soak were in better condition. 5. Combustion chamber unchanged from post-heat soak inspection. 6. Pronounced tendency of longer bricks to fracture into shorter segments. **PRE-TEST 33 PREPARATION** 1. Installed Coors 10.9, 12.6, and 13.8 w/o yttria bricks to replace broken ones and to level top of bed.							
33	1-15-70	500	550	4150	132	2340	
34	1-15-70	500	600		152	2430	
35	1-15-70	1000	1000		25	2480	
36	1-15-70	1000	1000		53	2440	
37	1-16-70	1000	1050		60	2330	
POST-TEST 37 INSPECTION 1. Several bricks placed in matrix pre-run 33 were inspected. Some hairline cracks. No open cracks. 2. Heater combustion chamber refractories showed increased degradation. **PRE-TEST 38 PREPARATION** 1. One Zircoa low density 12.5 w/o yttria brick added to matrix. 2. One Coors high density 10.9 w/o yttria brick added to matrix. 3. New heater combustion chamber refractories installed.							
38	2-23/27-70	---	---	3950	---	---	Hold setting of 3850°R was maintained for 60-1/2 hr followed by 3 hr of fast reheat
POST-TEST 38 CONCLUSION AND INSPECTION 1. Burner damage caused by nitric acid erosion. Zirconium-copper material not compatible with burner combustion gas with oxygen enrichment. 2. Selected matrix bricks inspected were in good condition with only a few additional hairline cracks. **PRE-TEST 39 PREPARATION** 1. Initiated design of new burner.							

*This is an approximate value because heater pressure data were not recovered during this test period.

TABLE III (Continued)

Test Number	Test Date	Pressure, psig		Temperature, °R	Steady-State Run Time, sec	Interface Temperature, °R	Comments
		Desired	Actual				
39	5-14-70	1000	100	3950	0	2220	Unsuccessful run. Oxidizer isolation valve leaked. Also a leak in the high pressure air control valve caused partial blowdown. Valve was replaced. On second run attempt, proper profile could not be obtained. Suspected burner water leak.
POST-TEST 39 INSPECTION 1. Selected matrix bricks inspected were practically unchanged since post-test 38. PRE-TEST 40 PREPARATION 1. No changes made to matrix configuration.							
40	6-25-70	1000	1000	3950	22	2440	
41	6-25-70	1000	1050	3950	17	2420	
42	6-25-70	1000	650	3950	0	2620	Unsuccessful run. Rough opening of 1-1/2-in. control valve caused excessive bed differential pressure resulting in automatic closing of the air supply valve. Began heater pressurization unaware of this. Decaying supply pressure caused excessive restrictor throat temperature which closed the 1-1/2-in. control valve. This restored film cooling air when heater pressure decayed.
43	6-25-70	1000	1000	3950	30	2420	
44	6-26-70	1000	1000	3950	70	2240	

POST-TEST 44 INSPECTION

1. Removed top foot of matrix.
2. Monoclinic analysis of bricks revealed no destabilization.

PRE-TEST 45 PREPARATION

1. Bricks removed for inspection were replaced with Coors and Zircoa high density (about 90 percent theoretical) zirconia sample bricks.
2. Yttria content ranged from 10.6 to 16.5 w/o.
3. A portion of the bricks supplied by Zircoa was to have contained 14.5 w/o; however, an error in manufacturing of the bricks resulted in an actual yttria content of 10.8 w/o.
4. Coors high density bricks were manufactured in lengths of about 1/2 in., 1 in., and 2 in., whereas, most of Zircoa high density bricks were about 2 in. in length with only a very few 1-in. bricks and no 1/2-in. bricks. Therefore, several of the 2-in. bricks were cut at AEDC to form 1/2-in. and 1-in. bricks so that a better comparison could be made between Zircoa and Coors bricks.
5. Several low density (about 70 percent theoretical) bricks were furnished by Zircoa with 12.5 and 14.5 w/o yttria. Maximum length of these bricks was about 4.5 in.
6. Yttria stabilizer content (w/o) of the new sample bricks was as follows:

Coors High Density	Zircoa High Density	Zircoa Low Density
10.9	10.8	12.5
12.6	12.5	14.5
13.8	16.5	

TABLE III (Continued)

Test Number	Test Date	Pressure, psig		Temperature, °R	Steady-State Run Time, sec	Interface Temperature, °R	Comments
		Desired	Actual				
45	8-5-70	1000	900	3450	11	2120	Heater air pressure control valve and restrictor film cooling valves responded sluggishly and shortened run.
46	8-5-70	1000	800		25	2250	Same trouble as in run 45. Run terminated because of inadequate film cooling flow rate.
47	8-5-70	1000	1100		45	2080	
48	8-8-70	1000	1150		65	2120	
48	8-6-70	1000	1050		70	2070	
50	8-8-70	1000	1000		50	2060	
51	8-8-70	1000	1000		17	2070	
52	8-8-70	1000	1050		33	2080	
53	8-6-70	1000	1050		52	2080	
54	6-6-70	1000	1000		46	2090	
POST-TEST 54 INSPECTION 1. Zircoa high density bricks inspected had some hairline cracks in vertical direction. 2. A few Zircoa buffers were fractured. 3. No hairline cracks in Zircoa low density or Coors high density bricks inspected. PRE-TEST 55 PREPARATION 1. No significant changes were made.							
55	8-26-70	1500	300	3450	70	2300	Desired operating pressure was not obtained because a hand valve, not completely closed, caused an abnormally high matrix differential pressure.
58	8-26-70	1500	1300		10	2130	
57	8-28-70	1500	1350		16	2230	
58	8-26-70	1500	1150		≈20	2080	
59	8-27-70	1500	1500		24	2140	
80	8-27-70	1500	1600		31	2020	
61	8-27-70	1500	1550		27	2070	Run accomplished on third attempt after problems with high pressure air leak through oxidizer isolation valve.
82	8-27-70	1500	1400		38	2060	
83	8-27-70	1500	1500		6	2240	Run shortened because of high pressure air leak into the low pressure air blower system.
64	8-28-70	1500	1100		4	2240	Two unsuccessful attempts. Same trouble as during run 83.
POST-TEST 84 INSPECTION 1. Bricks inspected were unchanged since Post-54 inspection. PRE-TEST 65 PREPARATION 1. No significant changes were made.							
65	9-17-70	1000	900	3850	12	2520	Run accomplished on second attempt. Same trouble as run 63. Run time shortened.

TABLE III (Continued)

Test Number	Test Date	Pressure, psig		Temperature, °R	Steady-State Run Time, sec	Interface Temperature, °R	Comments
		Desired	Actual				
66	9-17-70	1000	950	3950	9	2410	Run accomplished on second attempt. Same trouble as run 63. Run time shortened.
67		1000	1000		20	2440	
68		1000	1000		12	2460	Run accomplished on second attempt. Same trouble as run 63. Run time shortened.
69		1000	1150		80	2160	

POST-TEST 69 INSPECTION

1. Second major heater inspection due to water leak on burner tube tip exterior.
2. All bricks placed into matrix before run 45 were inspected.
3. All high density bricks contained hairline cracks.
4. All Coors high density bricks in column 4 beneath the burner were fractured into small pieces.
5. The other Coors high density bricks contained hairline cracks and four were fractured.
6. Coors buffers ranged from those with hairline cracks to fractured.
7. All high density Zircoa bricks and buffers contained hairline cracks, and 11 bricks were fractured.
8. Zircoa low density bricks in excellent condition and most were free of hairline cracks.
9. All sample bricks remained stabilized.
10. Practically all cracks in vertical direction.

PRE-TEST 70 PREPARATION

1. Second generation burner was installed.
2. New combustion chamber refractories installed to accompany new burner.
3. Sample bricks removed for inspection were re-installed in matrix with the following exceptions:
   a. Seven new bricks were placed in columns 2, 3, 6, and 18 to replace fractured ones.
   b. All sample bricks were replaced in column 4 (Coors 13.8 w/o), which was previously destroyed by water leak, and in column 15 (Coors 12.6 w/o), which is adjacent to column 4.
   c. All new bricks were of the same composition and manufacturer as those being replaced.
4. Column 3 (Coors 10.9 w/o) also adjacent to column 4, was to have been replaced also, but the old bricks (with exception of the fractured ones) were inadvertently placed into the matrix instead and were not replaced until after run 74.

70	2-11-71	500	500	3950	60	2590	
71	2-12-71	500	500		135	2800	
72	2-12-71	1000	1000		65	2450	
73	2-12-71	1000	1050		45	2450	
74	2-12-71	1000	1050		60	2470	

POST-TEST 74 INSPECTION

1. Inspection of selected matrix bricks revealed hairline cracks in approximately one-half of bricks inspected.
2. Practically all cracks were in the vertical direction.
3. New burner was in excellent condition.

PRE-TEST 75 PREPARATION

1. No significant changes were made.

75	3-17-71	500	500	4450	15	3040	
76	3-17-71	500	500		10	2960	Run terminated prematurely because of excessive noise.
77	3-18-71	1000	900 max		0	2640	Unusually high matrix differential pressure (1.9 psi)
78	3-18-71	1000	850 max		0	2840	Unusually high matrix differential pressure (2.2 psi)
79	3-18-71	1000	550 max		0	2900	Unusually high matrix differential pressure (2.5 psi)

TABLE III (Concluded)

Test Number	Test Date	Pressure, psig		Temperature, °R	Steady-State Run Time, sec	Interface Temperature, °R	Comments
		Desired	Actual				
POST-TEST 79 INSPECTION 1. Columns 2, 3, and 14 were inspected. 2. Some hairline cracks and a few fractures were present. All were in the vertical direction. 3. Several anomalies were discovered as possible causes of the high differential pressure. However, it is felt that a problem in the heater differential pressure measuring system caused the trouble. 4. New burner in excellent condition. PRE-TEST 80 PREPARATION 1. All anomalies were corrected.							
80	4-7-71	500	500	4450	40	2860	
81	4-7-71	1000	1000		30	2640	
82	4-7-71	1500	1450		15	2520	
83	4-7-71	2000	1750 max		0	2500	Run terminated prematurely because cutoff parameter temperature limit was reached.
84	4-8-71	2000	1600 max		0	2690	Run terminated prematurely because of restrictor over-temperature.
85	4-8-71	2000	1850 max		0	2350	Run terminated prematurely because of restrictor over-temperature.
POST-TEST 85 INSPECTION 1. Approximately one-half of ceramics removed from heater for major inspection and replacement of zirconia matrix.							

APPENDIX III
COMPARISON OF PREVIOUS SUBSCALE TESTS WITH PILOT HEATER SHAKEDOWN RUNS

During the development program of ceramics suitable for use as the matrix core of high temperature storage heaters, subscale tests performed by others led to the selection of yttria stabilized zirconia as the most suitable ceramic for heaters operating in the range of 4600°R. The following three types of subscale tests were performed (Ref. 2):

1. High temperature heat soak
2. Thermal cycling
3. Performance of stability

The heat soak, conducted at 4600°R, demonstrated the chemical stability of zirconia at this high temperature. During the thermal cycling tests, a single horizontal column of yttria-zirconia bricks was cycled through temperatures and at pressures simulating maximum operating conditions of a large storage heater. The permanence of stability tests involved cycling 1-in. cube samples slowly through the zirconia inversion zone. Thermal stresses were avoided so that any deterioration of the test samples could be traced directly to destabilization. However, the samples were placed inside an enclosure to prevent contamination by dust from the furnace insulation. Therefore, the samples were not subjected directly to combustion gases.

Results of the subscale testing included the following:

1. Dense 9.25 w/o yttria-zirconia did not destabilize when cycled through the inversion zone (in the absence of a flowing gas environment) if the initial monoclinic content was less than 5 percent.

2. Thermal cycling of yttria-zirconia above the inversion zone in flowing combustion products and with high thermal stresses did not result in destabilization.

3. Six weight percent yttria-rare earth is sufficient to stabilize zirconia fired at 4600°R.

4. Yttria-zirconia is chemically and structurally stable in flowing combustion products at 4600°R.

Since the results of the AEDC pilot heater shakedown runs were inconsistent with those of the subscale tests, differences between the two types of testing environments were examined. These differences included test pressure, thermal stresses incurred by the pilot heater matrix during blowdown, flowing combustion products in the pilot heater, variation of contaminants, and the presence of water vapor in the pilot heater combustion products.

Although these and other differences in test conditions existed between the subscale tests and the pilot heater tests, the cause of the PTU matrix destabilization was determined to have been the presence of 3 to 5 weight percent second-phase monoclinic zirconia randomly distributed throughout the as-fabricated bricks. The kinetics for the destabilization apparently resulted from a combination of monoclinic/tetragonal stresses realized in the zirconia bricks as a result of force cooling the zirconia matrix through the inversion zone during the shakedown runs, thermal stress cyclings and water vapor from the combustion products.

APPENDIX IV
MATRIX RESTABILIZATION HEAT SOAK

FACTORS INFLUENCING THE HEAT SOAK DECISION

After the heater matrix inspection after shakedown run 27, several samples of the destabilized material were refired in two separate kiln tests at Coors Porcelain Company and AFML/WPAFB at temperatures of approximately 3950°R. The high temperature heat soak treatment changed the sample characteristics from weak, friable, and chalky white to strong, hard, and a uniform shiny grayish color. Monoclinic contents were reduced in every case to an undetectable level (less than 0.5 percent by weight). Subsequently, a high temperature heat soak was conducted at Coors Porcelain Company to determine the length of time required to restabilize and resinter samples at 3450°R (maximum allowable interface temperature between the zirconia and alumina bricks in the PTU). Samples included ten sets of both the white friable material and the gray-white material. One sample of each material was removed from the kiln every 24 hr. Monoclinic analysis of the samples after the tests indicated that a 3450°R heat soak would reduce the monoclinic content of the white material to a minimum of 3.5 percent and the gray-white material to approximately 2.5 percent. The heat soak time period required would be approximately 72 hr. These kiln test results were the basis for refiring the pilot heater for a heat soak in an attempt to resinter the brick microstructure and restabilize the cored bricks.

PREPARATIONS

The following preparations were made to prepare the pilot heater for the heat soak:

1. Additional yttria stabilized zirconia cored bricks were obtained from NASA/Ames and Coors Porcelain Company to replace those bricks which had been removed from the heater for inspection and analysis. Of these bricks, approximately 4.7 linear feet contained 9.25 w/o stabilizer and approximately 8.0 linear feet contained 10.4 w/o stabilizer. Also obtained were 64 buffer bricks ranging in thickness from approximately 0.25 to 1.5 in. These buffer bricks were placed atop each matrix column to level the top of the bed and to provide thermal shock protection to the longer bricks immediately beneath them. A minimum of three buffers was placed on each of the 19 matrix columns.

2. Small matrix brick samples of both the white friable material and the stronger gray-white material, originally removed from the upper portion of the matrix, were placed into the heater through the horizontal view ports at the 9-, 11-, and 13-ft levels. The samples were placed on matrix bricks adjacent to the bed liner and on bed liner bricks. This was accomplished to evaluate the effect of lower temperatures at these locations on restabilization of the samples.

3. The heater vessel air outlet neck was originally designed to utilize Fiberfrax® as a second layer of insulation in the section upstream of the restrictor. However, the maximum working temperature of the material (2750°R) was not satisfactory for the proposed 4450°R heater operation. The Fiberfrax was, therefore, removed and replaced with low density alumina bricks.

OBJECTIVES AND PROCEDURES

The heater was refired for the heat soak with the objective being to resinter and restabilize the zirconia-cored bricks. The 94-hr high temperature heat soak was accomplished after a 98-hr reheat of the heater to obtain the desired thermal conditions. Temperatures along the centerline of the zirconia portion of the matrix during the heat soak ranged from 4550 ± 50°R at the matrix top to $3450 \,^{+70}_{-100}$ °R at the zirconia/alumina interface.

During reheat for the heat soak, the matrix centerline temperatures at the 9-, 11-, and 13-ft levels were measured by sacrificial thermocouples and optical pyrometers. Three pyrometers were used interchangeably to record the temperatures. The mean deviation between the thermocouple and optical pyrometer measurements was 32°R. A comparison of data from the two types of measuring devices was desired since the matrix centerline thermocouples at the 9-, 11-, and 13-ft bed levels would be destroyed by the high temperature of the heat soak leaving only the optical pyrometers.

After termination of the heat soak, the refractories were allowed to cool without passing air through the cored brick matrix. The heater refractories were then inspected. Access to the refractories was provided through the burner opening at the top of the heater.

INSPECTIONS

Cored Brick Matrix

Removal and inspection of the new matrix bricks (9.25 and 10.4 w/o yttria) after heater cooldown showed that these bricks remained strong, hard, and tan in color. The bricks with 9.25-percent yttria were slightly darker in color toward the edge than at the center. Segments of the original matrix bricks (9.25 w/o yttria) were removed and found to be strong, hard, and grayish in color in contrast to being weak, friable, and chalky white before the test. (Most original cored bricks were in segments as a result of the severe fracturing during the previous tests.) In removing the brick segments, partial fusing with adjacent bricks was noted. The fusing was apparently caused by ceramic particles which were lodged between adjacent bricks and subjected to compression forces and high temperature.

The small samples of destabilized material inserted into the bed through the horizontal view ports were also removed and visually inspected. All samples which were located on matrix bricks adjacent to the bed liner were strong, hard, and grayish in color. Those

samples located on the cooler bed liner bricks remained weak, crumbly, and gray-white in appearance (destabilized).

Insulation Bricks

Visual inspection of the heater vessel shell insulation showed that, with the exception of the combustion chamber bricks and the arch bricks adjacent to the dome skew bricks, the various insulating refractories were basically in good condition. The combustion chamber bricks, found fractured and spalled after run 27, remained essentially unchanged since the post-run 27 inspection.

The arch brick deterioration noted was some peripheral crumbling at their interface with the dome skew bricks. This deterioration apparently resulted from a material deformation at the prolonged high temperatures. The arch brick material was calcia stabilized zirconia. It appeared to have deformed about 0.25 in., allowing the entire dome and combustion chamber to sag. It was difficult to visually determine the extent of the deterioration without removing the adjacent refractories. This was not deemed necessary.

ANALYSIS OF MATRIX BRICK SAMPLES

Samples from the yttria stabilized matrix bricks removed from the top of the matrix and those samples which were located on the matrix bricks adjacent to the bed liner at the 9-, 11-, and 13-ft levels were sent to the Aerospace Research Laboratory (ARL) at Wright-Patterson Air Force Base (WPAFB) for photomicrographic and monoclinic crystalline structure (X-ray diffraction) analysis. Photomicrographs showed resintering of the microstructure. Results of the monoclinic analysis are summarized in Table IV-1.

The monoclinic crystalline structure content of the NASA/Ames brick sample (10.4 w/o yttria) remained undetectable. This brick was located at the top of the matrix. However, the Coors brick sample (9.25 w/o yttria) indicated an increase in monoclinic content from an undetectable percentage to 0.9 percent at the center and 1.4 percent near the edge. (The coloration of this brick was noted to be darker at the outer surface.) The reason for the increase in monoclinic content is uncertain. It is known that the brick was subjected to temperatures approximately 400 to 500°R lower than the matrix centerline temperature since it was located to the outside of the matrix. In addition, the surface of the brick protruded upward above the top of the matrix, thereby exposing the brick surface to the hot combustion products of the burner. This would be expected to cause nonuniform temperature gradients in the brick and give rise to undesirable thermal stresses.

TABLE IV-1
MONOCLINIC CRYSTALLINE STRUCTURE ANALYSIS[1]

Specimen	Monoclinic Content, percent after Heat Soak Test
Original 9.25 w/o Yttria-Zirconia	<0.5
"New" 9.25 w/o Yttria-Zirconia	
a. Outer Surface (Darker Color)	1.4
b. Inner Surface (Lighter Color)	0.9
"New" 10.4 w/o Yttria-Zirconia	<0.5
Destabilized Sample Located at	
a. 9-ft Level	5.2
b. 11-ft Level	2.5
c. 13-ft Level	2.9

[1]The analysis was performed by ARL/WPAFB.

APPENDIX V
OPERATING HISTORY OF THE FIRST GENERATION BURNER

The original burner remained in excellent condition throughout the initial 27 heater shakedown runs, conducted at maximum matrix temperatures up to 3450°R. After run 27 and prior to the heat soak, the exterior surface of the water-cooled combustion chamber was plasma spray coated with 0.030 in. of AVCO® No. 41 ceramic powder. This zirconium oxide coating was an attempt to prevent condensation on the outer surface of the combustion chamber.

Inspection after the heat soak (conducted with a maximum matrix temperature of 4550°R) revealed severe erosion of the burner combustion chamber. Localized pitting and relatively large areas of shallow surface erosion were observed. Figures V-1a and b are photographs of the burner tube after the heat soak showing the types of erosion encountered. Pit depths varied, with the maximum depth being approximately 1/16 in. Spalling of the ceramic coating near the burner tip was also observed. It is significant to note that oxygen enrichment was utilized for the first time during the heat soak to achieve the desired burner flame temperatures.

Prior to the test series consisting of runs 28 through 32, the pitted and eroded areas in the combustion chamber were repaired by electrodeposition of copper and remachining. The spalled areas on the outside burner wall were repaired by addition of the zirconium oxide coating. The gold plating was replaced in the combustion chamber and injector head.

Runs 28 through 32 were conducted with maximum matrix temperatures of 3450°R. After run 32, the burner was removed and inspected. No apparent erosion of the combustion chamber walls had occurred during the five previous runs, although deposits of nickel oxide were observed to have formed in the flow channels of the injector head, and additional spalling had occurred in the outer insulation layer near the burner tube tip. The regenerative burner was cleaned and coated with the zirconium oxide insulation prior to the next test series.

With the completion of test series 33 through 37 (conducted with maximum matrix temperatures of 4150°R) severe erosion to the combustion chamber wall was noted. Again, oxygen enrichment was utilized and the erosion was of the same general nature as that observed after the heat soak. In addition, large deposits of oxides of nickel were observed in the injector head flow channels and near the tip of the combustion chamber. Figure V-1c is a photograph of the burner after run 37. With the second appearance of significant erosion, blowdown testing was discontinued while the burner deterioration problem was investigated.

The appearance of the eroded areas pointed to two possible causes of burner damage, nitric acid etching and galvanic corrosion. Nitric acid formation is governed by the following two process reactions:

$$2\ NO + O_2 \rightarrow 2\ NO_2$$

$$H_2O + 3\ NO_2 \rightarrow 2\ HNO_3 + NO$$

The first reaction requires the presence of free oxygen, which was present both during the heat soak and during run series 33 through 37. Water in the liquid phase is required for the second of the above reactions. Areas exist within the burner which, because of water cooling, could provide condensation sites for the water vapor present in the burner combustion products. Hence conditions favorable to the formation of nitric acid can occur in the burner when oxygen enrichment is utilized to achieve the desired burner flame temperatures (as realized for runs at 3950°R and above).

Galvanic corrosion requires the presence of an electrolyte with free hydrogen ions and hydroxyl ions. The reaction is initiated when metal at the anode dissolves into the electrolyte and releases a metal ion and an electron. The electron passes through the electrolyte to the cathodic area and combines with a hydrogen ion to form atomic hydrogen. The positive metallic ion simultaneously combines with a free hydroxyl ion present in the electrolyte to form a neutral metal hydroxide. Formation of atomic hydrogen gas at the cathode tends to blanket the surface and eventually retard the corrosive action. However, with the presence of excess oxygen a reaction occurs at the cathode which removes the protective hydrogen film and allows the corrosion to continue.

As the burner was originally designed, all the elements necessary for galvanic corrosion were present since condensation could provide the necessary electrolyte, combustion produces the excess oxygen, and the gold-copper (combustion chamber) and gold-nickel (injector head) combinations provide the necessary cathodic and anodic materials.

Test 38 was conducted to determine whether galvanic corrosion or nitric acid erosion was the dominant contributor to burner damage. The presence of two dissimilar metals or a single metal with nonuniformities is required for galvanic corrosion to occur. Therefore, prior to the test the gold was removed from the combustion chamber and injector head, thus eliminating galvanically dissimilar metals. The test consisted of a normal reheat from room temperature to a maximum matrix temperature of 3950°R and a slow cooldown to room temperature.

Posttest inspection indicated that burner damage, evidenced by severe combustion chamber wall pitting, had again occurred. Galvanic corrosion was thus eliminated as a major contributor to burner deterioration while nitric acid erosion was considered the prime contributor.

A study of conditions which enhance nitric acid formation and subsequent burner erosion suggested two important considerations for maximizing life of the existing burner. These considerations were: (1) limitation of maximum matrix temperatures to approximately 3450°R thus eliminating oxygen enrichment and (2) minimization of excess oxygen in the exhaust products.

The first consideration imposed an obvious upper limit to the test capabilities of the existing burner. Because of this limit, testing of the ceramic matrix at the upper limit of its operating range became impossible. It was realized at this time that the combination of free oxygen in the burner exhaust products with high temperature resulted in the nitric acid erosion and that the severity of the erosion increased with an increase in burner

flame temperature. Therefore, the decision was made to limit maximum matrix temperatures to 3950°R with the existing burner and to relax the equivalence ratio from approximately 0.9 and 0.95 thus reducing the amount of free oxygen in the combustion products. (An equivalence ratio less than one is necessary because the heater refractories require an oxidizing atmosphere.) It was felt that the 3950°R temperature limit would represent a reasonable compromise permitting useful test results to be obtained in conjunction with restricting nitric acid erosion to a tolerable level.

Burner damage suffered during test 38 was repaired by electrodeposition of copper and replating with gold. The gold plating was applied to the lower 7-1/2 in. of the burner tube interior and the lower 2 in. of the burner tube exterior. Zirconium oxide powder insulation was applied to the exterior of the burner in areas which did not receive gold plating. Photographs of the burner tube and injector heat prior to run 39 are presented in Figs. V-1d and e.

During run 39 (conducted at a maximum matrix temperature of 3950°R), a high pressure air valve leak caused a partial blowdown of the bed, and the test was subsequently aborted. While reheat for run 40 was underway, the matrix temperature stabilized below the desired test level, and all efforts to increase this temperature failed. The test series was subsequently cancelled. Investigations conducted both before and after burner extinguishment were inconclusive as to the exact cause of the temperature stabilization problem. The most probable cause of the problem was a high temperature dependent cooling-water leak from the burner tip into the flame.

Inspection of the burner tube after cooldown indicated that additional nitric acid erosion had occurred near the tip. While undergoing repair, it became apparent that repeated acid erosion and repair had fatigued the burner tube to a point where its structural integrity was questionable. A decision was then made to completely rebuild the lower 7 in. of the zirconium-copper combustion chamber section of the burner tube prior to further testing.

Runs 40 through 44 (conducted at maximum matrix temperatures of 3950°R) were initiated with the rebuilt burner. In addition to replacement of the combustion chamber, the lower 7-1/2 in. of the burner interior wall and the lower 2 in. of the exterior wall along with the tip were replated with a 0.002-in. thickness of gold.

After run 44, inspection revealed no acid erosion in areas where the gold plating had been deposited. However, several locations on the burner exterior had developed fields of small pits where the ceramic coating had flaked away. The pits were subsequently machined off, and the burner tube exterior surface was gold plated up to a point 3 in. above the tip. The remaining exterior surface was again coated with the zirconia insulation.

The following test periods comprised runs 45 through 64 and were accomplished at maximum matrix temperatures of 3450°R. The burner remained in good condition throughout these runs and required no maintenance prior to run 65 except cleaning.

Runs 65 through 69, comprising the next test period, were accomplished at maximum matrix temperatures of 3950°R. After the test period, a water leak was found on the burner tube exterior surface at the tip. The water leak had a deleterious effect on one column of matrix sample bricks, fracturing them into pieces.

After this test period, the decision was made to terminate pilot heater testing until the second generation burner could be fabricated since the existing burner assembly, with the exception of the actual burner tube, would be utilized on the new burner and required modification.

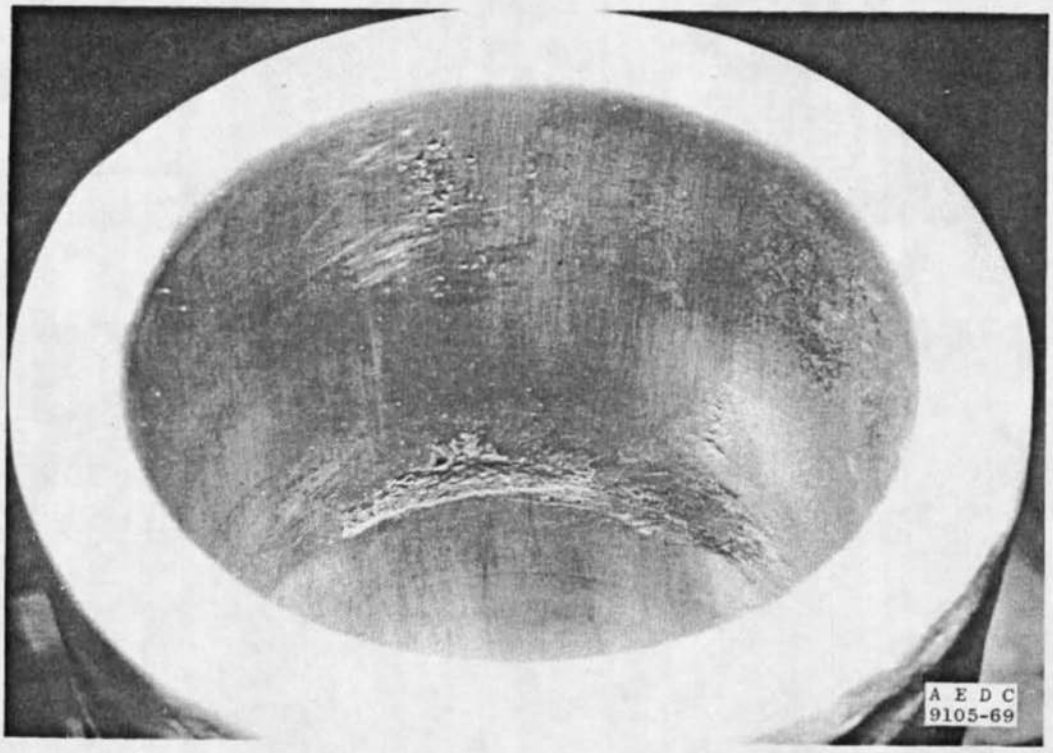

a. Post-Heat Soak

Fig. V-1 First Generation Burner

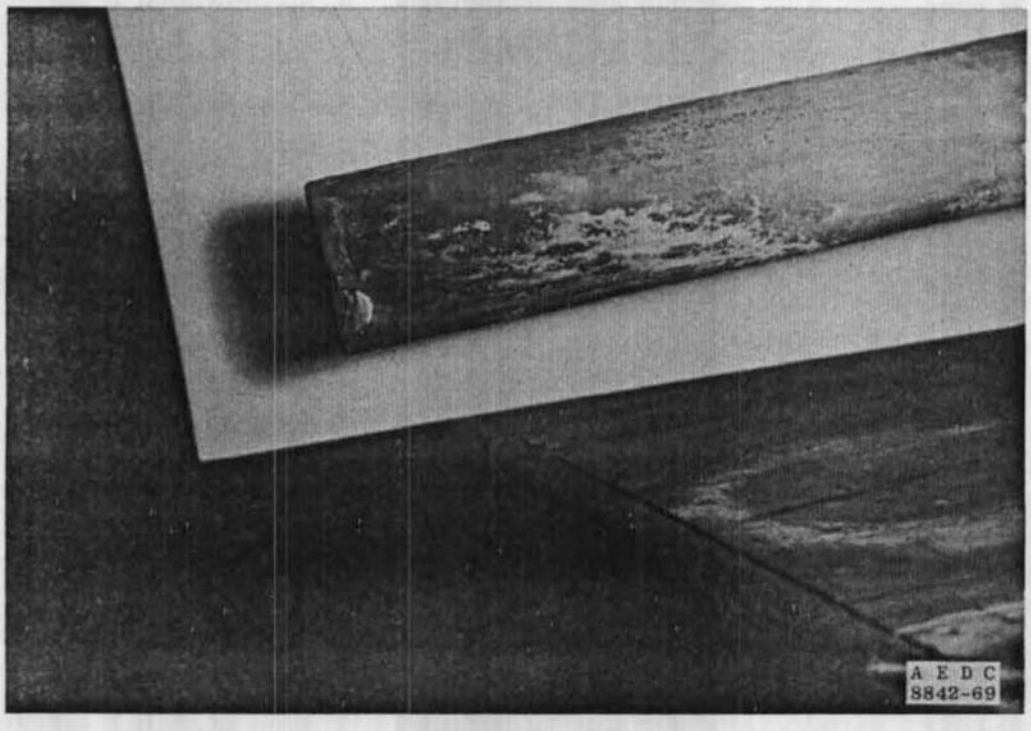

b. Post-Heat Soak

c. Post-Run 37
Fig. V-1 Continued

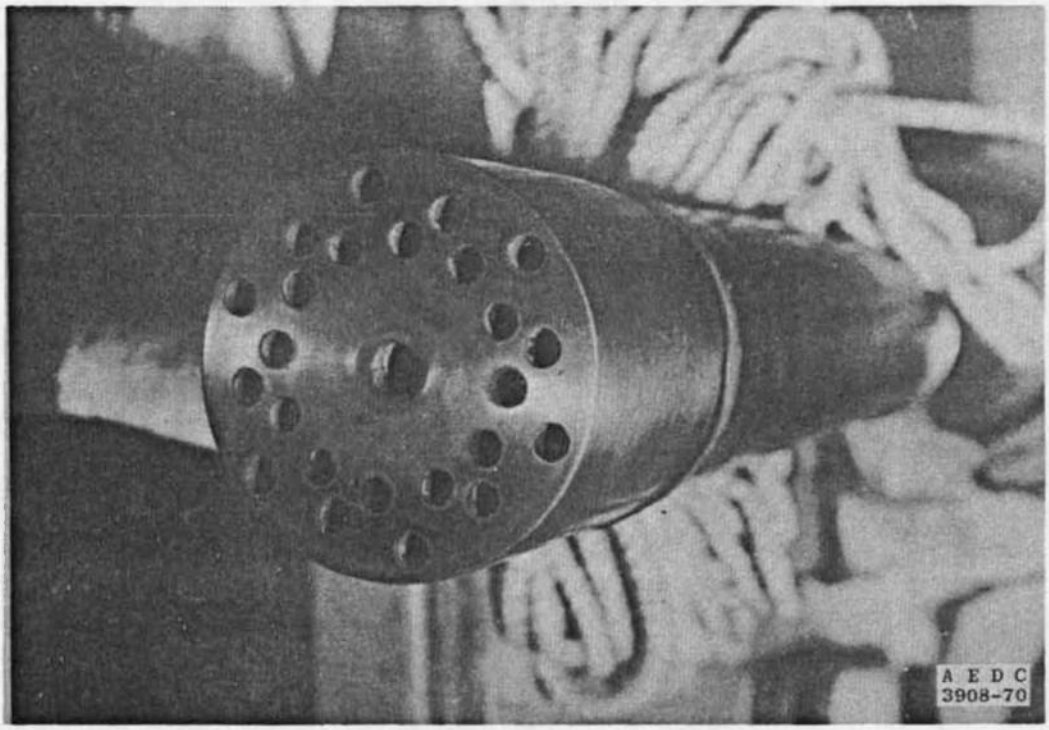

d. Pre-Run 39

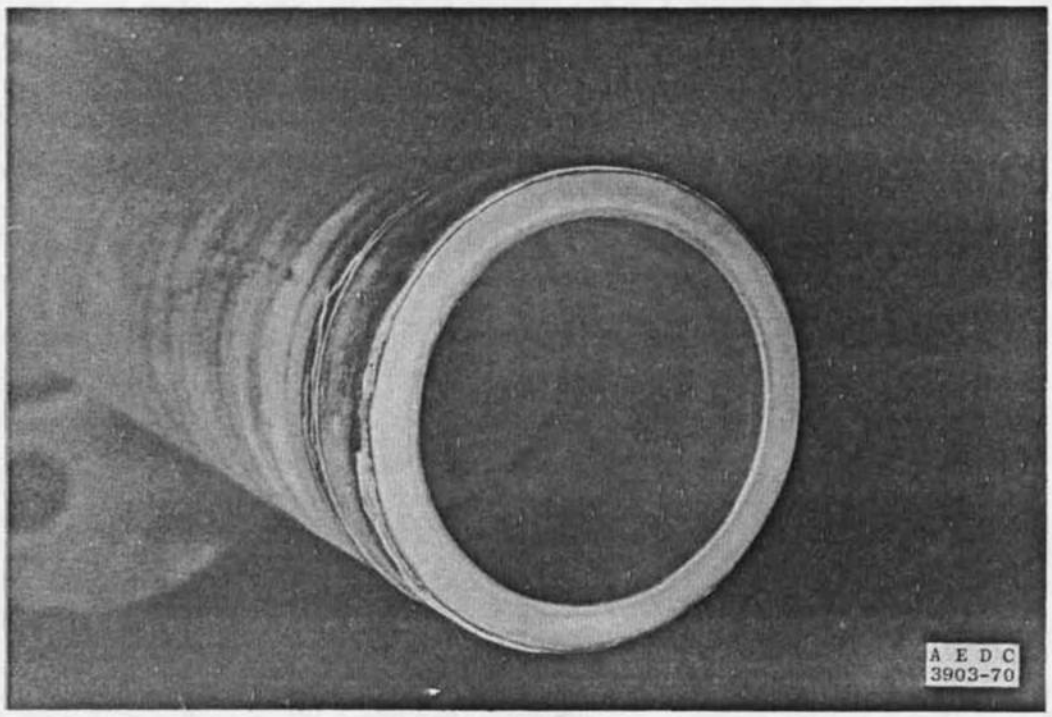

e. Pre-Run 39
Fig. V-1 Concluded

APPENDIX VI
REACTANT FLOW ANOMALY

During reheat in preparation for run 28, an irregularity was realized in the propane flow rate to the burner. At initiation of the fast reheat mode of operation, the propane flow was set at the desired rate of 25.7 lb/hr. Approximately 30 min later, during a periodic recording of matrix bed temperatures, the top of bed temperature was discovered to have dropped from 3220°R to approximately 2400°R. Burner reactant flow settings were checked and the propane flow was found to be reading 12.2 lb/hr. Airflow rate was found to be reading correctly at 514 lb/hr. The propane flow rate was adjusted to the desired value and was observed to be stable. Approximately 5 min later, another check of the propane flow rate revealed the flow had again dropped; however, the value was not recorded. After again making the necessary flow correction, no other problems were encountered with the system for the remainder of the test period (runs 28 through 32).

After the test period, sample bricks were removed from the heater for inspection and excessive cracking was noted in the bricks inspected. Posttest inspection of the propane system revealed a significant quantity of nonidentifiable debris in a pressure relief valve upstream of the propane rotameter.

Burner fuel-oxidizer ratios were calculated to have been 0.050 and 0.0237 for the correct and perturbed burner flows, respectively. Theoretical adiabatic flame temperatures corresponding to the normal and abnormal burner flows are 3440 and 2130°R, respectively.

The time period for which the anomalous flow setting existed is unknown. Based on the measured and predicted matrix temperature profiles, the abnormal conditions apparently lasted for only a relatively short duration. The cooling of the refractory matrix and/or the rapid heating which followed probably produced excessive thermal stresses resulting in cracking of the refractories at the top of the bed.

APPENDIX VII

ANALYTICAL STUDY OF ZIRCONIA REFRACTORIES FROM AEDC'S AIR STORAGE HEATER: POSTMORTEM IN-SERVICE ANALYSES

L. L. Fehrenbacher and D. F. Frank
Aerospace Research Laboratories

INTRODUCTION

A postmortem analytical study of yttria stabilized cored block and hot face bed liner insulation brick removed from the 14-in.-diam AEDC pilot storage heater after completion of an 85-run checkout program was conducted at the Aerospace Research Laboratories (ARL). Matrix brick samples were selected at one foot intervals from the top of the ZrO_2 bed portion (15 ft) to the alumina block (7ft 7 in.) interface from both a center column and outer (next to insulation) column. A few fractured tongue and groove ZrO_2 insulation brick and 2800°F firebrick of special interest were also chosen for evaluation.

These pilot heater refractories were subjected to crystal structure and compositional analyses via X-ray diffraction, X-ray fluorescence, and electron probe techniques; microstructure examination for grain growth, porosity, and second phase determinations; and impurity analyses using optical emission spectrographic (OES) and spark source mass spectrographic (SSMS) methods.

RESULTS

MATRIX CORED BLOCK

Crystalline Phase Stability

The results of X-ray diffractometer analyses on both powder and solid ZrO_2 cored brick samples are shown in Table VII-1. All samples examined were fully cubic with the exception of a very friable sample at the bottom of the ZrO_2 bed which contained 5.85-percent monoclinic phase.

Microstructure

Photomicrographs of cored block polished sections are shown in the composite of Fig. VII-1. The ZrO_2 materials at the top of the bed (14- to 15-ft-level) exhibit large equiaxed grains containing microstructures, a condition indicative of exposure at high temperatures. Pores also have become more rounded and larger as expected. No solid second phase is apparent. In the midportion of the ZrO_2 bed (11- to 12-ft-level), the microstructure

was markedly different as reflected by Figs. VII-1d and e, consisting of large, rounded grains and a slightly darker reflecting second phase between the primary grain structure. Since this grain boundary phase was not detectable by X-ray diffraction, the electron microprobe method was employed to determine the chemistry of this phase. These results are discussed in the next section. A ZrO_2 specimen cut from a block in the center column (col. 3) near the alumina interface showed a small grain, equiaxed structure (Fig. VII-1f) and the absence of a second phase, a result consistent with X-ray diffraction on this sample. A polished section of the ZrO_2 sample that contained approximately 6-percent monoclinic ZrO_2 was not examined metallographically, but the monoclinic phase would, undoubtedly, have been readily discernible microstructurally.

Electron Microprobe Analysis

The polished section of the YRE_2O_3-ZrO_2, 12-ft-level sample (photomicrograph Fig. VII-1d) that contained the large ZrO_2 grain structure surrounded by a grain boundary second phase was subjected to electron probe analysis. The electron backscatter photograph of Fig. VII-2a is representative of one of the areas that was studied. The relative yttrium and zirconium concentrations in the grain and boundary phases were measured first.

The ratio of Zr to Y intensities was essentially constant within in the grains while the $Zr_{L\alpha}$ and $Y_{L\alpha}$ (strongest X-radiation peaks of these elements) peaks were absent in the unknown phase, indicating that this boundary phase was not a yttria-zirconia based composition.

The second phase was next examined for the presence of impurities. As seen in the accompanying X-ray pulse photographs of Fig. VII-2, the boundary phase consisted principally of barium and silicon along with small amounts of calcium and aluminum and possibly other impurities such as phosphorous and iron. Probe analysis of other second-phase areas gave similar elemental concentration.

Impurity Analysis

The optical emission and spark source mass spectrometric impurity analyses for the ZrO_2 matrix brick are presented in Table VII-2. The ZrO_2 matrix brick analyzed were designated as samples 1, 2, 3, and 11 in the table. Of note is the slightly lower overall impurity levels in the brick sample from the upper portion of the storage heater (sample 2, 14-ft-level) and the significant increase in barium and silicon concentrations in samples 1, 3, and 11 from the lower levels of the ZrO_2 matrix. The differences between OES and SSMS concentration values may result from sample inhomogeneity as well as the difference in the precision of the two methods. SSMS should give better values below 0.1 (1000 ppm) w/o and OES more accuracy above 0.1 w/o. Since a series of standards for a Y_2O_3-ZrO_2 matrix were not available, the values quoted in Table VII-2 should be accurate within a factor of two.

The Y_2O_3 values reported in OES column are not significant even on a relative basis. However, the X-ray fluorescence data of Table VII-3 provide a relative difference accuracy of at least ±0.15 weight percent Y_2O_3. The Y_2O_3 values for the matrix ZrO_2 brick

(sample 1 and 11) are within the as-batched compositional range (8.2- to 8.3-percent Y_2O_3 is the 90-percent concentration value of the 9.25 w/o yttria mixed rare earth stabilizer).

INSULATION REFRACTORIES

Crystalline Phase Stability

The X-ray diffraction analyses of selected ZrO_2 insulation samples are shown in Table VII-4. The monoclinic content for both solid and powdered samples taken from various locations on the tongue and groove brick was measured. Only a solid chunk from the cold face of dome brick CC-9 showed any detectable monoclinic phase (~1 percent). Since earlier X-ray results of Y_2O_3-ZrO_2 hot face insulation (Fluidyne No. 1049-5**) had exhibited significant destabilization (16- to 20-percent monoclinic) in the tongue and groove fracture zone, the absence of monoclinic ZrO_2 phase in the fracture zones of the AEDC insulation brick was unexpected. Therefore, the 1049-5** fracture zone was again examined by the powder diffractometer method, yielding a concentration of 17 percent monoclinic as before. In order to resolve these experimental anomalies, polished sections from the hot, fracture, and cold faces of the 1049-5** sample were analyzed with the electron probe. The probe study revealed that the 1049-5** sample was a calcia stabilized zirconia bedliner insulation brick and not a Y_2O_3-ZrO_2 refractory as designated. Further X-ray diffraction analysis is required to corroborate the contributory role of destabilization in causing the Y_2O_3-ZrO_2 brick to fracture along the tongue and groove section.

Microstructure

Only sections from the hot and cold surfaces of dome brick CC-9 were prepared for microstructure analysis. The hot face surface consisted of a wide range of grain sizes, all exhibiting very angular shaped boundary morphology (Fig. VII-3a). The cold face structure appeared to consist of more rounded grains, but still possessed a wide difference in sizes (Fig. VII-3b).

Impurity Analyses

There appears to be no measurable difference in impurity concentrations of the as-fabricated 8-1/4-percent Y_2O_3-ZrO_2 insulation and the fracture face of the 8-1/4-percent CC-9 dome brick. However, both the hot and cold faces of the 9-1/4-percent Y_2O_3-ZrO_2 brick No. 1077** show a decrease in impurities compared to the as-fabricated (sample 8). Silicon, Al, Mg, Ti, and Fe all experienced factors of 2 to 10 reduction in impurity levels. The fire-brick specimens (samples 4 and 9, Table VII-2) gave almost identical OES results with the major impurities being Mg, Ti, and Fe.

**Not from AEDC pilot heater.

CONCLUSIONS

1. The yttria rare earth stabilized zirconia cored block (9.25 w/o YRE_2O_3) did not undergo cubic phase deterioration. Portions of the blocks near the alumina-zirconia interface that still contained monoclinic ZrO_2 had (a) not been totally restabilized during the 96-hr bed restoration heat soak and (b) not seen the necessary temperature-time combination during the remaining heater checkout runs to complete the cubic stabilization process.

2. Microstructure-microprobe analyses identified the presence of a barium silicate glassy phase throughout the cubic ZrO_2 grain matrix in the cored blocks in the center section of the ZrO_2 block matrix (10- to 12-ft-level). The large increase in barium and silicon concentrations in brick from this region of the bed were also confirmed by bulk impurity analyses (SSMS and OES). The glassy nature of this second phase was inferred by (a) the rounded grain corners and boundaries of the primary ZrO_2 grains and (b) the lack of X-ray diffraction evidence for a crystalline phase.

3. The mechanism of formation of this glassy impurity phase is not known. It appears that barium and silicon impurities from ZrO_2 blocks near the top of the bed may have been transported (probably by vaporization and condensation) to these intermediate levels where the thermal conditions are favorable for the formation of a barium silicate glass. There was no evidence that this boundary phase was deleterious to the performance of the cored block; i.e., enhanced destabilization, creep, or reheat shrinkage.

4. The fractures in the tongue and groove sections of the ZrO_2 insulation brick were not correlated with destabilization and thermal expansion stress discontinuities. Since many of the as-fabricated ZrO_2 bed liner refractories contain visible cracks along the length of the tongue and groove area, it is possible that thermal gradient stresses during reheat and blowdown produce fractures in the bed liner above the matrix. Shear stress loading of the backup insulation probably contributes to the cracking in the tongue and groove region of the ZrO_2 dome brick.

5. The aluminum silicate firebrick insulation that gave evidence of melting was not fluxed by other impurities. The temperatures were evidently too high near the viewports, and higher temperature insulation is required in these areas.

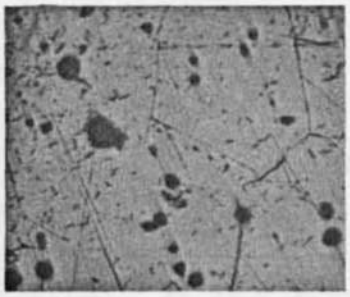

a. 10.8-Percent Y_2O_3-ZrO_2
Column 14, Top of Bed (200x)

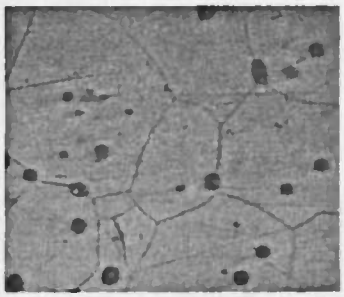

b. 9.25-Percent YRE_2O_3-ZrO_2
15-ft-Level Outer Segment (200x)

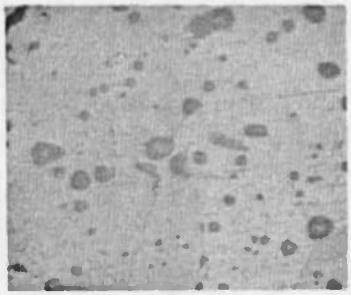

c. 9.25-Percent YRE_2O_3-ZrO_2
14-ft Level, Outer Segment (128x)

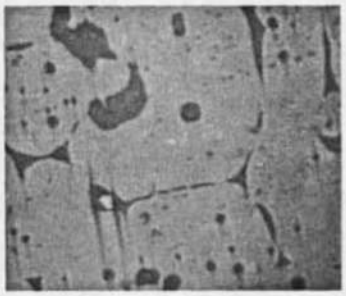

d. 9.25-Percent YRE_2O_3-ZrO_2
12-ft Level, Column 2 (Outer) (200x)

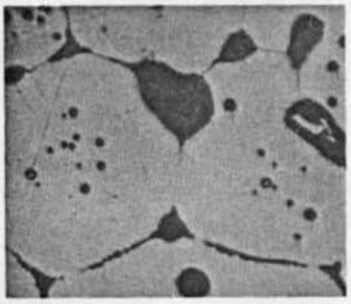

e. 9.25-Percent YRE_2O_3-ZrO_2
11-ft Level, Column 3 (Center)
(200x)

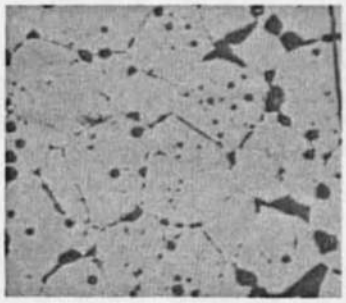

f. 9.25-Percent YRE_2O_3-ZrO_2
8-ft Level, Column 3 (Center)
(200x)

Fig. VII-1 Photomicrograms of Stabilized ZrO_2 Cored Block Samples

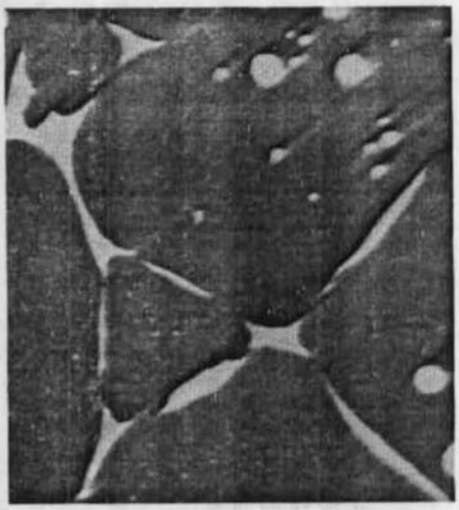

a. Electron Backscatter Photo Showing Second Phase between ZrO_2 Grains

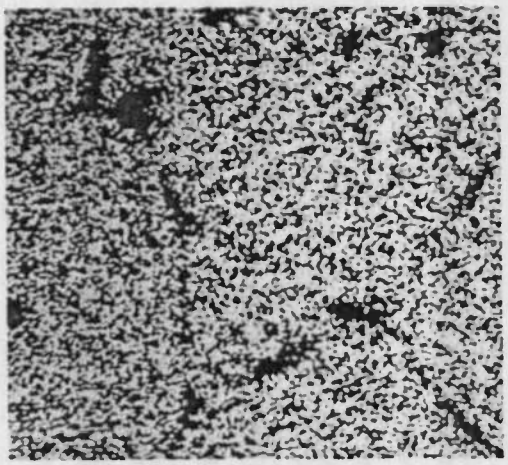

b. $Zr_{L\alpha}$ (500x)

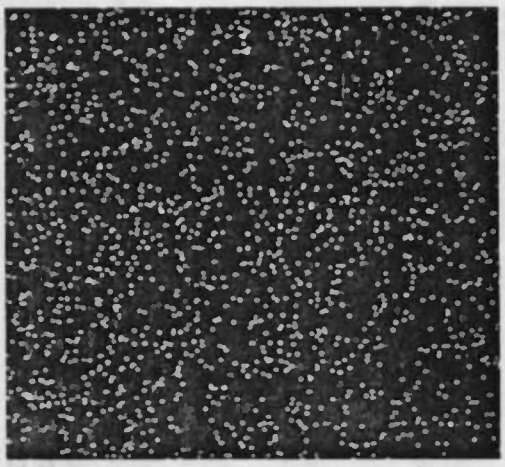

c. $Y_{L\alpha}$ (500x)

Fig. VII-2 Electron Microprobe X-Ray Photographs of 9.25 w/o YRE_2O_3-ZrO_2 Sample from 12-ft Level

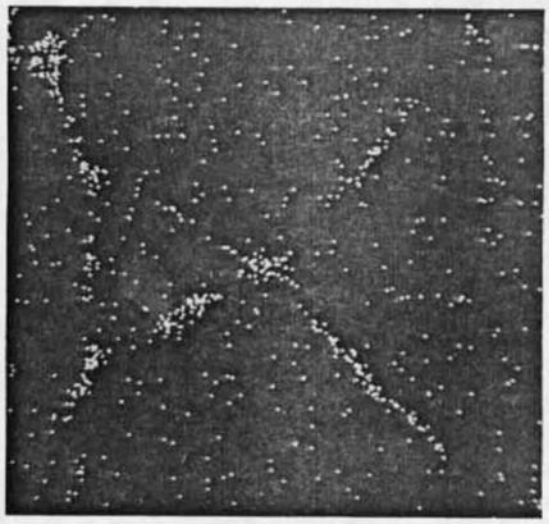

d. $Ba_{L\alpha}$ (500x)

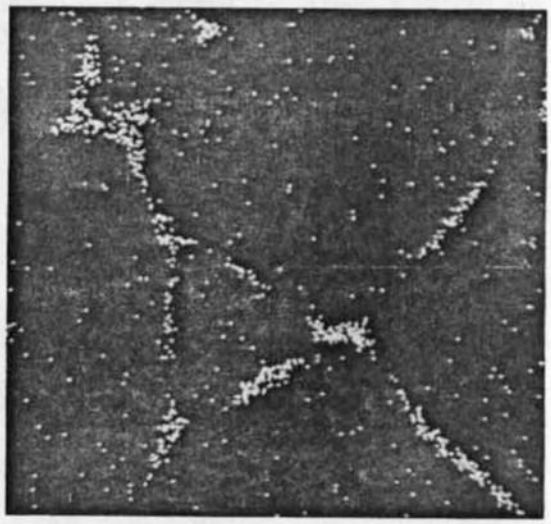

e. $Si_{L\alpha}$ (500x)

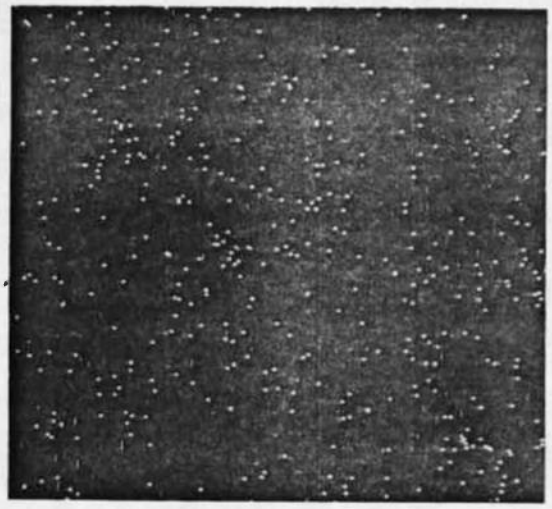

f. $Ca_{L\alpha}$ (500x)

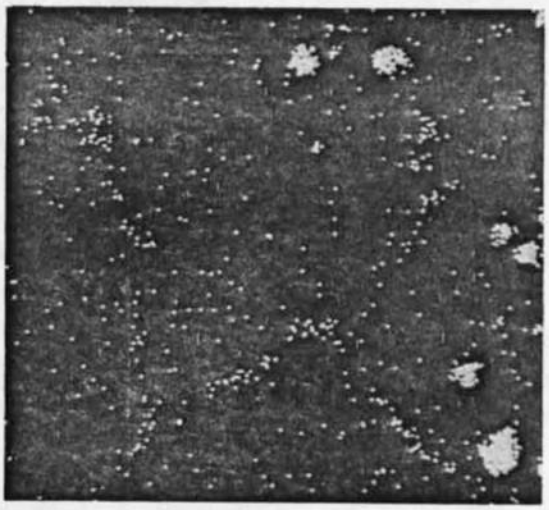

g. $Al_{L\alpha}$ (500x)

Fig. VII-2 Concluded

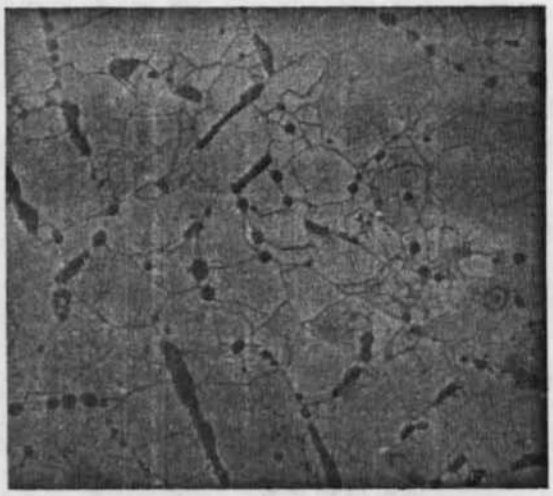

a. Hot Face Microstructure
(200x)

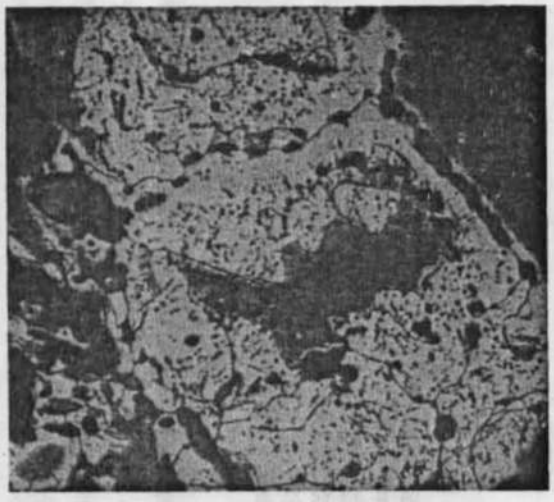

b. Cold Face Microstructure
(200x)

Fig. VII-3 Photomicrographs of 8-¼-percent Y_2O_3-ZrO_2 Dome Brick CC-9, Fourth Course

TABLE VII-1
X-RAY DIFFRACTION ANALYSES
MATRIX BRICK

Brick Description	Sample Location	X-Ray Setting	Percent Monoclinic
Zircoa 10.8% Y_2O_3 Solid	Col. 14, 15'3" Brick 1 (Top of Bed)		0% (Well Defined Cubic)
Coors 9.25% YRE_2O_3 Solid	12' Col. 1 (Outside)		0%
Coors 9.25% YRE_2O_3 Solid	14' Col. 1 (Outside)		0%
Coors 9.25 9.25% YRE_2O_3 Solid	8' Col. 3 (Center)		0%
Coors 9.25% YRE_2O_3 Solid	15' Outer Segment		0%
Coors 9.25% YRE_2O_3 Solid	11' Col. 3 (Center)	30 ku 20 ma* 8 1 4	0%
	Matrix Brick - Rerun Powder Samples		
9.25% YRE_2O_3 Powder	14' Level Col. 5		0%
9.25% YRE_2O_3 Powder	12' Level Col. 3		0%
9.25% YRE_2O_3 Powder	11' Level Col. 3		0%

*All diffractometer traces were run at 1/4°2θ/minute with $Cu_{K\alpha}$-Ni filtered radiation.

TABLE VII-2
OPTICAL EMISSION AND SPARK SOURCE MASS SPECTROMETRIC IMPURITY ANALYSES

	Matrix Brick Col. 3 11' Level Sample # 1 Weight %		Matrix Brick Col. 3 14' Level Sample # 2 Weight %		Matrix Brick Col. 3 8' Level Sample # 3 Weight %		2800 F Firebrick Under Heater Shelf Sample # 4 Weight %		Dome Brick CC-9 4th Course Hot Face Sample # 5 Weight %		CC-9 Fracture Face Sample # 6 Weight %		8¼ Bed Liner ASFAB No. 1078 Sample # 7 Weight %	
Element	Emission	SSMS*	Emission	SSMS	Emission	SSMS	Emission	SSMS	Emission	SSMS	Emission	SSMS	Emission	SSMS
Be	< 0.001	< 0.00001	< 0.001	< 0.00001	< 0.001	0.000006	< 0.001	-	< 0.001	< 0.00001	< 0.001	< 0.00001	< 0.001	< 0.00001
B	0.05	0.08	0.1	0.05	0.05	0.04	0.2	-	0.03	0.04	0.03	0.03	0.02	0.03
P	-	0.0002	-	0.0001	-	< 0.0001	-	-	-	< 0.0001	-	0.0001	-	0.0001
Na	-	0.0002	-	0.0002	-	0.0002	-	-	-	0.0002	-	0.0002	-	0.0001
Mg	0.03	0.04	0.03	0.045	0.02	0.04	0.1	-	0.1	0.4	0.1	0.2	0.1	0.15
Al	0.05	0.02	< 0.02	0.008	< 0.02	0.015	Matrix	-	< 0.02	0.002	< 0.02	0.005	< 0.02	0.003
Si	0.2	0.35	0.01	0.02	0.03	0.2	Matrix	-	0.01	0.01	0.02	0.05	0.02	0.035
P	-	0.00005	-	0.0001	-	0.0001	-	-	-	0.0001	-	0.0001	-	0.0001
S	-	0.0010	-	0.001	-	0.0010	-	-	-	0.0010	-	0.001	-	0.002
Cl	-	0.003	-	0.004	-	0.0010	-	-	-	0.01	-	0.01	-	0.001
K	-	0.0005	-	0.0001	-	0.0001	-	-	-	0.004	-	0.0004	-	0.0002
Ca	< 0.1	0.063	< 0.1	0.075	< 0.1	0.065	< 0.1	-	< 0.1	0.4	< 0.1	0.4	< 0.1	0.2
Sc	-	Masked	-	Masked	-	Masked	-	-	-	Masked	-	Masked	-	Masked
Ti	0.03	0.02	0.03	0.02	0.03	0.025	~ 0.5	-	0.03	0.025	0.1	0.06	0.05	0.03
V	< 0.02	< 0.00001	< 0.02	< 0.00001	< 0.02	< 0.00003	< 0.02	-	< 0.02	< 0.0001	< 0.02	< 0.0001	< 0.02	< 0.0001
Cr	< 0.03	0.002	< 0.03	0.002	< 0.03	0.0040	0.03	-	< 0.03	0.0004	< 0.03	0.015	< 0.03	0.005
Mn	0.003	0.003	0.002	0.0005	0.002	0.0030	0.03	-	< 0.002	0.0002	< 0.002	0.0002	< 0.002	0.0002
Fe	0.05	0.05	0.02	0.025	0.05	0.073	0.3	-	0.01	0.04	0.02	0.025	0.02	0.03
Co	< 0.03	< 0.0001	< 0.03	< 0.0001	< 0.03	< 0.0001	< 0.03	-	< 0.03	< 0.0001	< 0.03	< 0.0001	< 0.03	< 0.0001
Ni	< 0.05	0.002	< 0.05	0.002	< 0.05	0.0080	0.1	-	< 0.05	0.0008	< 0.05	0.0020	< 0.05	0.0020
Cu	< 0.003	0.0001	< 0.003	0.0002	< 0.003	0.0002	≤ 0.003	-	< 0.003	0.0006	< 0.003	0.0003	≤ 0.003	0.0020
Zn	-	0.0008	-	0.0003	-	0.0005	-	-	-	0.0030	-	0.0008	-	0.0005
Ga	-	< 0.0001	-	< 0.0001	-	< 0.0001	-	-	-	< 0.0001	-	< 0.0001	-	< 0.0001
Ge	-	< 0.0001	-	< 0.0001	-	< 0.0001	-	-	-	< 0.0001	-	< 0.0001	-	< 0.0001
As	-	< 0.0001	-	< 0.0001	-	< 0.0001	-	-	-	< 0.0001	-	< 0.0001	-	< 0.0001
Se	-	≤ 0.0002	-	< 0.0001	-	< 0.0001	-	-	-	< 0.0001	-	< 0.0001	-	< 0.0001
Br	-	0.0001	-	< 0.0001	-	< 0.0001	-	-	-	< 0.0001	-	< 0.0001	-	< 0.0001
Rb	< 0.03	0.0001	< 0.03	< 0.0001	< 0.03	< 0.0001	< 0.03	-	< 0.03	< 0.0001	< 0.03	< 0.001	< 0.03	< 0.0002
Sr	-	0.02	-	0.01	-	0.01	-	-	-	0.002	-	0.007	-	0.0070
Y_2O_3	9.1	Matrix	7.9	Matrix	13.0	Matrix	-	-	8.0	Matrix	8.0	Matrix	7.6	Matrix
Zr	Matrix	Matrix	Matrix	Matrix	Matrix	Matrix	0.3	-	Matrix	Matrix	Matrix	Matrix	Matrix	Matrix
Nb	< 0.03	0.0001	< 0.03	< 0.0001	< 0.03	< 0.0001	< 0.03	-	< 0.03	< 0.0001	< 0.03	< 0.0001	< 0.03	< 0.0001
Mo	< 0.01	< 0.0001	< 0.01	< 0.0001	< 0.01	< 0.0001	< 0.01	-	< 0.01	< 0.0001	< 0.01	< 0.0001	< 0.01	< 0.0001
Ru	-	< 0.0001	-	< 0.0001	-	< 0.0001	-	-	-	< 0.0001	-	< 0.0001	-	< 0.0001
Rh	-	< 0.0001	-	< 0.0001	-	< 0.0001	-	-	-	< 0.0001	-	< 0.0001	-	< 0.0001
Pd	-	< 0.0001	-	< 0.0001	-	< 0.0001	-	-	-	< 0.0001	-	< 0.0001	-	< 0.0001

TABLE VII-2 (Continued)

Element	Sample # 1 Weight % Emission	Sample # 1 Weight % SSMS	Sample # 2 Weight % Emission	Sample # 2 Weight % SSMS	Sample # 3 Weight % Emission	Sample # 3 Weight % SSMS	Sample # 4 Weight % Emission	Sample # 4 Weight % SSMS	Sample # 5 Weight % Emission	Sample # 5 Weight % SSMS	Sample # 6 Weight % Emission	Sample # 6 Weight % SSMS	Sample # 7 Weight % Emission	Sample # 7 Weight % SSMS
Ag	< 0.005	-	< 0.005	-	< 0.005	-	< 0.005	-	< 0.005	-	< 0.005	-	< 0.005	-
Cd	< 0.03	0.0002	< 0.03	0.0002	< 0.03	0.0002	< 0.03	-	< 0.03	0.0002	< 0.03	0.0002	< 0.03	< 0.0002
In	-	< 0.0001	-	< 0.00001	-	< 0.000001	-	-	-	< 0.0001	-	< 0.0001	-	< 0.0001
Sn	< 0.01	0.0001	< 0.01	< 0.0001	< 0.01	< 0.0001	< 0.01	-	< 0.01	< 0.0001	< 0.01	< 0.0001	< 0.01	< 0.0001
Sb	< 0.03	0.0001	< 0.03	< 0.0001	< 0.03	< 0.0001	< 0.03	-	< 0.03	< 0.0001	< 0.03	< 0.0001	< 0.03	0.0001
Te	-	0.0003	-	0.0003	-	0.0008	-	-	-	0.003	-	< 0.0001	-	< 0.0001
I	-	< 0.0001	-	< 0.0001	-	< 0.0001	-	-	-	< 0.0001	-	< 0.0001	-	< 0.0001
Cs	-	< 0.0001	-	< 0.0001	-	< 0.0001	-	-	-	< 0.0001	-	< 0.0001	-	< 0.0001
Ba	0.3	1.8	0.03	0.04	0.3	1.0	0.03	-	0.01	0.005	0.03	0.01	< 0.01	0.0040
La	-	0.003	-	0.0010	-	0.003	-	-	-	0.001	-	0.0004	-	0.001
Ce	-	0.003	-	0.010	-	0.003	-	-	-	0.01	-	0.03	-	0.03
Pr	-	0.0003	-	0.0001	-	0.0003	-	-	-	0.001	-	0.001	-	0.001
Nd	-	0.004	-	0.004	-	0.004	-	-	-	0.02	-	0.02	-	0.02
Sm	-	0.015	-	0.003	-	0.01	-	-	-	0.035	-	0.035	-	0.035
Eu	-	0.02	-	0.02	-	0.03	-	-	-	0.003	-	0.0003	-	0.0003
Gd	-	0.015	-	0.007	-	0.015	-	-	-	0.04	-	0.04	-	0.02
Tb	-	0.015	-	0.035	-	0.015	-	-	-	0.015	-	0.03	-	0.01
Dy	~ 0.5	1.2	~ 0.5	0.55	~ 0.5	1.2	< 0.1	-	~ 0.5	0.55	~ 0.5	0.55	< 0.3	0.55
Ho	0.13	0.3	0.14	0.15	0.22	0.35	< 0.1	-	< 0.1	0.015	< 0.1	0.015	≲ 0.1	0.01
Er	-	0.04	-	0.03	-	0.03	-	-	-	0.03	-	0.03	-	0.03
Tm	-	0.005	-	0.001	-	0.003	-	-	-	0.01	-	0.01	-	0.01
Yb	0.021	0.035	0.016	0.015	0.035	0.035	< 0.002	-	0.058	0.1	0.07	0.1	0.05	0.05
Lu	-	0.004	-	0.004	-	0.004	-	-	-	0.01	-	0.01	-	0.06
Hf	2.0	1.4	2.0	1.2	2.0	1.2	< 0.1	-	2.0	1.2	2.0	1.3	2.0	0.8
Ta	< 0.1	< 0.0001	< 0.1	< 0.0001	< 0.1	< 0.0001	< 0.1	-	< 0.1	< 0.0001	< 0.1	< 0.0001	< 0.1	< 0.0001
W	< 0.1	0.0010	< 0.1	0.0002	< 0.1	0.0004	< 0.1	-	< 0.1	0.001	< 0.1	0.0006	< 0.1	0.0004
Re	-	< 0.0001	-	< 0.0001	-	< 0.0001	-	-	-	< 0.0001	-	< 0.0001	-	< 0.0001
Os	-	< 0.0001	-	< 0.0001	-	< 0.0001	-	-	-	< 0.0001	-	< 0.0001	-	< 0.0001
Ir	-	< 0.0001	-	< 0.0001	-	< 0.0001	-	-	-	< 0.0001	-	< 0.0001	-	< 0.0001
Pt	-	< 0.0001	-	< 0.0001	-	< 0.0001	-	-	-	< 0.0001	-	< 0.0001	-	< 0.0001
Au	-	< 0.0001	-	< 0.0001	-	< 0.0001	-	-	-	< 0.0001	-	< 0.0001	-	< 0.0001
Hg	-	< 0.0001	-	< 0.0001	-	< 0.0001	-	-	-	< 0.0001	-	< 0.0001	-	< 0.0001
Tl	-	< 0.0001	-	< 0.0001	-	< 0.0001	-	-	-	< 0.0001	-	< 0.0001	-	< 0.0001
Pb	< 0.01	0.0008	< 0.01	0.0002	< 0.01	0.0004	< 0.01	-	< 0.01	0.0002	< 0.01	0.0002	< 0.01	0.0002
Bi	< 0.01	< 0.0001	< 0.01	< 0.0001	< 0.01	< 0.0001	< 0.01	-	< 0.01	< 0.0001	< 0.01	< 0.0001	< 0.01	< 0.0001
Th	< 0.1	0.0007	< 0.1	0.0005	< 0.1	0.0007	< 0.1	-	< 0.1	0.005	< 0.1	0.005	< 0.1	0.0070
U	-	0.0007	-	0.0010	-	0.0010	-	-	-	0.002	-	0.025	-	0.03

*SSMS-Spark-Source Mass Spectrometer

TABLE VII-2 (Continued)

Element	9% Y_2O_3-ZrO_2 Bedliner ASFAB Sample # 8 Weight %		2800°F Firebrick 11' Viewport Sample # 9 Weight %		9% Bedliner Cold Face No. 1077 Nasa Ames** Sample # 10 Weight %		Matrix Brick Col. 5 7'6" Level Sample # 11 Weight %		9% Bedliner Hot Face No. 1077 Nasa Ames** Sample # 12 Weight %		9% Bedliner L-43 9' Level Sample # 13 Weight %	
	Emission	SSMS	Emission	SSMS	Emission	SSMS	Emission	SSMS	Emission	SSMS	Emission	SSMS
Be	< 0.001	-	< 0.001	-	< 0.001	< 0.0001	< 0.001	< 0.0001	< 0.001	< 0.0001	< 0.001	< 0.0001
B	0.03	-	0.5	-	0.02	0.01	0.05	0.08	0.02	0.03	0.02	0.02
F	-	-	-	-	-	0.0001	-	0.0004	-	< 0.0001	-	< 0.0001
Na	-	0.0001	-	-	-	0.0002	-	0.0001	-	0.0001	-	0.0001
Mg	0.07	0.15	0.1	-	0.1	0.05	0.05	0.07	0.05	0.045	0.05	0.075
Al	0.2	0.1	Matrix	-	< 0.02	0.005	0.05	0.05	0.03	0.003	0.02	0.01
Si	0.02	0.06	Matrix	-	0.03	0.02	0.05	0.1	~ 0.005	0.002	0.02	0.03
P	-	0.0001	-	-	-	0.0001	-	0.0005	-	0.0001	-	0.0001
S	-	0.002	-	-	-	0.0020	-	0.0030	-	0.0020	-	0.0010
Cl	-	0.003	-	-	-	0.0010	-	0.003	-	0.0005	-	0.0015
K	-	0.0004	-	-	-	0.0004	-	0.0004	-	0.0001	-	0.0003
Ca	< 0.1	0.2	< 0.1	-	< 0.1	0.4	< 0.1	0.1	< 0.1	0.2	< 0.1	0.4
Sc	-	Masked	-	-	-	Masked	-	Masked	-	Masked	-	Masked
Ti	0.2	0.25	≥ 1.0	-	0.05	0.055	0.03	0.02	0.03	0.016	0.1	0.025
V	< 0.02	0.0005	≤ 0.02	-	< 0.02	< 0.0001	< 0.02	< 0.0001	< 0.02	< 0.0001	< 0.02	< 0.0001
Cr	< 0.03	0.0040	0.03	-	< 0.03	0.0040	< 0.03	0.0020	< 0.03	0.0004	< 0.03	0.0020
Mn	< 0.002	0.0002	0.05	-	< 0.002	0.0003	0.005	0.0020	< 0.002	0.0001	0.002	0.0005
Fe	0.02	0.02	0.5	-	0.05	0.03	0.05	0.05	0.02	0.0150	0.03	0.025
Co	< 0.03	< 0.0001	< 0.03	-	< 0.03	0.0004	< 0.03	< 0.0001	< 0.03	< 0.0001	< 0.03	0.0002
Ni	< 0.05	0.003	0.05	-	< 0.05	0.002	< 0.05	0.0030	< 0.05	0.0010	< 0.05	0.0015
Cu	0.01	0.015	0.003	-	0.005	0.006	< 0.003	0.0002	0.003	0.0006	~ 0.003	0.0006
Zn	-	0.0010	-	-	-	0.0005	-	0.0002	-	0.0001	-	0.0003
Ga	-	< 0.0001	-	-	-	< 0.0001	-	< 0.0001	-	< 0.0001	-	< 0.0001
Ge	-	< 0.0001	-	-	-	< 0.0002	-	< 0.0001	-	< 0.0001	-	< 0.0001
As	-	< 0.0001	-	-	-	< 0.0002	-	< 0.0001	-	< 0.0001	-	< 0.0001
Se	-	< 0.0001	-	-	-	< 0.0002	-	< 0.0001	-	< 0.0001	-	< 0.0001
Br	-	< 0.0001	-	-	-	< 0.0001	-	< 0.0001	-	< 0.0001	-	< 0.0001
Rb	< 0.03	< 0.0001	< 0.03	-	< 0.03	< 0.0001	< 0.03	< 0.0001	< 0.03	< 0.0001	< 0.03	< 0.0001
Sr	-	0.010	-	-	-	0.0070	-	0.007	-	0.0070	-	0.0030
Y_2O_3	11.0	Matrix	-	-	8.8	Matrix	8.5	Matrix	8.3	Matrix	8.9	Matrix
Zr	Matrix	Matrix	~ 0.5	-	Matrix	Matrix	Matrix	Matrix	Matrix	Matrix	Matrix	Matrix
Nb	< 0.03	< 0.0001	< 0.03	-	< 0.03	0.0001	< 0.03	< 0.0001	< 0.03	< 0.0001	< 0.03	< 0.0001
Mo	< 0.01	< 0.0001	< 0.01	-	< 0.01	< 0.0001	< 0.01	< 0.0001	< 0.01	< 0.0001	< 0.01	< 0.0001
Ru	-	< 0.0001	-	-	-	< 0.0001	-	< 0.0001	-	< 0.0001	-	< 0.0001
Rh	-	< 0.0001	-	-	-	< 0.0001	-	< 0.0001	-	< 0.0001	-	< 0.0001
Pd	-	< 0.0001	-	-	-	< 0.0001	-	< 0.0001	-	< 0.0001	-	< 0.0001

**Not from AEDC pilot heater

TABLE VII-2 (Concluded)

Element	Sample # 8 Weight % Emission	Sample # 8 Weight % SSMS	Sample # 9 Weight % Emission	Sample # 9 Weight % SSMS	Sample # 10** Weight % Emission	Sample # 10** Weight % SSMS	Sample # 11 Weight % Emission	Sample # 11 Weight % SSMS	Sample # 12** Weight % Emission	Sample # 12** Weight % SSMS	Sample # 13 Weight % Emission	Sample # 13 Weight % SSMS
Ag	< 0.005	-	< 0.005	-	< 0.005	-	< 0.005	-	< 0.005	-	< 0.005	-
Cd	< 0.03	0.0002	< 0.03	-	< 0.03	0.0002	< 0.03	0.0002	< 0.03	0.0002	< 0.03	0.0002
In	-	< 0.0001	-	-	-	< 0.0001	-	< 0.0001	-	< 0.0001	-	< 0.0001
Sn	< 0.01	< 0.0001	< 0.01	-	< 0.01	< 0.0001	< 0.01	< 0.0001	< 0.01	< 0.0001	< 0.01	< 0.0001
Sb	< 0.03	< 0.0001	< 0.03	-	< 0.03	0.0001	< 0.03	< 0.0001	< 0.03	< 0.0001	< 0.03	< 0.0001
Te	-	< 0.0001	-	-	-	< 0.0001	-	0.0003	-	< 0.0001	-	< 0.0001
I	-	< 0.0001	-	-	-	< 0.0001	-	< 0.0001	-	< 0.0001	-	< 0.0001
Cs	-	< 0.0001	-	-	-	< 0.0001	-	< 0.0001	-	< 0.0001	-	< 0.0001
Ba	0.02	0.02	0.1	-	< 0.01	0.0070	0.3	1.0	< 0.01	0.0005	0.03	0.1
La	-	0.03	-	-	-	0.001	-	0.001	-	0.001	-	0.0002
Ce	-	0.05	-	-	-	0.035	-	0.002	-	0.035	-	0.075
Pr	-	0.01	-	-	-	0.001	-	0.0001	-	0.0003	-	0.0002
Nd	-	0.06	-	-	-	0.02	-	0.002	-	0.015	-	0.03
Sm	-	0.01	-	-	-	0.035	-	0.01	-	0.05	-	0.05
Eu	-	0.0009	-	-	-	0.0003	-	0.009	-	0.0002	-	0.0003
Gd	-	0.07	-	-	-	0.02	-	0.007	-	0.02	-	0.035
Yb	-	0.07	-	-	-	0.1	-	0.015	-	0.1	-	0.1
Dy	~ 0.7	1.8	< 0.1	-	~ 0.5	0.55	~ 0.5	1.2	~ 0.5	1.8	~ 0.5	1.8
Ho	< 0.1	0.005	< 0.1	-	< 0.1	0.0030	0.14	0.3	< 0.1	0.005	< 0.1	0.015
Er	-	0.015	-	-	-	0.01	-	0.015	-	0.015	-	0.05
Tm	-	0.005	-	-	-	0.005	-	0.002	-	0.01	-	0.008
Yb	0.046	0.05	< 0.002	-	0.056	0.075	0.017	0.0150	0.056	0.05	0.077	0.17
Lu	-	0.02	-	-	-	0.01	-	0.002	-	0.01	-	0.05
Hf	2.0	1.3	< 0.1	-	2.0	1.4	2.0	1.4	2.0	1.4	2.0	2.0
Ta	< 0.1	< 0.0001	< 0.1	-	< 0.1	< 0.0001	< 0.1	0.0010	< 0.1	< 0.0001	< 0.1	< 0.0001
W	< 0.1	0.0004	< 0.1	-	< 0.1	0.0004	< 0.1	0.0004	< 0.1	0.0002	< 0.1	0.0002
Re	-	< 0.0001	-	-	-	< 0.0001	-	< 0.0001	-	< 0.0001	-	< 0.0001
Os	-	< 0.0001	-	-	-	< 0.0001	-	< 0.0001	-	< 0.0001	-	< 0.0001
Ir	-	< 0.0001	-	-	-	< 0.0001	-	< 0.0001	-	< 0.0001	-	< 0.0001
Pt	-	< 0.0001	-	-	-	< 0.0001	-	< 0.0001	-	< 0.0001	-	< 0.0001
Au	-	< 0.0001	-	-	-	< 0.0001	-	< 0.0001	-	< 0.0001	-	< 0.0001
Hg	-	< 0.0001	-	-	-	< 0.0001	-	< 0.0001	-	< 0.0001	-	< 0.0001
Tl	-	< 0.0001	-	-	-	< 0.0001	-	< 0.0001	-	< 0.0001	-	< 0.0001
Pb	< 0.01	0.0002	< 0.01	-	< 0.01	0.0008	< 0.01	0.0002	< 0.01	0.0004	< 0.01	0.0005
Bi	< 0.01	< 0.0001	< 0.01	-	< 0.01	< 0.0001	< 0.01	< 0.0001	< 0.01	< 0.0001	< 0.01	< 0.0001
Th	< 0.1	0.015	< 0.1	-	< 0.1	0.005	< 0.1	0.0007	< 0.1	0.007	< 0.1	0.0075
U	-	0.05	-	-	-	0.05	-	0.0020	-	0.007	-	0.035

**Not from AEDC pilot heater

Analysis performed by Oak Ridge Y-12 Plant.

TABLE VII-3
YTTRIUM OXIDE CONCENTRATIONS IN ZrO_2
MATRIX AND INSULATION REFRACTORIES

Sample	Description	Weight Percent Y_2O_3*
1	9.25 w/o YRE_2O_3-ZrO_2 11' Level Col. 3 Matrix	8.31
7	8.25 w/o Y_2O_3 ASFAB Bed Liner No. 1078 Front Face	8.06
8	9.25 w/o Y_2O_3 ASFAB Bed Liner (AEDC)	8.43
10	9.25 w/o Y_2O_3 B.L. Cold Face NASA AMES** No. 1049	8.98
11	9.25 w/o YRE_2O_3-ZrO_2 7'6" Level Col. 5 Matrix	8.51
12	9.25 w/o Y_2O_3 B.L. Hot Face NASA AMES** No. 1077	8.87

*X-Ray Fluorescence Analysis performed by Oak Ridge Y-12 Plant.
**Not from AEDC Pilot Heater

TABLE VII-4
X-RAY DIFFRACTION ANALYSES
INSULATION BRICK

Brick Description	Sample Location	Percent Monoclinic
1078 Fluidyne AS-FABD 8-1/4% Y_2O_3	Front Face	0%
1077 Fluidyne* 9-1/4% Y_2O_3 Ames Heater	Front Hot Face	0%
1077 Fluidyne* 9-1/4% Y_2O_3 Ames Heater	Fractured Faced	0%
1077 Fluidyne* 9-1/4% Y_2O_3 Ames Heater	Rear Cold Face	0%
L-43 9-1/4 Y_2O_3	9' Level Front Face Viewport	0%
L-43	9' Level Back Face Viewport	0%
L-15 9-1/4 Y_2O_4	15' Level Hot Face Viewport	0%
L-15	15' Level Viewport	0%
9-1/4 w/o AS-FAB Front	Front Face	0%

*Not from AEDC pilot heater

TABLE VII-4 (Continued)

Brick Description	Sample Location	Percent Monoclinic
CC-9	Cold Face L. H. Side (Solid Sample No. 2)	0%
CC-9	Side Hot Face	0%
	Insulation Brick	
L-8 Bed Liner 8-1/4% Y_2O_3	Cold Face Center Rear (Solid)	0%
L-8	Fracture Surface (Powder)	0%
CC-9 Dome Brick 8-1/4% Y_2O_3	Cold Face Center Rear (Powder)	0%
ARL 1049-5* $CaO-ZrO_2$	Fracture Zone (Solid)	17%
ARL 1076-2*	Intermediate Zone (Solid)	0%
ARL 1076-2*	Intermediate Zone (Powder)	0%

*Not from AEDC pilot heater

TABLE VII-4 (Concluded)

Brick Description	Sample Location	Percent Monoclinic
L-8 (Above Matrix Bed Liner) 8-1/4% Y_2O_3-ZrO_2	Fracture Face (Powder)	0%
L-8	Front Face (Powder)	0%
L-8	Back Face (Powder)	0%
	Dome Brick	
CC-9 8-1/4% Y_2O_3-ZrO_2	4th Course Dome Brick R. H. Side Hot Face Front Face (Powder)	0%
CC-9	Fracture Face (Powder)	0%
CC-9	Back Face R. H. Side (Solid Sample No. 5)	0%
CC-9	Front Edge Hot Face L. H. Side (Solid Sample)	0%
CC-9	Side Hot Face L. H. Side (Solid Sample)	0%
CC-9	Cold Face L. H. Side (Solid Sample No. 2)	Peak at 29-45° Other Anomalous Peak Counter Electronics Acting Up.

UNCLASSIFIED

Security Classification

DOCUMENT CONTROL DATA - R & D

(Security classification of title, body of abstract and indexing annotation must be entered when the overall report is classified)

1 ORIGINATING ACTIVITY *(Corporate author)* Arnold Engineering Development Center Arnold Air Force Station, Tennessee 37389	2a. REPORT SECURITY CLASSIFICATION UNCLASSIFIED 2b. GROUP N/A

3 REPORT TITLE

RESEARCH AND DEVELOPMENT TESTING OF YTTRIA/RARE EARTH STABILIZED ZIRCONIA MATRIX BRICKS IN THE PILOT TEST UNIT (PTU) AT AEDC

4 DESCRIPTIVE NOTES *(Type of report and inclusive dates)*

February 1969 to April 1971--Final Report

5. AUTHOR(S) *(First name, middle initial, last name)*

C. R. Tinsley, ARO, Inc.

6 REPORT DATE November 1972	7a. TOTAL NO. OF PAGES 132	7b. NO. OF REFS 2

8a. CONTRACT OR GRANT NO. b. PROJECT NO. c. Program Element 65802F d. Task T-2	9a. ORIGINATOR'S REPORT NUMBER(S) AEDC-TR-72-161 9b. OTHER REPORT NO(S) *(Any other numbers that may be assigned this report)* ARO-ETF-TR-72-80

10 DISTRIBUTION STATEMENT

Approved for public release; distribution unlimited.

11. SUPPLEMENTARY NOTES Available in DDC	12 SPONSORING MILITARY ACTIVITY Arnold Engineering Development Center, Air Force Systems Command, Arnold Air Force Station, Tenn.

13 ABSTRACT Presented herein are the comprehensive results of research testing accomplished with the Pilot Test Unit (PTU) at AEDC since February 1969. The major objective of this continuing test program is to develop operational techniques and suitable ceramic materials in direct support of a full-scale, intermittent airflow, high enthalpy, high pressure test facility capable of testing aircraft and missile models, components, and engines in the Mach 2 to 8 flight regime. Eighty-four blowdown runs accomplished in the PTU are reported herein. Heater maximum operating conditions of 1850 psi and 4450°F were accomplished during testing.

DD FORM 1 NOV 65 1473

UNCLASSIFIED

Security Classification

14. KEY WORDS	LINK A ROLE	LINK A WT	LINK B ROLE	LINK B WT	LINK C ROLE	LINK C WT
test facilities						
development						
bricks						
ceramics						
heaters						
yttrium oxides						
zirconium oxides						
aluminum oxides						
rare earth elements						